Design and development of intelligent actuator control methodologies for morphing wing in wind tunnel

by

Shehryar KHAN

MANUSCRIPT BASED THESIS PRESENTED TO ÉCOLE DE TECHNOLOGIE SUPÉRIEURE IN PARTIAL FULFILLMENT FOR THE REQUIREMENTS OF THE DEGREE OF DOCTOR OF PHILOSOPHY
Ph.D.

MONTREAL, 2020-01-06

ÉCOLE DE TECHNOLOGIE SUPÉRIEURE
UNIVERSITÉ DU QUÉBEC

BOARD OF EXAMINERS

THIS THESIS HAS BEEN EVALUATED

BY THE FOLLOWING BOARD OF EXAMINERS

Professor Ruxandra Botez, Thesis Supervisor
Department of Automated Manufacturing Engineering at École de technologie supérieure

Professor Vincent Demers, President of the Board of Examiners
Department of Mechanical Engineering at École de technologie supérieure

Professor Vincent Duchaine, Member of the jury
Department of Automated Manufacturing Engineering at École de technologie supérieure

Professor Ramin Sedaghati, External Evaluator
Department of Mechanical and Industrial Engineering at Concordia University

THIS THESIS WAS PRENSENTED AND DEFENDED

IN THE PRESENCE OF A BOARD OF EXAMINERS AND PUBLIC

ON 3RD DECEMBER 2019

AT ÉCOLE DE TECHNOLOGIE SUPÉRIEURE

ACKNOWLEDGMENT

I would like to dedicate this work to my mother; without her sacrifices, I would not have been able to achieve too much in life, and to my father, who served in the aviation industry and at the United Nations and he had to stay far from home, to make sure we could receive the best education.

I offer my sincere gratitude to my research director Professor Ruxandra Botez for recognizing my potential, and for giving me an opportunity to pursue research and development under her leadership, and for giving me an opportunity to continue research in the prestigious international project CRIAQ MDO 505. I also wish to thank her for her supervision to help me to complete my exchange studies at McGill University, and also to complete the course work requirements for my PhD. I want also to thank Dr. Teodor Lucian Gregory for many useful discussions and for his leadership in various aspects of research. I would also like to thank Mr. Oscar Carranza for his cordial collaboration in the LARCASE, his discussions and his supervision in ensuring the sensitive equipment to be handled in a safe and appropriate manner. I would like to thank my colleague Tchatchueng Kammegne for many useful duscussions on various research aspects, that led to useful results. I would also like to express my gratitude to Mohammed Sadok Guezguez for his non-stop efforts during the project, and for his support in the validation of the controller during bench testing, and finally at the wind tunnel at the IAR-NRC Ottawa. I would also like to thank Miss Andrea Koreanschi and Mr.Oliviu Sugar Gabor for their useful discussions and brainstorming on the aerodynamic aspects of the project, and also would like to thank very much Manuel Flores, for the useful discussions during the evolution of the project. I would like to acknowledge the expertise of George Ghazi for our numerous productive discussions during various debugging sessions, and also to thank very much Yvan Tondji for his collaboration in the post-processing of the wind tunnel data.

I would like to express my sincere appreciation to the CRIAQ MDO 505 project's academic partners from the University of Naples Mr.Rosario Pecora, Mr.Leonardo Lecce and Professor Eric Laurendeau from Ecole Polytechnique, and to industrial partners Mr. Phillippe Molaret

and Mr.Louis Xavier from Thales Canada, and Patrick Germain and Mr. Fassi Kafyeke from Bombardier Aerospace.

Special thanks are due to Mr. Mahmoud Mamou and Mr. Youssef Mebarki for the supervision of the wind tunnel testing at the IAR-NRC. Without the contributions of committed experts and students it would not have been possible to realize the CRIAQ MDO 505 project. This project has helped me to develop many technical and leadership skills from countless interactions with academic and industrial partners.

Finally, I would like to thank my wife for being with me throughout all these challenging times. I would also like to thank my sons Muhammad Musa and Haroon for being an inspiration to pursue excellence in my career. I would also like to acknowledge the support of my friends whom presence during all this time helped me to finalize this PhD thesis.

Conception et développement de méthodes de commande intelligente d'actionneurs pour la déformation d'ailes en soufflerie

Shehryar KHAN

RESUME

Afin de protéger notre environnement en réduisant les émissions de carbone de l'aviation et en rendant les opérations aériennes plus économiques en carburant, plusieurs collaborations ont été établies à l'échelle internationale entre les universités et les industries aéronautiques du monde entier. Suite aux efforts de recherche et développement du projet CRIAQ 7.1, le projet MDO 505 a été lancé dans le but de maximiser le potentiel des avions électriques. Dans le projet MDO 505, de nouveaux actionneurs basés sur des moteurs à courant continu sans balai sont utilisés. Ces actionneurs sont placés le long de la corde sur deux lignes d'actionnement. L'aile de démonstration, composée de longerons et d'un revêtement souple, est composée de fibres de verre. Les modèles 2D et 3D de l'aile ont été développés en XFOIL et Fluent. Ces modèles d'ailes peuvent être programmés pour déformer l'aile dans diverses conditions de vol tel que le nombre de Mach, l'angle d'attaque et le nombre de Reynolds, permettant ainsi de calculer des profils optimisés. L'aile a été testée dans la soufflerie de l'IRA NRC (Ottawa).

Les actionneurs sont montés avec des capteurs LVDT pour mesurer le déplacement linéaire. Le revêtement flexible est intégré aux capteurs de pression pour détecter l'emplacement du point de transition laminaire - turbulent. Cette thèse présente à la fois la modélisation linéaire et non linéaire du nouvel actionneur de déformation. Les techniques classiques et modernes de l'IA pour la conception du système de commande d'actionneur sont présentées.

La conception et la validation de la commande de l'actionneur l'aide de la soufflerie renvoient à trois articles, le premier article présente la conception du contrôleur et les tests ensoufflerie du nouvel actionneur de déformation pour l'extrémité d'une aile d'avion. Les nouveaux actionneurs de déformation sont constitués d'un moteur BLDC couplé à un engrenage qui convertit le mouvement de rotation en mouvement linéaire. La modélisation mathématique est

effectuée afin de dériver une fonction de transfert basée sur les équations différentielles. Afin de pouvoir déformer l'aile, il a été conclu qu'un contrôle de la position, de la vitesse et du courant de l'actionneur devait être effectué. Chaque contrôleur est conçu en utilisant la méthode de contrôle de modèle interne (IMC) à partir de la théorie de contrôle classique sur le modèle linéaire de l'actionneur. Les gains obtenus ont été testés avec succès sur le modèle non linéaire de l'actionneur à partir de simulations. Enfin, l'essai de l'actionneur sur un banc de test est suivi d'un essai en soufflerie. Les données de la thermographie infrarouge et des capteurs de Kulite ont révélées qu'en moyenne, dans tous les cas de vols étudiés, le point de transition laminaire à turbulent était retardé au bord de fuite de l'aile.

Le deuxième article porte sur l'application de l'optimisation de l'essaim de particules pour la conception du contrôle de l'actionneur du nouvel actionneur de déformation. Récemment, l'algorithme d'optimisation d'essaims de particules a acquis une réputation dans la famille des algorithmes évolutifs pour la résolution de problèmes non convexes. Bien qu'il ne garantisse pas la convergence, toutefois, s'il est exécuté plusieurs fois en variant les conditions initiales, il permet alors d'obtenir les résultats souhaités.

Dans l'optimisation des essaims de particules, toutes les particules sont associées au vecteur de position et de vitesse. À chaque itération, la vitesse de la particule est calculée sur la base de la meilleure particule et de la meilleure particule globale en association avec des paramètres cognitifs et sociaux ainsi que du moment d'inertie de la particule. Une fois la vitesse calculée, la position suivante de la particule est calculée à l'aide de la somme de la position actuelle de la particule et de la vitesse. Bien que l'optimisation des essaims de particules ne garanti pas de converger vers un minimum global, son algorithme moins coûteux en terme de calcul repose néanmoins sur un nombre réduit d'opérations pour explorer l'espace de recherche. Suite au calcul réussi de la conception du contrôleur utilisant l'optimisation de l'essaim de particules, ses essais sur un banc de test ont été réalisés avec succès. Enfin, les essais en soufflerie ont été effectués sur la base du contrôleur conçu. Les résultats des capteurs infrarouge et Kulite ont révélé une extension des écoulements laminaires sur l'aile en train de se déformer.

Le troisième et dernier article présente la conception du contrôleur par logique floue. Le moteur BLDC est couplé au réducteur qui convertit le mouvement rotatif en mouvement linéaire, ce phénomène est utilisé pour pousser et tirer le revetement flexible qui se déforme. Le moteur BLDC lui-même et son interaction avec l'engrenage et le revetement déformant sont exposés aux charges aérodynamiques, ce qui en fait un système non linéaire complexe. Il a donc été décidé de concevoir un contrôleur flou capable de contrôler l'actionneur de manière appropriée. Trois contrôleurs flous ont été conçus pour le contrôle du courant, de la vitesse et de la position de l'actionneur de déformation. Les résultats de la simulation ont révélé que le contrôleur devellopé peut contrôler l'actionneur avec succès. Enfin, le contrôleur conçu a été testé en soufflerie et les capteurs infrarouge et Kulite ont révélé une amélioration de la position du point de transition de l'aile déformée.

Design and development of intelligent actuator control methodologies for a morphing wing in a wind tunnel

Shehryar KHAN

ABSTRACT

In order to protect our environment by reducing the aviation carbon emissions and making the airline operations more fuel efficient, internationally, various collaborations were established between the academia and aeronautical industries around the world. Following the successful research and development efforts of the CRIAQ 7.1 project, the CRIAQ MDO 505 project was launched with a goal of maximizing the potential of electric aircraft. In the MDO 505, novel morphing wing actuators based on brushless DC motors are used. These actuators are placed chord-wise on two actuation lines. The demonstrator wing, included ribs, spars and a flexible skin, that is composed of glass fiber. The 2D and 3D models of the wing were developed in XFOIL and Fluent. These wing models can be programmed to morph the wing at various flight conditions composed of various Mach numbers, angles of attack and Reynolds number by allowing the computation of various optimized airfoils. The wing was tested in the wind tunnel at the IAR NRC Ottawa.

In this thesis actuators are mounted with LVDT sensors to measure the linear displacement. The flexible skin is embedded with the pressure sensors to sense the location of the laminar-to-turbulent transition point. This thesis presents both linear and nonlinear modelling of the novel morphing actuator. Both classical and modern Artificial Intelligence (AI) techniques for the design of the actuator control system are presented. Actuator control design and validation in the wind tunnel is presented through three journal articles; The first article presents the controller design and wind tunnel testing of the novel morphing actuator for the wing tip of a real aircraft wing. The new morphing actuators are made up of BLDC motors coupled with a gear system, which converts the rotational motion into linear motion. Mathematical modelling is carried out in order to obtain a transfer function based on differential equations. In order to control the morphing wing it was concluded that a combined position, speed and current

control of the actuator needs to be designed. This controller is designed using the Internal Model Control (IMC) method for the linear model of the actuator. Finally, the bench testing of the actuator is carried out and is further followed by its wind testing. The infra red thermography and kulite sensors data revealed that on average on all flight cases, the laminar to turbulent transition point was delayed close to the trailing edge of the wing.

The second journal article presents the application of Particle Swarm Optimization (PSO) to the control design of the novel morphing actuator. Recently PSO algorithm has gained reputation in the family of evolutionary algorithms in solving non-convex problems. Although it does not guarantee convergence, however, by running it several times and by varying the initialization conditions the desired results were obtained. Following the successful computation of controller design, the PSO was validated using successful bench testing. Finally, the wind tunnel testing was performed based on the designed controller, and the Infra red testing and kulite sensor measurments results revealed the expected extension of laminar flows over the morphing wing.

The third and final article presents the design of fuzzy logic controller. The BLDC motor is coupled with the gear which converts the rotary motion into linear motion, this phenomenon is used to push and pull the flexible morphing skin. The BLDC motor itself and its interaction with the gear and morphing skin, which is exposed to the aerodynamic loads, makes it a complex nonlinear system. It was therefore decided to design a fuzzy controller, which can control the actuator in an appropriate way. Three fuzzy controllers were designed each of these controllers was designed for current, speed and position control of the morphing actuator. Simulation results revealed that the designed controller can successfully control the actuator. Finally, the designed controller was tested in the wind tunnel; the results obtained through the wind tunnel test were compared, and further validated with the infra red and kulite sensors measurments which revealed improvement in the delay of transition point location over the morphed wing.

TABLE OF CONTENTS

LIST OF TABLES

LIST OF FIGURES

LIST OF ABBREVIATION

IATA	International Air Transport Association
ICAO	International Civil Aviation Organization
PSO	Particle Swarm Optimization
BLDC	Brushless Dc Motor
CRIAQ	Consortium Of Research In Aerospace Quebec
IAR-NRC	Institute Of Aerospace Research National Research Center
LVDT	Linear Variable Differential Transducer
PID	Proportional Integral Derivative
MDO	Multi-Disciplinary Optimization
NASA	National Aeronautics And Space Administration
SMA	Shape Memory Alloy
MF	Membership Function
FFT	Fast Fourier Transform
BLDC	Brushless Dc Motor

STD Standard Deviation

IR Infra Red Thermography

LIST OF SYMBOLS

M	Mach numbers
α	Angle of attack
δ	Aileron deflection angles
c_1	Cognitive parameter
c_2	Social parameter
w	Moment of inertia
p^i	Best position of particle i experienced upto iteration *k*
p_k^g	Global best till iteration *k*
r_1	Cognitive random factor (0,1) at iteration *k*
r_2	Social random factor (0,1) at iteration *k*
v_k^i	Velocity of particle i at iteration *k*
qc	Quad counts
M	Mutual Inductance of the motor
R	Phase resistance of the motor
T_l	Load torque
T_e	Electromagnetic torque
U_{AB}	Line voltage

Tl	Load torque
$w(\Omega)$	Speed of the motor
ke	Coefficient of line back EMF
kt	Torque constant of the motor
I	Phase current of the BLDC motor
J	Moment of inertia of the motor
Ud	DC bus voltage
dY_{opt}	Desired vertical displacements of the optimized airfoil at the actuation points
dY_{real}	Real vertical displacements at the actuation points
e_i	Back EMF generated in phase "i" of the BLDC motor
i_k	Current in phase "k" of the BLDC motor
k_e	Coefficient of the line back EMF
k_t	Torque constant of the motor
q_c	Quad counts
u_d	DC bus voltage
u_i	Voltage in phase "i" of the BLDC motor
u_{ij}	Line voltages for the BLDC motor
$w(\Omega)$	Angular speed of the motor
B	Viscous friction coefficient
J	Moment of inertia of the motor
K_P	Proportional gain in SI units
K_{Pc}	Proportional gain for electrical current controller

K_{Pp}	Proportional gain for position controller
K_{Ps}	proportional gain for angular speed controller
K_I	Integral gain in SI units
K_{Ic}	Integral gain for electrical current controller
K_{Is}	Integral gain for angular speed controller
K_{P_EPOS}	Proportional gain in EPOS units
K_{I_EPOS}	Integral gain in EPOS units
$\mathscr{L}$	Laplace transform
L	Inductance of the phase winding
L_a	Line inductance of winding
M	Mutual inductance of the motor
R	Phase resistance of the motor
T_l	Load torque
T_e	Electromagnetic torque
IMC	Internal Model Control
EMF	Electromagnetic Force
PWM	Pulse Width Modulation
A_i	Fuzzy membership function for each input variable (i=1,N)
a, c	Parameters locating the feet of the triangular membership function
a_k^i	Parameters of the linear function($k, i= 1,n$)

b	Parameter locating the peak of the triangular membership function
b_o^i	Scalar offset($i=1,N$)
x	Input vector
y	Output of the fuzzy model
RPM	Rotation Per Minute
P	Proportional
I	Integral
A, B, C	Three phases of the BLDC motor
M	Mach number
A	Angle of attack
δ	Aileron deflection angle
k_e	Angular speed constant
K_t	Torque constant
R	Winding resistance
L	Inductance
e	Induced voltage
w_m	Rotational speed of the motor
T_e	Motors torque
T_l	Load torque
K_f	Friction coefficient
K_t	Torque constant
J	Moment of inertia

CHAPTER 1 INTRODUCTION

1.1 Motivation and previous work at the LARCASE

Aeronautical transport has evolved at a very rapid pace; the traffic has increased by threefold over the last decade, and by 2025 it is expected to double its current level. An approximate 3% increase in the number of passengers is expected annually, reaching approximately 1 billion passengers by 2016. The percentage of global CO_2 emissions from the aviation industry is 2%, based on the most recent statistics, as shown in Figure 1.1.

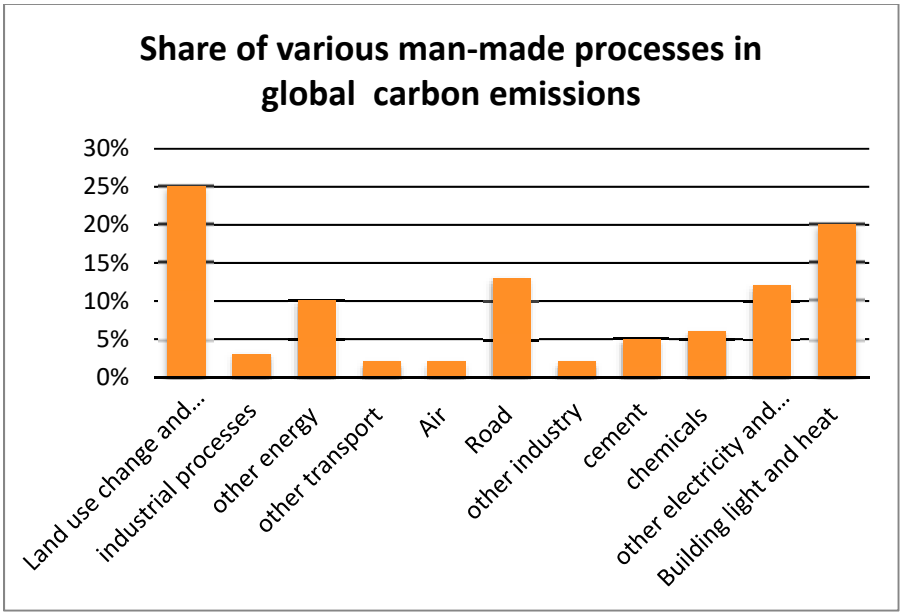

Figure 1.1 Share of various man-made processes in global aviation emissions (IATA)

Thousands of aircraft fly every day, transporting people (and some goods) from one part of the world to another. However the ever-growing number of flights are increasing the carbon

emissions; it is predicted that by 2050, the carbon emissions due to the aeronautical industry will increase from 2% to 3% of the total man made CO_2 emissions. This fact has become an important issue from the point of view of international policy. The International Air transport association (IATA) has decided to make a joint effort to reduce these carbon emissions by setting the targets visualized in Figure 1.2:

- Fuel efficiency improvement from 2009 and 2020 levels;
- Carbon-neutral growth by 2020; and
- Reducing the CO_2 emissions to 50% relative to 2005 levels by 2050.

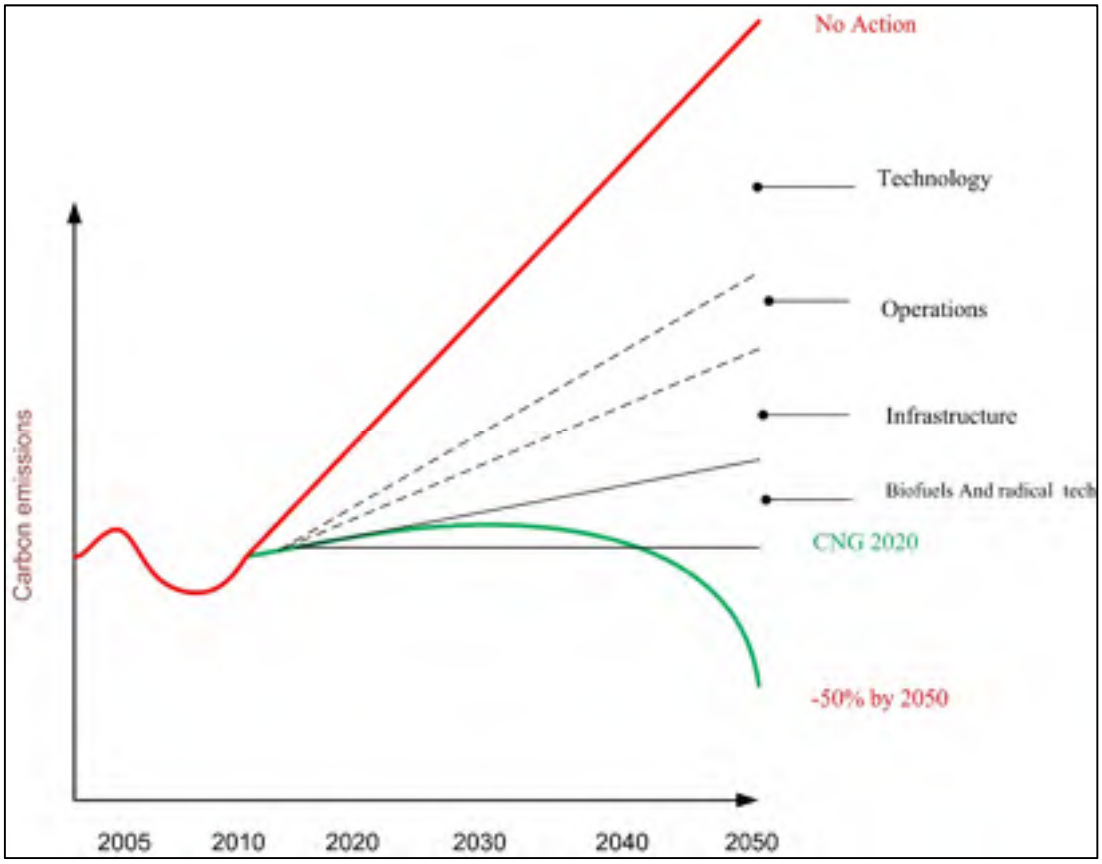

Figure 1.2 CO_2 emission reduction plan (IATA website)

To accomplish the above environmental goals, the international air transport association (IATA) in partnership with the international aerospace community has set forward a technology road map based on a four pillar strategy:

- Technological advancement in airframe, engine and biofuels;
- Efficiency in flight operations;
- Development in airspace and airport infrastructure; and
- Economical measures

Historically, fuel efficiency has been the key driver for technological development. The growing concerns regarding fuel cost and CO_2 emissions have led the governments in the Europe, USA and Canada to realize research and development projects in various areas such as lightweight materials, structures and propulsion, aerodynamics and equipment systems. All these diverse research areas are being evaluated for their potential to reduce fuel burn. Among these areas, the most promising green aircraft technologies needed for fuel reduction were identified as those involving:

- Laminar flow control;
- Structural health monitoring;
- Composite structures for wing and fuselage; and
- Engine architectures.

The major subsystems involved in morphing wing technology for laminar flow control are shown in Figure 1.3 (Gianluca Amendola PhD thesis, 2016). These subsystems cover aerodynamics, structural systems, sensors, actuators and control systems.

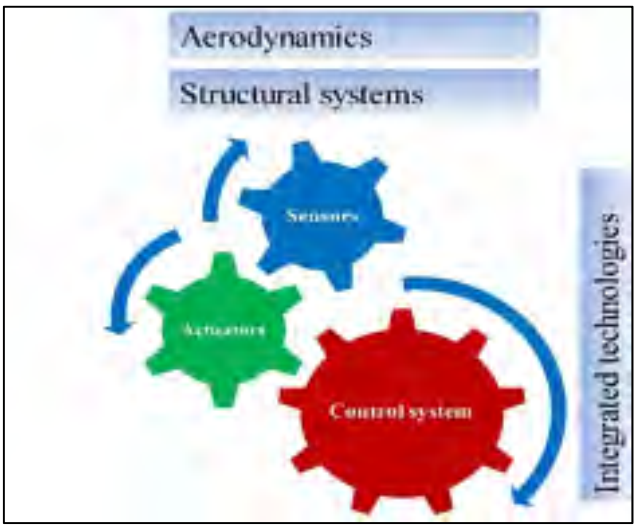

Figure 1.3 Major subsystems involved
in morphing wing technology

Air travel has become the most popular means of long-distance transportation over the last several decades. According to the Annual Report of the International Air Transport Association (IATA), which is composed of 290 member airlines, 4.1 billion passengers travelled on scheduled flights during the year 2017, which is 280 million more than in 2016. The growing number of flights is contributing to the continous increase of the aeronautical industry's share of global CO_2 emissions. In addition, rising fuel prices have become another important concern for airline operators and the aviation industry in general. Both climatic and financial concerns have led to academic and industrial collaborations around the world to develop advanced aircraft systems to address these global concerns.

State-of-the-art aircraft still have conventional hinged flight control surfaces. Conventional hinged control surfaces can be optimized for certain flight phases, but they produce drag due to gaps between the main body of the wing and its adjacent control surfaces. Unnecessary drag on the airfoil results in degraded aircraft performance and increased fuel burn by adding to CO_2 emissions and increasing fuel costs. Aeronautical engineers have always strived to develop aircraft systems that can mimic the bird flight. However, these attempts have not

reached the required level of technology readiness so they can be installed on commercial passenger aircraft due to weight and safety issues raised by certifying authorities.

Neverthless, with the emerging technologies, research teams around the world are working to develop new aircraft systems that would be more fuel efficient and climate friendly. With the advent of smart materials and shape-memory alloys, researchers are trying to replace conventional aircraft wings with morphing wings. Morphing wings structures involve the use of shape memory alloys, flexible materials which change their shape according to temperature variations. Another technology which has revolutionized many other industries, including aviation, is power electronics. This technology, has led to a new research area in aeronautical industry, known as more electric aircraft. In aircrafts, four different powers are extracted from engine: mechanical, pneumatic, electrical and hydraulic. The more electric aircraft goal is to use only one source of power, “electrical power”. The electrical power can be used for various purposes like cabin air-conditioning or actuator control.

The flight of birds in nature has always inspired scientists, that resulted in the development of aircraft. From the development of the first aircraft, aeronautical engineering researchers have taken their inspiration from bird flight to improve the efficiency of overall aircraft design. The concept of a morphing wing is not new. The Wright brothers were able to roll their aircraft by twisting the wing and by using wires that actuated directly. Conventional flight control surfaces, such as flaps and slats, have been successfully incorporated to control aircraft during various flight conditions, but their aerodynamic efficiency was suboptimal. Historically, morphing wings have been associated with various kinds of complexities such as increased weight as well as cost and safety issues. Over the last few decades, morphing wing technology has not been enough successful in making significant improvement in aerodynamic efficiency. Most of the large shape modifications over the last several decades have been carried out in military aircraft. During recent years, the researchers’ focus has also shifted towards UAVs due to their less-strict certification requirements.

New developments in the various fields, such as materials and actuation devices may apply to morphing wing developments. Current morphing wing research is a multidisciplinary field, as researchers can choose from a variety of materials, actuation devices and sensors. Some of the more important objectives in morphing wing design are the type of morphing, the time when the shape change occurs, and the choice of materials, actuation devices and sensors.

1.2 Morphing wing classification

Morphing wings can be classified into three categories: planform, out of plane and airfoil adjustment. Planform morphing can be achieved by varying the span, chord and sweep of the morphing wing either individually or in combination. Planform morphing results in modification of the aircraft aspect ratio, which has a direct effect on the lift to drag ratio. From aerodynamics point of view, increasing the aspect ratio will result in increased range and endurance. A larger span results in a broader range and improved fuel efficiency, however it reduces the manoeuvrability. Wing out of plan morphing is achieved by combination of twist, span wise bending and dihedral gull. Dihedral gull is the angle between the wing root and the wing tip, dihedral wings provide the capability to enhance the flight control and performance of the aircraft; in case when the wing is at a lower angle than the wing root than its known as the “anhedral wing”. Twist is added to the wing in order to distribute the lift over the wing with an aim to increase its flight performance. Simillary the aim of spanwise bending is also to improve the flight performance, however fewer studies have been carried out on this subject (Barbarino et al., 2011).

Developments in the field of smart technologies such as microelectronics, support hardware, actuators and sensors have led to breakthroughs in many scientific disciplines. These developments have the potential to advance the edges of aircraft technology in various aspects, including safety, environmental compatibility and affordability. At NASA, the goal of the Aircraft Morphing program is to develop smart devices based on active component technologies. The ultimate aim of the research is the development of self adaptive flight, which will lead to improved aircraft efficiency. Many of these research endeavors ended up not being qualified for the real aircraft, mainly due to the high cost of implementation or because of the

fact that the overall benefit was too small to conduct the system into production. One of the key enabling technologies is the control system design, which is helpful in the mathematical modelling and feedback control in the Aircraft Morphing program. Once the choices of actuator and sensor type have been made, the next key decision was to determine the number of actuators and their locations (NASA website). Various types of actuators, including electromechanical, hydrauic, pnematic and piezo electric actuators have been used for applications ranging from flaps/Slats, ailerons, rudders and spoilers to landing deployment and retraction control. The following section explains the various types of actuators and controllers used for morphing applications.

1.3 Types of actuators and control techniques

Pierre and Jacques Curie first discovered the piezoelectric effect in 1880. Piezo is a greek word which means pressure. When pressure is applied on certain materials they generate electricity and vice versa when electricity is applied to them they change their shape. Thus piezoelectricity is a phenomenon which relates electrical and mechanical systems (Inman, d. et al, 1998).

Macro Fiber Composites (MFC) are materials whose properties can be modified by an external stimulas in order to meet certain objectives. These are the kind of materials which can sense their envirnment and accordingly change their physical characteristics, furthermore when voltage is applied to them, they deform and change their shape. Based on the electrode patern inside the material, it either elongates or contracts. NASA has used MFC for alleviating uncontrolled vibrations and unsteady aerodynamics.

At virginia tech a hinged trailing edge was replaced with the deformable surface, and hence the camber could be changed continously by embedding the MFC actuator in the wing surface (Kelvin, P et al, 2014).In the past few decades Macro Fiber Composite have been used widely, because they provide high actuation and structural stability. A common drawback with the piezo ceramic actuators is that they may require high voltages in the range of 1.8 KV to 10 KV, however the current drain is extremely low which results in small power consumption.

MFC are made up of piezo ceramic fibers embedded in a polymer matrix (Bilgen, O. et al, 2010).

Patches of MFC were bonded to a wing and voltage was applied to change the camber of the wing, it was concluded that MFC are one of the best means of shape modifications for structural and aerodynamic applications. Some of their useful characteristics are high flexibility and large displacements(Bilgen, O., Alper et al, 2010).

Shape memory alloys are used to design morphing wing actuators. A morphing wing actuator varies the camber of the wing, which causes the same effect as a mechanical flap, and reduces the overall drag caused by the discontinuous parts of the conventional flap control surface. Various tests, including material property and actuation characteristics tests were performed; these led to the selection of Flexinol wire as an appropriate actuator for the morphing wing. An Hardware In the Loop (HIL) interface based on Matlab/Simulink was used to analyze the displacement response of the actuator to a commanded input current (Misun et al, 2014).

A morphing flap was designed based on the application of Shape Memory Alloy. As their names suggest, SMAs can change their shape when their temperature is changed. This principle was used to morph the shape of the wing. Aerodynamic analysis was conducted using Fluent and Gambit. The morphing wing was composed of a spar, a rib, the wing skin and a quadrilateral frame. The quadrilateral frame was bonded with in the upper and lower part of the skin. When the actuation temperature was reached, the SMA wire shrinked, causing the trailing edge flap to move downward. Flexinol wire was used as an SMA actuator. The actuation test of the morphing wing was performed using a DC power supply and six Flexinol wires. The electric current was increased in the range of 1.5 to 3.3 mA, and the corresponding deflection angles were measured for each flight simulation case (Woo-Ram et al.,2012).

Another work consisted in morphing a wing's upper surface by using an electromechanical system. The actuator was custom-designed, as the off-the-shelf actuators did not suit the requirements. The morphing was carried out by two DC motors connected to two eccentric shafts. The two actuation lines were connected at 30% and at 50% of the chord. The purpose of the cam is to convert the rotational movement into vertical displacement. Rotary electric

actuators were used. The transfer function of the electromechanical system was developed, and a frequency domain analysis was conducted to satisfy the time domain requirements. The position controller was designed using the Ziegler-Nicholes technique (Majji et al, 2007).

A double loop fuzzy logic position and torque controller was designed to perform actuator control for a morphing wing. These morphing wing actuators were based on DC motors. The controllers were validated in simulations using Matlab/Simulink software. Wind tunnel testing was carried out in the Price-Paidoussis wind tunnel. Two actuation lines were controlled using their respective controllers, which supply voltage to the DC motors via programmable power supplies (Dimino et al, 2007).

Various airfoil optimization techniques have been investigated both theoretically and experimentally; however, their incorporation in real aircraft is still in progress. The purpose of this research was to mitigate the drag by improving the laminar flows over the wing. A morphing actuator was composed of a cam that has a translation motion relative to the structure. The movement of the cam resulted in the movement of a rod with one end connected to the roller and the other end connected to the skin. When the SMA was heated, the SMA moved to the right, which caused the cam to move to the right and the roller moved up, causing vertical displacement of the skin. In contrast, when the SMA cooled, the CAM moved to the left and caused the skin to move downward. In (Popov et al, 2010), a Quanser board controlled the power supplies, which in turn controlled the SMA actuators, that were programmed through Simulink. A Graphical User Interface allowed the user to select the optimized airfoil, which in turn generated the desired displacements to be actuated by the controller. The controller commands the power supply, connected to the SMA. The Linear Variable Differential Transformer (LVDT) sensors attached to each actuator provided the displacement feedback to the controller. The difference between the reference and the feedback from the LVDT sensors was computed, and then fed to the controller. Based on this difference, the associated controller decides whether to heat or cool the SMA to acquire the reference actuator displacement. The data from the Kulite pressure sensors was fed to the data acquisition module, which in turn was used for the computation of the transition point. The sampling rate of each channel was chosen

to be 15k samples/s. The pressure coefficient was calculated from the mean of the feedback signals fed from the Kulite pressure sensors, which was ultimately used to find the laminar to turbulent transition point.

Morphing Wing Technology has been pushing the edges of science in the fields of physics and mathematics in recent years. As a multidisciplinary research area, it consisted in a combination of various fields such as intelligent control, intelligent materials, high computational power, computational fluid dynamics, flight testing, signal acquisition, wind tunnel testing and signal detection using miniaturized sensors. Fuzzy logic was used to model nonlinear systems, multi dimensional systems and those with parameters variations. Fuzzy sets were utilized to design such a model. Complications appeared because it was not easy to design membership functions, and rules manually for each input. An Adaptive Neuro Fuzzy Inference System simplified the process of the generation and optimization of membership functions and rules using neural networks. Neural networks have found applications in various domains of the aeronautical industry, such as structural damage detection, autopilot controllers and detection of control surface failures. Takagi, Sugeno and Kang designed a Sugeno fuzzy model to generate fuzzy rules from a given input-output data (kang et al, 2012). ANFIS deployed a combination of gradient descent and least squares methods to compute the membership function parameters. The optimization of membership functions has been done using ANFIS to train epochs (Botez et al, 2009).

A novel actuation concept for a morphing wing was presented (Grigorie et al, 2010) in their approach optimized airfoils were computed for five different Mach numbers and seven different angles of attack. The transition point estimation was found using both Kulite and optical sensors. In closed loop morphing wing control, actuator control was performed using the feedback from the Kulite pressure sensors. In open loop morphing wing control, the simulation and experimental effort was focused on the aerodynamics of the morphing wing, actuator control, real time visualization, and the determination of the transition point using pressure sensors. The morphing wing had a span of 0.9m and chord of 0.5m, with a flexible upper skin. The actuation lines were chosen to be SMA wires. The SMA actuator wires were

composed of nickel-titanium, they have contracted and expanded similar to muscles when they were driven electrically. Three SMA wires were used in each actuation line (1.8 m in length) as actuators that were functioning as a cam which moved in translation compared to the structure by causing vertical movement of the rod with one end connected to the skin, and its other end was connected to the roller. Heating of the SMA caused the cam to move to the right, which resulted in the upward movement of the roller while in contrast, cooling of the SMA caused the cam to move to the left by causing the downward movement of the skin. The objective of the controller design is to apply appropriate current to the SMA based on the error signal obtained from the difference between the required skin displacement and the actual skin displacement (Grigorie, et al, 2010).

A real time closed loop morphing wing control was presented (Popov et al. 2010). The idea was to replace the previously computed optimized airfoils using CFD software and to embed the optimization algorithm was embedded in a processor that generated optimized airfoils in real time, and for various wind flow conditions. This optimization method was a mixture of simulated annealing and a gradient descent. The actuators were two oblique cam sliding rods positioned span-wise, thus converting the translatory motion along the span into perpendicular motion. Each actuator was placed in equilibrium by Ni-Ti alloy SMAs wires that pulled the sliding rod in one direction while the gas spring pulled the sliding rod in the opposite direction. The gas spring was included to nullify the effects of aerodynamic forces acting upon the flexible skin when the SMAs were not active and thus to return the airfoil into an unmorphed reference state. The SMAs, meanwhile, push or pull the flexible skin into an optimized airfoil state.

The SMA based actuators were powered by programmable power supplies. The power supplies received the commands from the Data Acquisition Card (DAC) which was interfaced via Matlab/Simulink. The open loop control program in Simulink received its temperature feedback from thermocouples attached to each SMA, and its position feedback from the LVDTs served to perform the desired position control. The temperature feedback was used to disconnect the current supply to the SMAs in case when safe temperature limits were

exceeded. The feedback from the LVDTs served to perform the desired position control. The optimized airfoil actuator displacements were stored in the computer's hard disk, and were further provided to the Matlab/Simulink control model.

The aim of this research was to push the laminar to turbulent transition point towards the trailing edge of the wing and thereby to improve the laminar flows. An array of Kulite sensors were embedded in the wing to detect the laminar flows. Pressure acquisition was done using a NI DAQ USB 6210 with sixteen analog inputs and a sampling rate of 250 kilo samples/s (Popov et al, 2010).

Shape Memory Alloys (SMA) were designed using nickel titanium alloys, and they stretched and shrinked like muscle tissues when they were electrically excited. When a current was applied to an SMA, heat was generated due to the resistivity of its internal crystalline structure. The generated heat caused changes to the internal crystalline structure of the SMA by changes in the length of the SMA wire. SMA wire's variation in length as a function of electrical current was used for morphing skin actuation purposes. The main reason for using Ni-Ti was its ability to withstand repeated heating and cooling phases without no signs of fatigue. While SMAs have many advantages, they also have various drawbacks, one such draw back was that they require high current to reach their transformation temperatures. Since the length of the wire changes, it cannot be welded to a surface directly, as after certain cycles of operation, the mechanical attachment would break. The heating and cooling of the SMA wire causes the left and right span wise movement of an oblique cam. The translatory motion of the cam was converted into the perpendicular motion of the rod with one end connected to the roller inside the cam, and the other end was connected to the flexible skin. Several step responses were recorded for both the cooling and heating phase of the SMA. Using Matlab's system identification tool box, the transfer function was identified based on the recorded step response. The Proportional Integral (PI) gains controlling the heating phase were computed using the Ziegler-Nichols PID controller tuning methodology. The proportional gain was increased to a level where sustained oscillations were obtained. The value of the proportional gain for which the sustained oscillations were obtained was recorded with in a semi time period. Having calculated these parameters, the respective PI parameters were calculated

Zieglerand Nichols' equations. Once the PI gains were computed, the closed loop transfer function can be derived. The closed loop transfer function revealed that the system was stable, since all the poles were on the left hand side of the *s*-plane. The state space equations indicated that the system was completely controllable and observable (Grigorie et al, 2011).

The control strategy developed by (Grigorie et al, 2011) was validated using Matlab and Simulink software, and then validated experimentally. The experimental validation was carried out using two programmable power supplies and a Quanser Q8 data acquisition card. The inputs to the data acquisition card were provided by LVDTs and thermocouples connected to the actuators. The Quanser Q8 data acquisition card generated appropriate signals to control the power supplies which in turn controled the actuator displacements to obtain the desired skin displacements. The actuator testing was first performed in a bench test and it was then tested in a wind tunnel. The optimized airfoils computed in the design phase were validated during the wind tunnel testing by morphing the skin using various actuator displacements; their analyis made it possible to identify the laminar-to-turbulent transition region.

Morphing wing intelligent control was performed using a fuzzy logic controller. The reason for which a fuzzy logic controller was chosen, it was because of the strong non linearities of the smart material actuator. The input/output mapping was designed, so that the error and its change were considered. Four important elements were required to design a fuzzy logic controller: a fuzzy inference engine, a fuzzifier, a fuzzy rule base and a defuzzifier. The fuzzifier element, converted crisp inputs into linguistic variables. A Takagi, Sugeno and Kang fuzzy model was selected to define the rules. The actuators were controlled using Quanser Q8 data acquisation card as shown in Figure 1.4 (Grigorie et al, 2012).

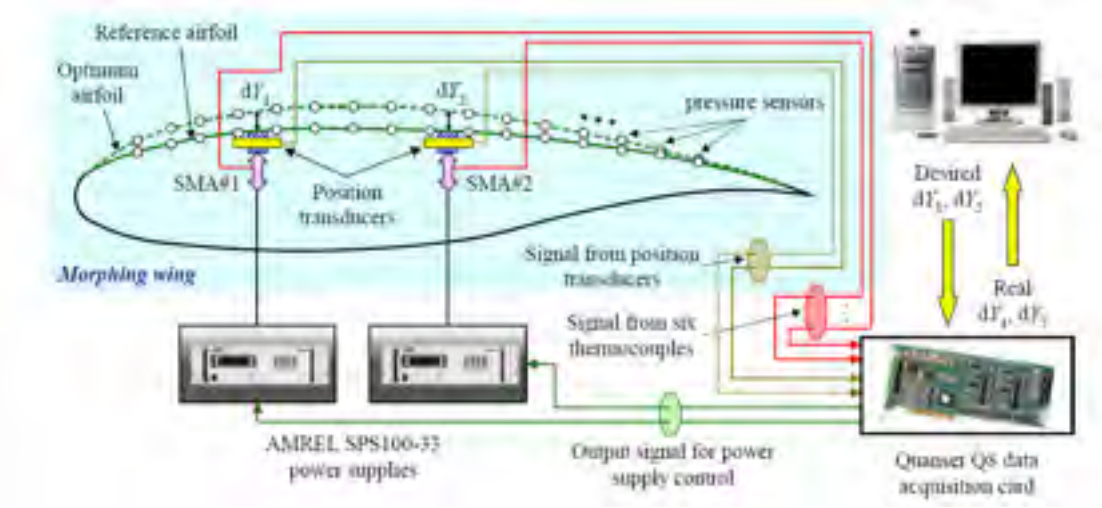

Figure 1.4 Morphing wing control using shape memory alloys

Two morphing wing control strategies were developed to obtain the optimized airfoils during wind tunnel testing. One way to perform morphing wing was to store the required displacements, Mach numbers and angles of attack on the computer. The feedback signals consisted in the position feedback from the LVDT sensors connected to the actuator. There was no feedback from the pressure sensors mounted on the flexible skin. This kind of configuration is called open loop morphing wing control. In the second kind of morphing wing control strategy, pressure feedback was measured by the Kulite sensors mounted on the skin in order to compute the actuator displacements required to increase the laminar flows over the wing (Kammegne, M.T et al,. 2015).

Position control of an electrical actuator for morphing ATR-42 airfoil in the Price-Païdoussis wind tunnel was presented by Popov et al. (2010). Electric actuators are usually stable than sma's and they are easy to integrate. The flexible skin was morphed at 10% and 70% of the chord. The electrical motors were coupled with the eccentric shaft in order to morph the flexible upper skin. A proportional derivative controller was designed to control the actuator. The transfer functions were derived for both the electrical and mechanical systems. Simulink was used to validate the electrical and mechanical transfer function model of the actuator. In order to perform position control, it was important that the electrical actuator provided the right

torque to move the mechanical system. This current controller was designed using the phase margin and gain margin analysis in order to provide an appropriate torque. Once the current controller was designed, the Ziegler and Nichols technique was applied to compute the proportional and derivative gains for the position controller (Popov et al, 2010).

Reference airfoil was morphed to compute the optimized airfoils for each combination of angles of attack, Reynolds numbers and Mach numbers. An optimization algorithm was used to generate various vertical displacements for the actuator. The optimization code was interfaced with the morphing skin and the CFD code. Incase of closed loop morphing wing control the input was the optimized airfoil for each airflow condition. The infrared thermography of the airfoil revealed that the transition point was located at 25% of the cord for the reference airfoil while in case of open loop control the transition point was located at 57%. For closed loop control the transition point was located at 58% (Kammegne et al, 2015).

fuzzy logic position controller has been designed for a morphing wing. The morphing wing actuators used were based on DC motors. The controller was validated in simulations with matlab simulink software. The wind tunnel testing was carried out in price-paidoussis wind tunnel. The controller was designed to control the two actuation lines which supply voltage to the DC motors via programmable power supplies (Kammegne et al, 2017).

In this research, instead of SMA actuators, miniature electric actuators are used. Since there was no actuator in the market which could fit in the wing, therefore electromechanical actuator was built in-house. The designed actuators could be useful for the aviation applications due to its light weight and low power consumption (15 Watts). The electrical motor was the BLDC motor. BLDC motors are known for their small size and high torque. An immense amount of research has been done to replace direct current motors by BLDC motors Actuator mathematical model was derived. Numerical validations were carried out based on the data sheet. A hysteresis and Ziegler Nichols technique has been used to design the current control and position control for the morphing actuator (Nguyen, 2016).

A real time control system was developed to control the position of the actuator in order to morph the wing shape for the specified flight condition. Although mathematical model of the actuator was developed, however the model did not include the integrated effects of the skin and actuator. To handle this nonlinear behavior, the fuzzy feedforward controller was developed. Input of the controller was the actuator position error while its output was the number of the pulses required to obtain the desired actuator position. Four identical fuzzy controllers were developed each of them was associated with its respective actuator. The membership parameters were chosen by trial and error method. The fuzzification process was composed of eleven rules. The wind tunnel testing results revealed that for some flight cases, such as, for the flight case 70 (Mach=0.2, $\alpha=1^{o}$, $\delta=4^{o}$), a 4% improvement in the transition was obtained from 48% unmorphed to 52% morphed (Kammegne et al, 2016).

The adaptive neuro fuzzy inference system has been applied to design a morphing wing actuator control. The knowledge base of fuzzy logic and self learning abilities of neural networks was combined. Neural networks have the ability to learn while fuzzy logic was easy to understand with the If-Then rules. The simulation and experimental results are obtained using Matlab, Simulink, NI veristand, NI PXI and Maxon drives. The input to the controller was the difference between the desired position and the feedback from the LVDTs attached to the flexible skin. The error was fed to the ANFIS controller, which produced the desired number of pulses required by the Maxon motor. Finally, Maxon drive rotated the motor and the gear mechanism, which converted the rotary motion into the vertical motion (Kammegne et al, 2016).

The electrical and mechanical dynamics of the actuator were modeled in Matlab and Simulink. Although motor had internal position sensing based on hall sensors however LVDT feedback was required due external gearing mechanism. Pole zero cancellation method was applied to design the torque controller. The zero of the current controller was used to cancel the pole of the transfer function (Botez et al, 2016).

Wind tunnel testing was performed in order to evaluate the aerodynamic performance of the wing. Various flight cases were combinations of nineteen angles of attack (varied from -3

degree to +3 degrees), 13 aileron deflection angles (-6 deg to +6 deg), and three values of Mach numbers (0.15,0.2,0.25). For each flight condition, the actuator displacements varied based on their values stored in the database (Joao Loureiro et al 2015).

Calibration of the open loop morphing wing control has been done in this work. After setting up the real time control of the morphing skin, it was observed that the actuator was unable to morph the skin to the desired displacement. Upon repeated attempts, it was established that the response of the actuator was nonrepeatable and nonlinear due to the play in the gear box and to the linkage between components. Furthermore, problems like dead zone nonlinearity, and uncertain reference point were solved by use of the closed loop position control. (Kammegne et al, 2010).

In recent aircrafts such as Boeing B787 and Airbus A-380 various hydraulic, pneumatic and mechanical systems have been replaced by electrical systems. Power electronics is key enabling technology employed for more electric aircraft; In conventional aircraft four different kinds of powers are derived from the aircraft, namely hydraulic, pneumatic, electrical and mechanical. The pneumatic power provided by the engine is used for cabin pressurization, and wing anti icing. The mechanical power is provided by the engine gear box. Similarly, the hydraulic system is used for the actuation of various aircraft systems. In contrast to the conventional topology, in more electric aircraft single source of power is derived from the engine, which is electrical, and is further used for all other applications. The replacement of conventional pneumatic and mechanical systems by electrical systems improves the overall weight and efficiency of the aircraft (Wheeler et al, 2012).

In various applications, it is required to control the position, altitude and retract or deploy the system. There is ever increasing need of miniature actuators in aeronautical and space applications. State of the art aircraft systems is based on hydraulic actuators, however future aircrafts will be either more electric or even all electric, which will result in weight reduction, and less maintenance. Although promising results could be achieved from this conversion,

there are still many challenges posed by the certification companies before more electric or all electric aircrafts could be brought into service (Janker et al, 2008).

Tuning rules for PID have been presented. The internal model control method proposed by (skogested et al, 1986) gained a widespread acceptance in the industry. Another classical technique to tune PID controller is Ziegler & Nicholes. The important step in this technique was to obtain sustained oscillation with a Proportional controller.

A new class of morphing actuators was integrated into a flexible UAV wing with the aim to reduce its overall complexity, weight and power consumption. The UAV has a span of 1.4 m and is equipped with two Posts-Buckled Pre-Compressed (PBP piezoelectric actuators) on its outboard. Various benefits were obtained by replacing the conventional aileron by the PBP morphing aileron. The morphing aileron did not employ any gears or linkages as compared to its conventional counterpart, which had the advantage of simplicity and reduction in the weight. It was observed that the morphing wing provided 38% more roll in comparison to the conventional one. Also the morphing aileron reduced the number of mechanical parts mounted on the wing from 56 to only 6. Power consumption was reduced from 24w to 100mw and current from 5A to 1.4mA (Roelof Vos et al, 2007).

Shape memory alloys (SMA's) have been used to perform the camber actuation of the trailing edge of the wing (Jodin et al, 2017). Three SMA wires move back and forth under the upper skin and over the lower skin. Temperature and deformation sensors were utilized to perform the precise shape control. One thermocouple per SMA wire was used for temperature sensing and strain gauge was used to measure the deformation. The SMA reference temperature was generated by the Proportional Integral controller. Wind tunnel testing revealed that the camber control proved its ability to modify the lift by 23%, the drag by 35% and the lift to drag ration by 16%.

An Unmanned Aerial Vehicle with morphing wings has been designed by the Virginia Tech morphing wing team. Servo-less and piezoelectric material have been used to control the camber of all control surfaces of the aircraft. Micro Fiber Composite is flexible (MFC) and

was thus used for morphing wing control. Extensive research has been carried out on the suitability of the MFC for actuation and structural control purposes. Combination of DSPIC30f2010 microcontroller and power electronics was used to perform the MFC actuation. It was concluded that MFC's can successfully control the camber of the RC aircraft in the laboratory and during flight. They successfully controlled the pitch and roll during the flight. A single lithium polymer battery was used to power all the systems. Lag was caused due to the large number of capacitance that were connected in parallel and were powered from the on board battery. The lag was proportional to the capacitance of the system, and affected the flight of the aircraft. A conclusion was made that if the nonlinearity of the control surfaces caused to the hysteresis was modelled, the power electronics and control circuit could be modified accordingly to avoid the lag, and to ensure more responsive and linear actuation (Bilgen et al, 2012).

A morphing wing strategy for enhanced aerodynamic performance has been proposed. The goal was to achieve aerodynamic efficiency while respecting the weight and performance constraints. An important objective was to design a concept of distributed actuation and sensing. Extensive research has been carried out in the field of monolithic joint less mechanisms known as complaint mechanisms. These devices transmited motion and force using flexure and deformation in contrast to conventional devices with joints. Improvements such as withdrawal of backlash, no wear and backlash from mechanical joints were denoted. This research took its inspiration from the biological creatures for monolithic systems design, resulting in more autonomous, adaptive and self contained systems. Genetic algorithms have been used for the purpose of parameters optimization (Trease, 2006).

CHAPTER 2 RESEARCH APPROACH AND OBJECTIVES

Following the same international trend, the Laboratory of Applied Research in Active Controls and Aeroservoelasticity (LARCASE) team participated in an international project involving a collaboration between industries and academia across Canada and Europe. The main research focus of the CRIAQ 7.1 project was the improvement of the laminar flows over a morphing wing. A morphing wing with a flexible upper skin was manufactured, and equipped with shape-memory alloys (SMAs) used as morphing actuators. Both classical and modern actuator control techniques were designed. The respective controllers were validated both during bench and wind tunnel testing. The CRIAQ 7.1 project led to the following conclusions.

- A strong nonlinear behavior was observed for the SMAs; and
- SMAs respond rapidly during the heating phase (10 Sec), but had a slow response in a cooling phase (1-2 min).

The CRIAQ 7.1 had known success from the perspective of integration of technologies as well as from the aerodynamic results point of view. Following the experiences of CRIAQ 7.1, it was decided to use brushless DC motors as morphing actuators due to their high weight-to-torque ratio and their growing popularity in many defense and avionics applications.

2.1 Background of the CRIAQ MDO 505 Project

Following the experience acquired in the CRIAQ 7.1 project, another major international collaboration was launched, that was funded by the Canadian and Italian governments and industrial partners. The CRIAQ MDO 505 project had the following governmental and business partners: the Consortium for Research and Innovation in Aerospace Quebec (CRIAQ), the National Sciences and Engineering Research Council of Canada (NSERC), Thales Avionics, Bombardier Aerospace and the National Research Council Canada Institute for Aerospace Research (NRC-IAR), and the following academic partners: the École die Technologie Supérieure, the Laboratory of research in Avionics and Aero-Servo-Elasticity

(LARCASE), École Polytechnique, the University of Naples and the Italian Aerospace Research Center (CIRA).

The CRIAQ MDO 505 project focuses on the design, manufacturing, bench and wind tunnel tests of a prototype system of a morphing wing-tip (wing and aileron, no winglet). This project includes the design, control and validation of the morphing system in a wind tunnel using actuators and sensors. To improve the aerodynamic performance of the morphing system, each team developed its own design, manufacturing and testing for the morphing wing and rigid aileron (Canada), and for the morphing aileron (Italy).

The distribution and integration of the tasks between the project partners are shown in Figure 2.1. The LARCASE team at ETS, as the project leader, was assigned the task of developing the actuator control methods, both in open and closed loop, along with aerodynamic analysis of the morphing wing as well as the embedding of the kulite sensors in the wing in collaboration with Ecole polytechnique. The structural team at the ETS, and at the IAR-NRC were responsible for the design and manufacture of the morphing wing and the rigid aileron. The purpose of the aerodynamic studies, in addition to determining the optimized airfoil shapes, was to compute the actuator displacements for the morphed airfoils, which must be implemented for various flight conditions during wind tunnel testing. The team at IAR-NRC was responsible for the wind tunnel testing and for the infrared measurements to locate the laminar-to-turbulent transition point in collaboration with the LARCASE team. As stated above, the Italian team was tasked with designing and manufacturing a morphing aileron.

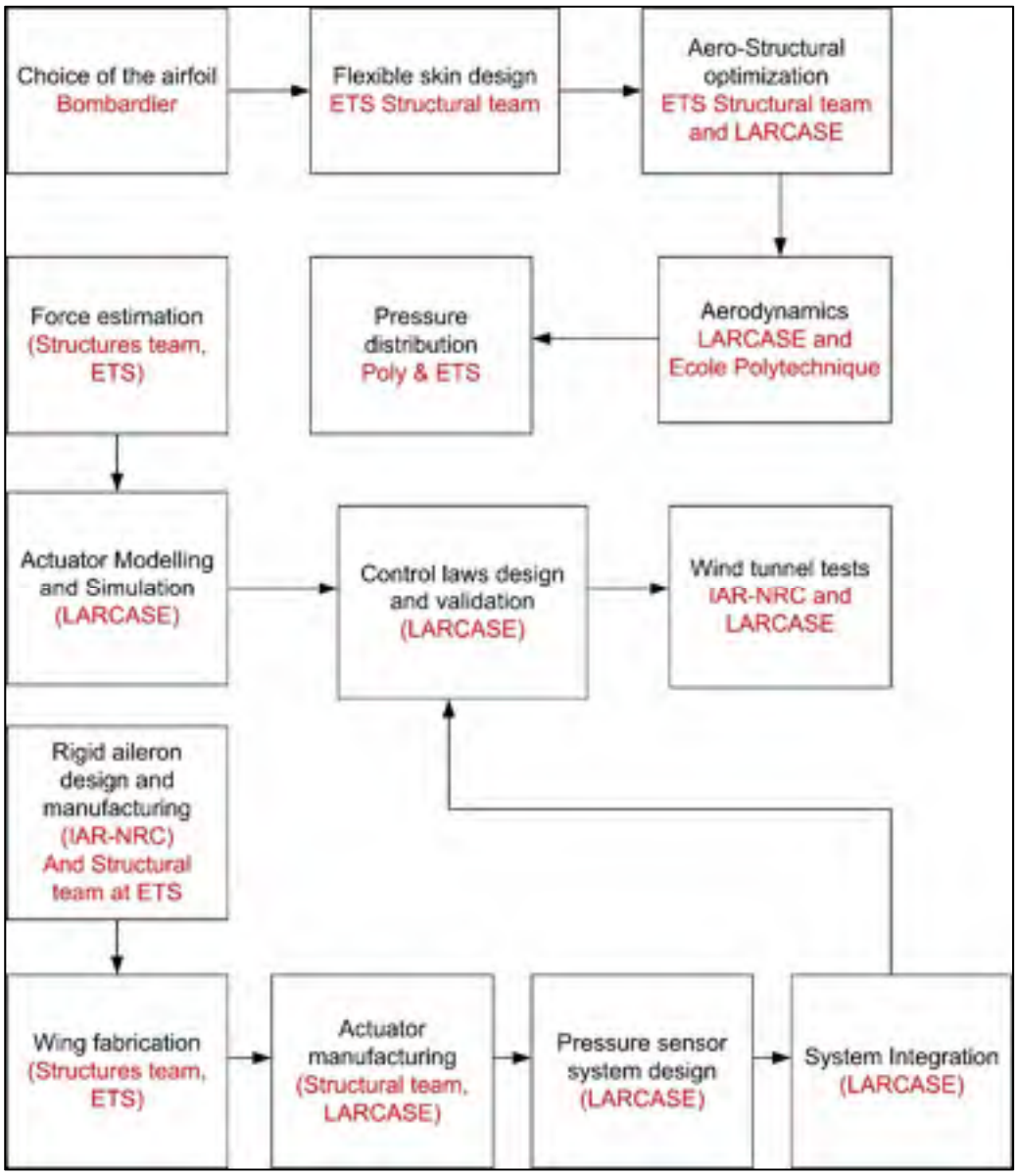

Figure 2.1 Project task distribution among the project partners

2.2 Morphing wing presentation

It was decided to design a wing with its cord and span length of 1.5m, as shown in Figure 2.2. These dimensions were chosen as they fitted the max model required dimensions in the wind

tunnel IAR-NRC. Actuation lines were placed at 32% and 48% of the chord. The rigid part of the wing was made of aluminium, but 20% to 65% of the wing's upper skin was made flexible. Figure 2.3 shows the position of the morphing actuators inside the wing box and the position of the morphing wing tip on the real aircraft wing. The morphing skin was designed by the structures team at ETS. The wind tunnel testing was carried out in the IAR-NRC wind tunnel in Ottawa.

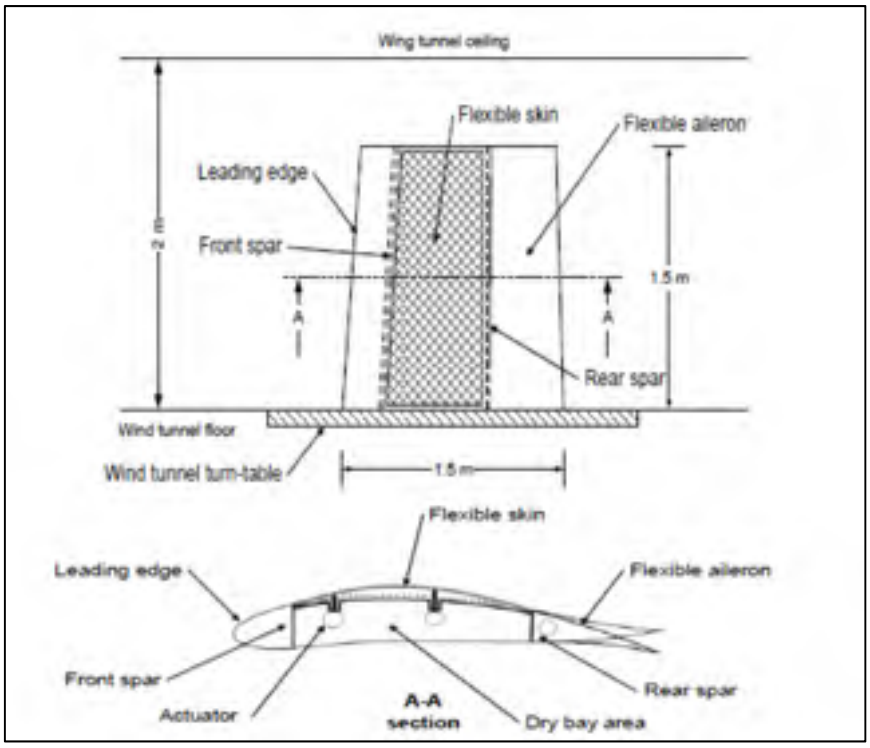

Figure 2.2 Features of the morphing wing demonstrator

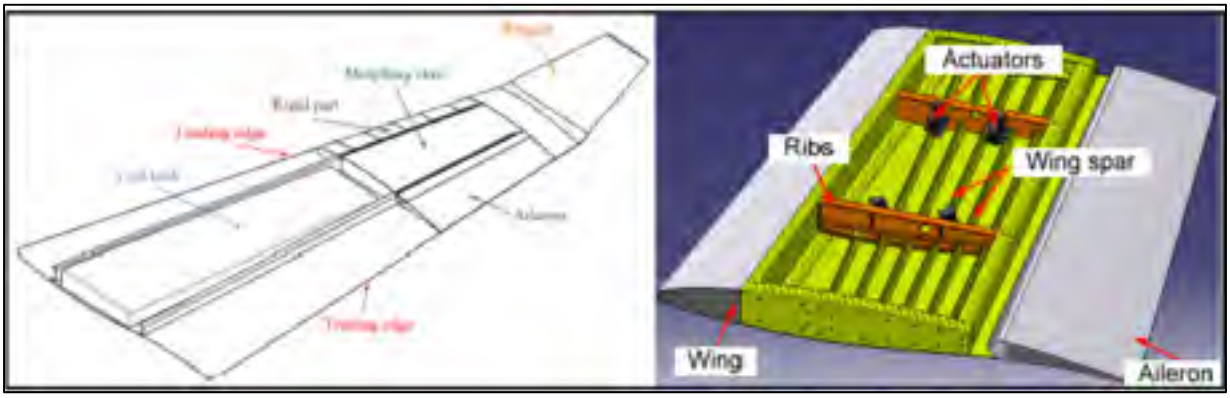

Figure 2.3 Position of the morphing wing tip on the real wing (left) and inside view of the wing box (right hand side)

Figure 2.4 shows the mounting of the actuator on the actuation line and its linkage to the flexible skin.

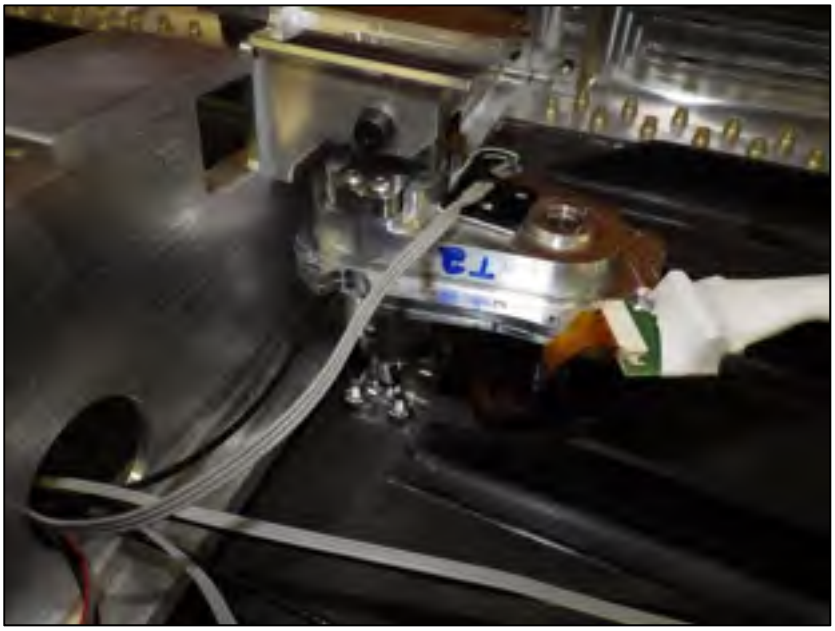

Figure 2.4 Mounting of the actuator inside the wing box

2.3 Features of the IAR-NRC wind tunnel testing facility in Ottawa

The IAR-NRC wind tunnel is used for subsonic aeronautical and industrial testing. It is used by commercial organizations, governments and universities for research and development in the field of aircraft aerodynamics, surface level aerodynamics, wind engineering and wind energy generation. The maximum speed of the IAR-NRC wind tunnel is 130 m/s. The dimensions of the test section are 1.9m×2.7m×5.2m (width×height×length).

2.4 Research Objectives

The global research objective of the CRIAQ MDO 505 project was to improve the laminar flows over a flexible wing skin. Laminar flows are improved by moving the laminar-to-turbulent transition point towards the trailing edge of a wing. The transition location is altered by morphing the upper flexible skin. Novel BLDC motor based morphing actuators were embedded under the wing's flexible skin. The research objectives within in the CRIAQ MDO 505 project for this thesis are:

- Obtain the linear model of the novel morphing actuator based on the transfer function;
- Design of an actuator nonlinear model;
- Design of an actuator control using classical control methods;
- Design of an actuator control using neural networks and fuzzy logic; and
- Design an actuator controller using a heuristic optimization technique.
- Validation of the designed controller using bench testing and wind tunnel testing

2.5 Research approach and thesis organization

This thesis focuses on the research work done during the international CRIAQ MDO 505 project to develop a morphing wing for a commercial passenger aircraft. This research focuses

on three core disciplines interactions: structural, aerodynamics and controls. The broad objectives of the project were:

- Determination of the best type of actuator;
- Determination of the actuation mechanism;
- Design a reliable controller for the actuator;
- System integration and calibration;
- Validation of the controller using bench testing without aeodynamic loads; and
- Experimental testing of the controller in a wind tunnel.

During the preliminary phases of the project, aerodynamic studies were performed to compute the optimized aero-structural morphing airfoils. Aero-structural studies were performed with the aim to choose the locations of actuator, this optimization was done by another team in the CRIAQ MDO 505 project, also to optimize the skin weight and ensure the structural stability, stiffness and strength of the wing. The structural optimization was carried out based on the aerodynamic results in order to design the wing and in specific the upper flexible skin of the wing. Since the initial wing setup was modified, therefore an aeroelastic analysis were carried out to perform the flutter analysis of the wing in order to make sure the structural integrity of the wing during the wind tunnel testing. In order to improve the aerodynamic performance of the wing, analysis were carried out using aerodynamic solvers to delay the transition region towards the trailing edge of the wing and hence reduce the drag coefficient.

It was decided to use BLDC motors as morphing actuators as shown in Figure 2.6, based on feasibility studies on the design constraints, such as the maximum height and the required actuator force. A Linear Variable Differential Transformer (LVDT) was attached to the actuator in order to measure its displacement.

Both linear and nonlinear models were developed for the actuators. A linear model was developed using differential equations; the transfer functions of the mechanical and electrical dynamics of the brushless DC motor-based morphing actuator, were determined, as shown in

as shown in Figure 2.5. The data sheet depicting the electrical characteristics of the brushless DC motor is presented in table 2.1. A gain was added to reflect the dynamics of the gears and the screw needed to convert the rotary motion to linear motion, which can be seen at the output of the transfer function blocks. The relation between the rotory motion and linear motion of the actuator is such that for 100 revolutions of the motor the actuator moves 1mm.

Table 2.1 Data sheet of the BLDC motor integrated in the morphing actuator

Characteristics of the BLDC Motor	
Nominal Voltage	12 volts
No load speed	4610 rpm
No load current	75.7 mA
Nominal speed	2810 rpm
Nominal Torque	25.1 mNm
Nominal Current	1 A
Stall torque	84.1 mNm
Starting Current	3.49 A
Terminal resistance	3.43 Ohm
Terminal Inductance	1.87 mH
Torque constant	24.1 mNm/A
Speed constant	397 rpm/V
Mechanical time constant	20.7 ms

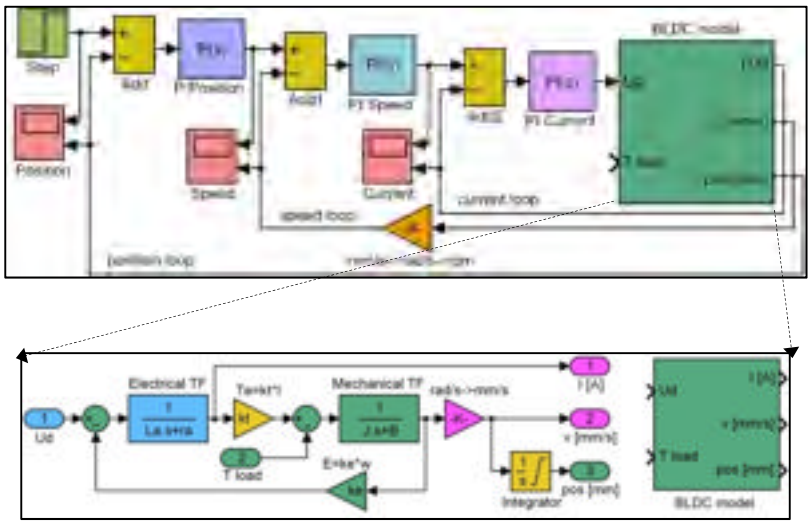

Figure 2.5 Linear model of the morphing actuator

The nonlinear model of the morphing actuator is shown in Figure 2.7. Pulse width modulation is used to control the position of the actuator.

Figure 2.6 BLDC motor-based
morphing actuator

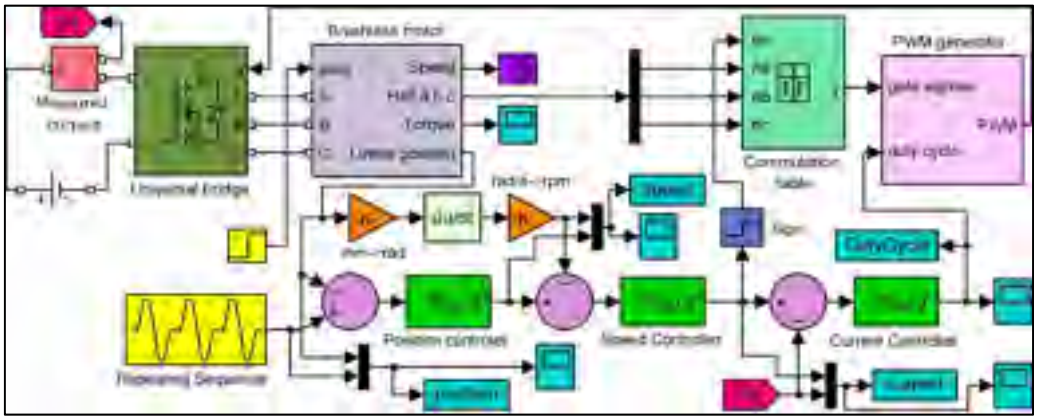

Figure 2.7 Nonlinear model of the morphing actuator

The hardware for the validation of the simulation model was acquired. Two methodologies were adopted to validate the simulation model, one used a Digital Signal Processor (DSP) and another one used NI PXI and Maxon motor control technology. DSP approach was to model the actuator in Matlab & Simulink, and then to apply both classical and intelligent actuator control techniques to design its controller. It was important to discretize the linear model at the sampling rate of the DSP. Pulse Width Modulation (PWM) was used to modulate the commutation signals. Signal conditioner was used to get feedback from the LVDT position sensor in order to close the loop with the error fed to the controller, thus the duty cycle of the

pulse-width modulated signal was used to modulate the commutation signals. The LDX 3A signal conditioner was calibrated to convert the AC voltage from the LVDT to DC voltage in order to perform analog to digital (A/D) conversion. Speed control of the BLDC motor could be performed by varying the duty cycle manually in Simulink, while the Simulink model was designed and loaded into the DSP.

Another approach consists in using the national instruments (NI) PXI technology in combination with a real time PXI 8135 controller. This loop is closed by the Signal Conditioning and Instrumentation Unit (SCXI) by taking feedback from the LVDT position sensors mounted on each actuator. Maxon motor drives are used for the actuators.

Bench testing of the actuators revealed that the displacements read on the LVDT sensors and the upper flexible skin are not same as the set points, as shown in Figure 2.8.

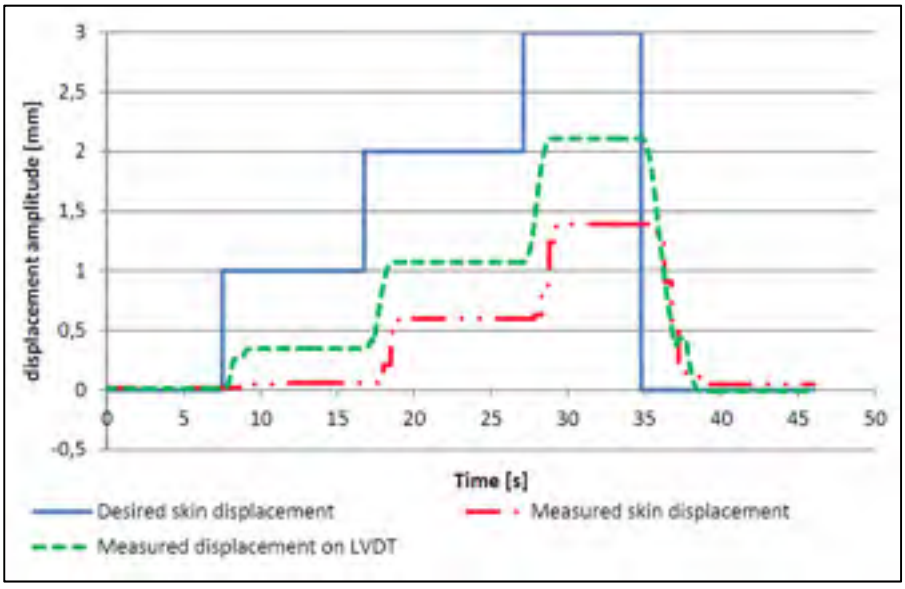

Figure 2.8 Morphing skin displacement
(Master thesis, Guzguez Sadok, 2016)

The reason for the difference between the measured skin displacement was the backlash between the gears which couple the motor with the screw. This situation led the actuator control research team to model the morphing actuator and investigate various ways to develop precise actuator control methods, and to minimize as much as possible the differences between the setpoint and skin displacement.

2.6 Contributions

The originality of this thesis lies in the following main contributions consisting of three journal articles.

- Mathematical modelling using three phase circuit analysis of the actuator model using the differential equations consisting of motor's phase winding resistance and inductance.

- Development of the transfer function of the actuator electrical and mechanical dynamics using the differential equations of its model.

- A three loop cascade design consisting of “position”, “speed” and “current control” loop to perform actuator control using the linear actuator plant dynamics.

- Modeling Mechanism converting the rotary motion into linear motion.

- A three loop cascade non-linear model consisting of non-linear blocks such as Insulated Gate Bipolar Junction Transistor (IGBT), three phase star connected motor windings, Hall sensor block, and Pulse Width Modulation (PWM) to perform actuator control.

- Actuator controller design using the Internal Model Control (IMC) methodology.

- Bench testing of the actuator controller by programming the gains into the EPOS Maxon motor drives.

- Successful performance of the actuator controller with insignificant time delay, while taking into account the duration of the flight.

- With zero steady state error the controller meets the requirement of reproducibility of the morphed wing shapes.

- Locating the laminar to turbulent transition point on the whole wing using Infra Red thermography (IR).

- Post-processing of the kulite sensor data using STandard deviation (STD) analysis of the pressure data obtained from the kulite channels.

- Post-processing of the kulite sensor data using Fast Fourier Transform (FFT) analysis of the pressure data obtained from the kulite channels.

- Infra Red (IR) thermography revealed that the morphing produced an extension of the laminar region over the whole wing upper surface with a mean value of about 2.46% of the chord.

- The average improvement in the laminar to turbulent transition based on all three methods was found to be 2.5% of the wing chord.

- Interfacing the Particle Swarm Optimization (PSO) with the actuator model in Matlab Simulink.

- Computation of the controller parameters at the levels of “position”, “speed” and “current” control of the morphing actuator using the PSO algorithm.

- Parametric analysis of the PSO algorithm.

- The best results were obtained for a swarm size of 20 “birds”, with a number of 50 “bird steps”, and with c_1=1, c_2=1.2 and w=0.9.

- Successful actuator performance with an insignificant delay and zero steady state error.

- Design of the sugeno fuzzy model proposed by Takagi, Sugeno and Kang for “position”, “speed” and “current control” of the morphing actuator.

- The designed controller was tested with repeated steps switching between positive and negative morphing skin displacement. The results revealed the successful operation of the designed controller.

- Average improvement at 2.5% of the chord in the laminar to turbulent transition point over the wing.

2.7 Summary of chapter 1

Chapter 1 provides introduction and literature review of the state-of-the-art of morphing wing technology. This chapter includes the way in which morphing wing technology has evolved, the types of materials used for actuation and the control techniques.

2.8 Summary of chapter 2

Chapter 2 provides the importance and background of the project. Brief details about the characteristics of the morphing wing and the novel BLDC motor based actuator are presented. It also describes the global objectives of the project and specific objectives of this thesis and finally the research approach adapted to achieve these objectives.

2.9 Summary of chapter 3

Design and experimental testing of a control system for a morphing wing model actuated by miniature BLDC motors

Teodor Lucian GRIGORIE[a, b], Shehryar KHAN[a], Ruxandra Mihaela BOTEZ[a,*],
Mahmoud MAMOU[c], Youssef MÉBARKI[c]

[a] *ETS, Laboratory of Active Controls, Avionics and AeroServoElasticity LARCASE, Montreal H3C-1K3, Quebec, Canada*
[b] *Military Technical Academy "Ferdinand I", Bucharest 040531, Romania,*
[c] *Aerodynamics Laboratory, NRC Aerospace, National Research Council Canada, Ottawa K1A0R6, Ontario, Canada*

This paper was published in the Chinese journal of aeronautics and it presents linear and nonlinear modelling of the novel morphing actuator and a position controller design for this morphing actuator using a classical control technique known as an internal model

control(IMC). Four different actuators were placed on two actuation lines chord wise. Differential equations representing the dynamics of the electrical and mechanical systems of the actuator were presented. The transfer function of the respective electrical and mechanical dynamics was derived. A linear actuator control model consisting of three loops was designed. The three loops being current, speed and position control. Moreover the nonlinear model of the actuator was designed. Internal model control (IMC) was applied for computation of Proportional and integral gains for the actuator control using the transfer function of electrical and mechanical dynamics of the linear actuator model. The gains obtained from the linear model were tested on the nonlinear model which is based on PWM and hall sensor signals. The simulation results revealed the satisfactory performance of the designed controller. The PI gains tested in simulations were validated based on NI-PXI technology using the bench testing facility. Finally the controller was tested in the wind tunnel and the wind tunnel results revealed an overall improvement in the laminar to turbulent transition point location. Following are the contributions of the authors

Teodor Lucian GRIGORIE

- Proposed the three loop cascade strategy for the controller design.
- Supervised the analysis, modelling and simulation of the linear actuator.
- Supervised the analysis, modelling and simulation of the non-linear actuator model.

Shehryar Khan

- Performed the analysis of the actuator to design a linear model.
- Designed the nonlinear model of the actuator.
- Designed the actuator control using IMC methodology.
- Performed the actuator control using bench testing.

Ruxandra Botez

- Research thesis supervisor

Mahmoud Mamou and Youssef Mébarki

- Concept of pressure data post-processing software for analysis and validation
- Wind tunnel testing and infrared thermography analysis

2.10 Summary of chapter 4

Novel morphing wing actuator control based Particle Swarm Optimization

Shehryar Khan[1], Teodor Lucian Grigorie[1,2], Ruxandra Mihaela Botez[1]
Mahmoud Mamou[3], Yousef Mébarki[3]

This chapter explains the controller design for a novel morphing actuator using huristic approach known as Particle Swarm Optimization (PSO). Recently, PSO algorithm has become famous in the family of evolutionary algorithms due to its simplicity and superior performance in solving non-convex problems. Contribution of this chapter is to present the application of the particle swarm optimization to design a controller for this new morphing actuator.

For the MDO 505 actuator we had five parameters to compute: proportional parameter for the position loop, and proportional and integral parameter for the speed loop and the current loop. For a swarm size of twenty, there are twenty particles, each particle containing 5 parameters. The algorithm works in such a way that from one iteration to another, each particle moves from one position to another position with a velocity and their positions being initialized in the search space defined using the limits of the desired parameters. If for a particular iteration or bird step the value of the cost function is minimized the new values are retained and the old are discarded for that specific particle in the swarm, this new value is known as particles best. Finally after evaluation of the whole swarm based on the cost function, the global best particle is choosen among the whole swarm. This information about the particle best position and the global best particle in the whole swarm is used to compute the velocity for each particle to move to a new position in the search space. Although PSO algorithm does not gaurentee

convergence, neverthless its application to the problem by varying the initialization of the particle positions, often results in obtaining the required results. The designed controller was tested in the wind tunnel and the results revealed the controller could successfully perform morphing wing actuation. Finally the infra-red and kulite sensor data revealed an improvement in the laminar to turbulent transition location on the morphing wing. Following were the contributions of the authors.

Shehryar Khan

- Analysis, modelling and simulation of the morphing actuator.
- Application of PSO algorithm for the design of actuator control in Matlab.
- Parametric analysis of the PSO algorithm.
- Post processing of the wind tunnel data.

Teodor Lucian Grigorie

- Recommendation for the parameteric analysis of the PSO algorithm.
- Recommendation on overall improvement of the paper.

Ruxandra Botez

- Research thesis supervisor

Mahmoud Mamou, Yousef Mébarki

- Concept of pressure data post-processing software for analysis and validation.
- Wind tunnel testing and infrared thermography analysis.

2.11 Summary of chapter 5

Fuzzy logic based control for a morphing wing-tip actuation system: design, numerical simulation and wind tunnel experimental testing

Shehryar Khan [1], Teodor Lucian Grigorie [1, 2, *], Ruxandra Mihaela Botez [1], Mahmoud Mamou [3] and Youssef Mébarki [3]

École de Technologie Supérieure, Laboratory of Active Controls, Avionics and AeroServoElasticity LARCASE, Montreal H3C-1K3, Quebec, Canada; sherykhann@yahoo.com, Ruxandra.Botez@etsmtl.ca

[2] Military Technical Academy "Ferdinand I", Faculty of Aircraft and Military Vehicles, Center of Excellence in Self-Propelled Systems and Technologies for Defense and Security, Bucharest 040531, Romania; ltgrigorie@yahoo.com

[3] Aerodynamics Laboratory, NRC Aerospace, National Research Council Canada, Ottawa K1A0R6, Ontario, Canada; Mahmoud.Mamou@nrc-cnrc.gc.ca, Youssef.Mebarki@nrc-cnrc.gc.ca

* Correspondence: ltgrigorie@yahoo.com

This chapter presents the application of the fuzzy logic controller design of the new morphing actuator. The BLDC motor and associated gearing mechanism along with its interaction with the morphing skin makes it a complex nonlinear system. Therefore, it was decided to design a fuzzy controller to design a controller for such a nonlinear system. In order to perform BLDC motor control, current control needs to be designed so that an appropriate amount of current flows inside the motor coils, and the required torque is generated to push or pull the morphing skin. "Speed control" is required to control how fast or slow the actuator can act. "Position control" is required to control the position of the actuator. The inputs in every loop are mapped to the input membership function known as the "antecedents", "antecedents" are used to design

"consequents" based on if-then principle. For a certain input the membership grades of the output are aggregated and the output is computed which is known as a crisp value. Finally, after analysis of the actuator model fuzzy proportional derivative (PD) controller was designed for the position control, proportional integral derivative (PID) control was designed for the speed control and a proportional integral (PI) controller for the current control was designed.

Simulation results revealed the successful operation of the designed fuzzy logic controller. Finally, this controller was tested in the wind tunnel. Both the quality sensor data and Infra red results confirmed that the designed controller was successfully able to actuate the morphing wing. Finally the wind tunnel results revealed an improvement in the laminar flows over the morphing, wing. The contributions of the authors are the following:

Shehryar Khan and Teodor Lucian Grigorie

- Control design, implementation and testing.
- Software development, control validation.
- Writing-original draft preparation.

Ruxandra Mihaela Botez

- Research project concept, aerodynamic optimization and funding acquisition.
- Supervision, project administration, writing-review and editing.

Mahmoud Mamou and Youssef Mébarki

- Concept of pressure data post-processing software for analysis and validation.
- Wind tunnel testing and infrared thermography analysis.

CHAPTER 3 FIRST ARTICLE

Design and experimental testing of a control system for a morphing wing model actuated with miniature BLDC motors

Teodor Lucian GRIGORIE[a, b], Shehryar KHAN[a], Ruxandra Mihaela BOTEZ[a,*], Mahmoud MAMOU[c], Youssef MÉBARKI[c]

[a] *ETS, Laboratory of Active Controls, Avionics and AeroServoElasticity LARCASE, Montreal H3C-1K3, Quebec, Canada*
[b] *Military Technical Academy "Ferdinand I", Bucharest 040531, Romania,*
[c] *Aerodynamics Laboratory, NRC Aerospace, National Research Council Canada, Ottawa K1A0R6, Ontario, Canada*

Proof of Publication :

Paper was accepted in "Chinese Journal of Aeronautics", 2019.

RÉSUMÉ

L'article traite de la conception et de la validation expérimentale d'un système de commande du mécanisme d'actionnement d'un modèle d'aile déformable. Le modèle expérimental d'aile déformable fabriqué dans le cadre de ce projet se torque à l'échelle d'une véritable aile d'avion. L'actionnement de la déformation du modèle est basé sur un mécanisme avec quatre actionneurs similaires conçus et fabriqués en interne, positionnés à l'intérieur de l'aile sur deux lignes parallèles. Chacun des quatre actionneurs utilise un moteur électrique à courant continu sans balais (BLDC) intégré à une partie mécanique effectuant la conversion des déplacements angulaires en déplacements linéaires. Les étapes suivantes ont été choisies comme étapes successives dans la conception du système de commande de l'actionneur : (A) Modélisation mathématique et logicielle de l'actionneur ; (B) Conception de l'architecture système de commande à l'aide de la méthodologie de contrôle du modèle interne ; (C) Simulation numérique de l'actionneur contrôlé, essais sur banc et en soufflerie. Le modèle expérimental d'aile déformable est testé en laboratoire, dans l'absence de d'air, pour évaluer l'intégration des

composants et le fonctionnement de l'ensemble du système, mais aussi en soufflerie, en présence de l' air, pour évaluer son comportement et le gain aérodynamique.

Abstract

The paper deals with the design and experimental validation of the actuation mechanism control system for a morphing wing model. The experimental morphable wing model manufactured in this project is a full-size scale wing tip for a real aircraft equipped with an aileron. The morphing actuation of the model is based on a mechanism with four similar in house designed and manufactured actuators, positioned inside the wing on two parallel lines. Each of the four actuators used a BrushLess Direct Current (BLDC) electric motor integrated with a mechanical part performing the conversion of the angular displacements into linear displacements. The following have been chosen as successive steps in the design of the actuator control system: (A) Mathematical and software modelling of the actuator; (B) Design of the control system architecture and tuning using Internal Model Control methodology; (C) Numerical simulation of the controlled actuator and its testing on bench and wind tunnel. The morphing wing experimental model is tested both at the laboratory level, with no airflow, to evaluate the components integration and the whole system functioning, but also in the wind tunnel, in the presence of airflow, to evaluate its behavior and the aerodynamic gain.

Keywords: Morphing wing; BLDC Motor; Control Tuning; Simulation and Experimental Testing; Wind Tunnel.

3.1 Introduction

One of the main priorities of each scientific field is the optimization, as long as it generates costs savings. From the aerospace industry perspective, efforts are focused on optimizing the various flight-related procedures, which deliver immediate positive effects on allocated financial resources and on the development of green technologies. This aerospace engineering trend has been sustained over time by governments and industry, by initiating and sustaining research programs and projects carried out in collaboration with research centers and

universities.

From the point of view of green aircraft technologies development, our research team from École de Technologie Supérieure (ÉTS) in Montréal, Canada, our Research Laboratory in Active Controls, Avionics and AeroServoElasticity (LARCASE) acted in the next main research directions: (A) development and numerical testing of various algorithms for flying vehicles trajectory optimization(Gagne J, Mendoza A-M et al, 2013); (B) design and validation of different optimal methods for flying vehicles high robustness model identification with the aim to reduce the flight tests number (Mota S, Botez RM, 2009); (C) design, numerical simulation and experimental testing, including wind tunnel testing, of various experimental models based morphing wing technologies (Labib M, Popov A et al, 2008).

Based on the multitude of research studies, projects and programs developed in the last two decades, it seems that for the next generations of aircrafts the morphing wing technology will be a serious alternative to the rigid control surfaces used currently. Actually, this technology added value in the aerospace field is given by the possibility to improve the aircraft performance by changing various characteristics and match the aircraft state with the requirements of the developed mission. The benefits are related to the flutter and vibration mitigation, drag reduction, fuel costs saving, emissions reduction, flight envelope expansion and improvements in aircraft range.

On the other way, the disseminated results from the worldwide research activities related to this technology proven its huge potential and feasibility. For example, the researchers from the Kentucky University in USA investigated the flow control using shape adaptive surfaces. A piezoceramic actuator bonded with a metallic substrate under the form of a circular arc has been used as adaptive airfoil. The actuator was powered by a bi-polar operational power supply, and tested in a subsonic wind tunnel. The designed architecture proved a good balance between the developed force and the obtained deflection (Pern NJ, Jacob JD, 1999). Few years later, at the same university a morphing study has been conducted to control the airflow in a

mechanism based on the use of some oscillating adaptive surfaces. The study has been realized both by using the numerical simulation, but also by using a modular experimental adaptive wing model, equipped with piezoelectric actuators. The actuation system architecture has been chosen in order to realize a fast actuation and to limit in this way the generation of laminar separation bubbles (Munday D, Jacob J, 2002).

Another morphing wing experimental model was also developed at University of Bristol, UK, in collaboration with specialists from the University of Limerick, Ireland. The change the wing camber the team used a composite Fish Bone Active Camber (FishBAC) device, equipped with an elastomeric skin and actuated through an antagonistic tendon mechanism. The wind tunnel experimental tests shown an important improvement of the lift coefficient by using this architecture (Rivero AE, Fournier S, 2018).

In a collaborative research project between the University of Tokyo and Japan Aerospace Exploration Agency a morphing wing was manufactured and wind tunnel tested based on the use of corrugated structures. The experimental tests suggested that the developed morphable structure exhibited superior properties in lift coefficients (Yokozeki T, Sugiura A, 2014). Over the last fifteen years the German Aerospace Center (DLR) developed lot of research projects related to the morphing aircraft technologies, financed both from the national resources, but also by using the European Union research funds. In a recent project, the researchers performed the 3D structural design of a large-displacement flexible leading edge (droop nose) equipping a morphable wing for a transport aircraft (Vasista S, Nolte F, 2018).

The research activity in the morphing aircraft domain is at peak this moment, having in mind that there are still several challenges related to high power requirement for actuation systems, and solutions necessary for dissipation of the heat generated by the actuators, but also reduction in the weights and large response times. As a direct consequence of this idea, but also correlated with the actual trend related to the “all-electric aircraft” concept associated to the green aviation, the “mechatronics” started to be more and more implied in the aerospace engineering field.

A special place has been reserved by the specialists to the development of electric actuation systems for aircraft, technological direction sustained also through various research projects. As an example, the More Open Electrical Technologies - MOET can be mentioned [30]. MOET has been financed in the 6th European RTD Framework Programme with the main aim to produce a new standard to be used by industry in the design of the electrical systems for the commercial aircraft. As main actuation solutions for aircraft during a lot of time, the actuators based on hydraulic and pneumatic forces started to be replaced with electrical actuators, lightweight and more efficient, especially when they are used to actuate the landing gear or the flight control surfaces (Jänker P, Claeyssen F et al, 2008).

3.2 Research project background

In this context, new research on morphing wing technologies was carried out by our team in a major research project ("Multi-Disciplinary Optimization 505" (MDO 505)), which targeted to obtain a fuel consumption economy by using these technologies in a real aircraft wing equipped with an aileron, and morphed by using an actuation mechanism with BLDC electric motors. This project, conducted at ÉTS in Montréal, was developed in an international research consortium, involving industrial partners such as Bombardier Aerospace and Thales from Canada, and Alenia from Italy, and universities and research institutes as ÉTS, École Polytechnique de Montréal and the National Research Council of Canada (IAR-NRC) from Canada, and Frederico II Naples University and CIRA from Italy. Within the context of this project, some new numerical studies related to the behavior of the airflow over the morphable wing and aileron were conducted (Koreanschi A, Sugar Gabor, 2014). In addition, a design approach for the aileron position controller was proposed and tested (Vincent J-B, Botez RM, 2015), followed by the design, numerical simulation and evaluation of various position controllers for the actuators equipping the morphable wing (Tchatchueng Kammegne MJ, Khan Set al, 2015).

The experimental model manufactured in this project is a full-size scale wing tip for a real

aircraft, which includes an aileron, as is presented in Figure 3.1. The obtained model had the structure and the stiffness like the wing of the real aircraft. To morph the model, its upper surface was chosen to a flexible one, manufactured by using some composite materials. Its actuation is performed by using a system integrating four similar electric actuators, disposed on two lines, which were placed at 32% (Act. #1 and Act. #3) and 48% (Act. #2 and Act. #4) from chord, respectively (see Figure 3.2). The structure of each actuator includes a BLDC motor and a mechanism which converts rotation movement into linear movement. Due to limited space and the high actuation force requirements imposed by our application, the actuators were manufactured in house using miniature BLDC motors acquired from the Maxon Motor Company.

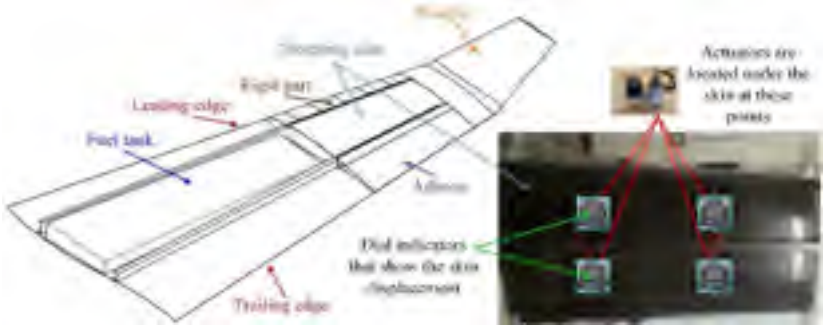

Figure 3.1General architecture of MDO 505
experimental model.

Figure 3.2 Actuation system of
morphing wing.

To monitor the airflow over the wing upper surface, 32 high precision Kulite pressure sensors

were installed on the flexible skin. They were disposed in equal number on two staggered lines positioned at 0.600 m and at 0.625 m from the wing root section.

The obtained pressure data were real time processed in order to provide information related to the laminar-to-turbulent transition location; the Fast Fourier Transforms (FFT) of the acquired pressure data have been conducted in the real time. As an additional method to evaluate the laminar-to-turbulent transition location, the Infra-Red (IR) thermography was used.

In the first phase of the project, a preliminary aerodynamic study was conducted by modifying the original (reference) airfoil for various flight conditions. This allowed for calculation of certain optimized airfoils corresponding to various airflow conditions considered as combinations of incidence angles (α), Mach numbers and aileron deflection angles (δ). This resulted in four morphing actuator displacements (dY_{1opt}, dY_{2opt}, dY_{3opt}, dY_{4opt}) for each optimized airfoil, characterizing the changes from the original (reference) airfoil and corresponding to the positions of the four actuators. All of these displacements were stored in a database to be used for the control system as reference actuation distances necessary to obtain the optimized airfoils. Therefore, the morphing shape control is realized by controlling the positions of the actuators until the real displacements (dY_{1real}, dY_{2real}, dY_{3real}, dY_{4real}) of the morphing skin in the four actuation points equal the desired actuation distances necessary to obtain the optimized airfoil (dY_{1opt}, dY_{2opt}, dY_{3opt}, dY_{4opt}) associated with a flight condition. All of the actuators used the same type of BLDC motor, and therefore, the same designed controller is used for all four actuators included in the actuation mechanism.

The results shown in the present paper characterize a part of this second major morphing wing research project (MDO 505) developed by our team, exposing the design and the validation of one of the developed variants for the control system of the morphing actuators integrated in the wing; as design methodology for the control system the Internal Model Control procedure has been adopted (Khan S, Botez RM et al, 2015). The rest of the paper is organized as follows: Section 2 presents the mathematical and software modelling of the used actuators; Section 3

exposes the tuning of the control loops by using the Internal Model Control (IMC) technique, while Sections 4 and 5 are reserved to the bench testing of the morphing wing control system, respectively to the evaluation of the morphing wing experimental model through wind tunnel testing.

Some parts from the mathematical model, which are also shown in this paper, describing the first steps in the development of our morphing wing project, have already been presented in few conference papers(Tchatchueng Kammegne MJ, Khan S et al, 2015) . In this study results reflect the behavior of the experimental morphing wing system as a whole, with numerical simulations, bench testing and wind tunnel testing.

3.3 Mathematical and software modelling of actuator

Figure 3.3 exposes the actuator physical model, which includes a BLDC motor and a mechanism which converts the angular movement into linear movement. This mechanism allows the four morphing actuators used in our application to deform, through direct actuation, the flexible skin on the wing upper surface.

In order to design a control system for the actuators which morph the wing, their preliminary mathematical and software modelling is required. The model includes two different parts: (A) the BLDC motor model and (B) the model of the conversion mechanism from angular actuation to linear actuation, linked to the BLDC motor output.

The general objective in the mathematical modelling is to identify a linear model for the actuator under the form of a transfer function (plant model), which can be used in the design phase of the actuator control system. On the other way, the model is further used in a software subroutine to analyze the controlled actuator performance. Having in mind the multitude of the possibilities to drive the actuator included motor, to derive this linear model and its associated transfer function a full bridge drive was considered for the BLDC motor, which operates in the two-phase conduction mode.

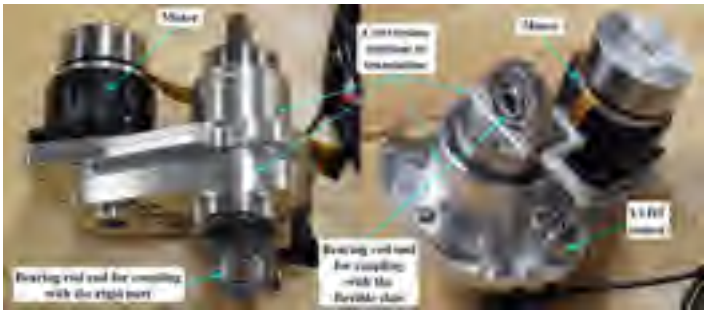

Figure 3.3 Actuator physical model.

From Figure 3.4(a) (Tchatchueng Kammegne MJ, Khan S et al, 2015), the equivalent electrical circuit of a BLDC motor is described as:

$$i_A + i_B + i_C = 0, \tag{3.1}$$

$$\begin{aligned} u_A &= Ri_A + (L-M)\frac{di_A}{dt} + e_A, \\ u_B &= Ri_B + (L-M)\frac{di_B}{dt} + e_B, \\ u_C &= Ri_C + (L-M)\frac{di_C}{dt} + e_C. \end{aligned} \tag{3.2}$$

where L is phase winding inductance; R is resistance of the phase; M is mutual inductance; i_A, i_B, i_C are electrical currents in the motor phases; u_A, u_B, u_C are voltages in the motor phases; e_A, e_B, e_C are back ElectroMagnetic Forces (EMF) generated in the motor phases (Xia CL., 2012).

In majority of situations, the windings of the stator are star-connected, and the neutral point is not brought out to an external physical connection, it is hard to measure the phase voltages. As a consequence, it is recommended to use model based on line voltages, having in mind that their measurement is easiest to be done in this configuration (Khan S, Botez RM, Grigorie, TL et al 2015). In this situation, the line voltages resulting from Eq. (3.2) are as follows:

$$
\begin{aligned}
u_{AB} &= u_A - u_B = \\
&= R(i_A - i_B) + (L-M)\left(\frac{\mathrm{d}i_A}{\mathrm{d}t} - \frac{\mathrm{d}i_B}{\mathrm{d}t}\right) + (e_A - e_B), \\
u_{BC} &= u_B - u_C = \\
&= R(i_B - i_C) + (L-M)\left(\frac{\mathrm{d}i_B}{\mathrm{d}t} - \frac{\mathrm{d}i_C}{\mathrm{d}t}\right) + (e_B - e_C), \\
u_{CA} &= u_C - u_A = \\
&= R(i_C - i_A) + (L-M)\left(\frac{\mathrm{d}i_C}{\mathrm{d}t} - \frac{\mathrm{d}i_A}{\mathrm{d}t}\right) + (e_C - e_A).
\end{aligned}
\tag{3.3}
$$

If the phases *A* and *B* are conducted and phase *C* is suspended (two-phase conduction mode), the simplified model in Figure 3.4 (b) is obtained. Therefore, the relationships between the phase currents i_A and i_B is:

$$
i_A = -i_B = i, \tag{3.4}
$$

which also means that:

$$
\frac{\mathrm{d}i_A}{\mathrm{d}t} = -\frac{\mathrm{d}i_B}{\mathrm{d}t} = \frac{\mathrm{d}i}{\mathrm{d}t}. \tag{3.5}
$$

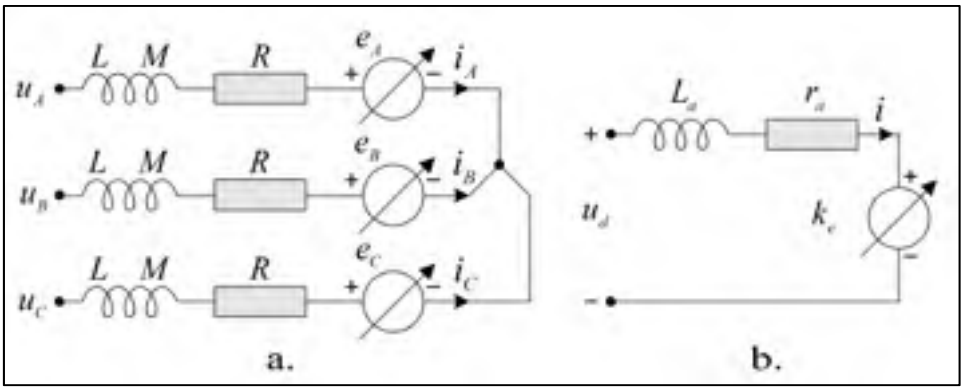

Figure 3.4 a) Equivalent electrical circuit of a BLDC motor;

b) Equivalent circuit in two-phase conduction mode

The line voltage u_{AB} from Eq. (3.3) becomes:

$$u_{AB} = 2Ri + 2(L-M)\frac{di}{dt} + (e_A - e_B). \quad (3.6)$$

Because the e_A and e_B amplitudes are the same and the signs are opposite, Eq. (3.6) becomes:

$$u_{AB} = 2Ri + 2(L-M)\frac{di}{dt} + 2e_A. \quad (3.7)$$

Therefore,

$$u_{AB} = u_d = r_a i + L_a \frac{di}{dt} + 2e_A = r_a i + L_a \frac{di}{dt} + k_e w. \quad (3.8)$$

u_{AB} is the line voltage; u_d is DC bus voltage; r_a is winding line resistance (r_a=2R); L_a is winding inductance (L_a=2(L–M)); k_e is line back EMF coefficient ($2e_A$=$k_e w$); w is motor speed of rotation.

The equation characterizing the dynamics of the motor is given by the next expression [42, 43]:

$$J\frac{dw}{dt} + Bw = T_e - T_l, \quad (3.9)$$

where J characterizes the rotor inertia, B is equivalent viscous friction coefficient, T_e is electromagnetic torque and T_l is load torque. Denoting the torque constant of the motor as k_t results in a simplified formula for the electromagnetic torque as a function of phase current i, for the two-phase conduction mode, as follows:

$$T_e = k_t i. \quad (3.10)$$

From Eqs. (9)-(10) we get:

$$i = \frac{T_e}{k_t} = \frac{J}{k_t} \cdot \frac{dw}{dt} + \frac{B}{k_t} \cdot w + \frac{1}{k_t} \cdot T_l, \quad (3.11)$$

which, substituted in Eq. (8), leads to:

$$u_{\mathrm{d}} = r_{\mathrm{a}}\left(\frac{J}{k_{\mathrm{t}}}\frac{\mathrm{d}w}{\mathrm{d}t} + \frac{B}{k_{\mathrm{t}}}w + \frac{T_{\mathrm{l}}}{k_{\mathrm{t}}}\right) + \\ + L_{\mathrm{a}}\frac{\mathrm{d}}{\mathrm{d}t}\left(\frac{J}{k_{\mathrm{t}}}\frac{\mathrm{d}w}{\mathrm{d}t} + \frac{B}{k_{\mathrm{t}}}w + \frac{T_{\mathrm{l}}}{k_{\mathrm{t}}}\right) + k_{\mathrm{e}}w. \tag{3.12}$$

As a consequence,

$$u_{\mathrm{d}} = \frac{L_{\mathrm{a}}J}{k_{\mathrm{t}}}\frac{\mathrm{d}^2w}{\mathrm{d}t^2} + \frac{r_{\mathrm{a}}J + L_{\mathrm{a}}B}{k_{\mathrm{t}}}\frac{\mathrm{d}w}{\mathrm{d}t} + \frac{r_{\mathrm{a}}B + k_{\mathrm{e}}k_{\mathrm{t}}}{k_{\mathrm{t}}}w + \\ + \frac{L_{\mathrm{a}}}{k_{\mathrm{t}}}\frac{\mathrm{d}T_{\mathrm{l}}}{\mathrm{d}t} + \frac{r_{\mathrm{a}}}{k_{\mathrm{t}}}T_{\mathrm{l}}. \tag{3.13}$$

With the Laplace transform, Eq. (13) implies:

$$U_{\mathrm{d}}(s) = \left(\frac{L_{\mathrm{a}}J}{k_{\mathrm{t}}}s^2 + \frac{r_{\mathrm{a}}J + L_{\mathrm{a}}B}{k_{\mathrm{t}}}s + \frac{r_{\mathrm{a}}B + k_{\mathrm{e}}k_{\mathrm{t}}}{k_{\mathrm{t}}}\right)\Omega(s) + \\ + \left(\frac{L_{\mathrm{a}}}{k_{\mathrm{t}}}s + \frac{r_{\mathrm{a}}}{k_{\mathrm{t}}}\right)T_{\mathrm{l}}(s), \tag{3.14}$$

where $\Omega(s)=\mathscr{L}\{w(t)\}$, $U_{\mathrm{d}}(s)=\mathscr{L}\{u_{\mathrm{d}}(t)\}$, and $T_{\mathrm{l}}(s)= =\mathscr{L}\{T_{\mathrm{l}}(t)\}$. In another form, Eq. (14) is:

$$\Omega(s) = \frac{k_{\mathrm{t}}}{(L_{\mathrm{a}}s + r_{\mathrm{a}})(Js + B) + k_{\mathrm{e}}k_{\mathrm{t}}}U_{\mathrm{d}}(s) - \\ - \frac{L_{\mathrm{a}}s + r_{\mathrm{a}}}{(L_{\mathrm{a}}s + r_{\mathrm{a}})(Js + B) + k_{\mathrm{e}}k_{\mathrm{t}}}T_{\mathrm{l}}(s). \tag{3.15}$$

which highlights the dependence between the motor speed and the two main variables which influence it: the DC voltage u_{d} and the load torque T_{l}. It can be easily observed that, for a fixed load, the increase of the u_{d} voltage produces the increase of the motor speed, while, for a fixed input voltage, the increase of the T_{l} load torque produces the decrease of the speed.

On the other way, Eq. (8) to Eq. (11) lead to:

$$I(s) = \frac{1}{L_{\mathrm{a}}s + r_{\mathrm{a}}}\left[U_{\mathrm{d}}(s) - k_{\mathrm{e}}\Omega(s)\right], \tag{3.16}$$

$$T_{\mathrm{e}}(s) = k_{\mathrm{t}} \cdot I(s), \tag{3.17}$$

and

$$\Omega(s) = \frac{1}{Js + B}\left[T_{\mathrm{e}}(s) - T_{\mathrm{l}}(s)\right], \tag{3.18}$$

conducting to the following block scheme with transfer functions of the modeled motor (see Figure 3.5(Khan S, Botez RM, Grigorie, TL, 2015), which considers the motor loaded with T_l.

To analyze the behavior of the motor integrated in the morphing actuator, a Matlab/Simulink software model was developed as in Figure 3.6 (“BLDC model”); it implements both mechanical and electrical mathematical models of the BLDC motor, but also the model of the conversion mechanism from angular actuation to linear actuation. It has as inputs the DC bus voltage “Ud” and the load torque “T load”, and as outputs the electrical current “I”, the actuation speed “v”, expressed in mm/s, and the actuation linear position “pos”, expressed in mm. In order to conduct numerical simulations, the “BLDC model” was integrated into the model in Figure 3.7 , which contains three control loops acting at the level of the electrical current, actuation speed and actuation position.

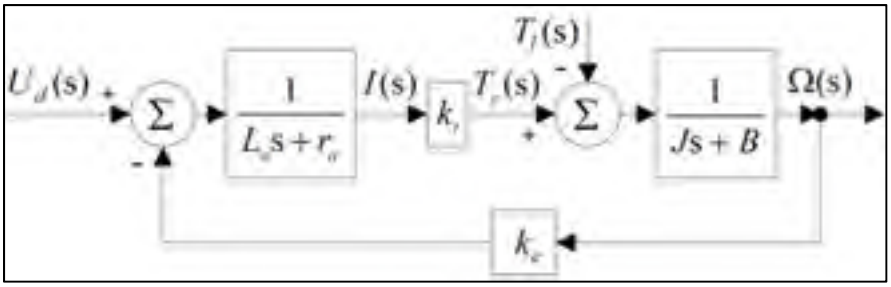

Figure 3.5 Motor block scheme

with transfer functions.

The electrical current is measured at the output of the “Electrical TF” block shown in Fig 3. 6, and is further used to provide feedback in the current control loop as it is shown in the control model presented in Figure 3.7. According to the control system model in Figure 3.7, the “BLDC model” provides also feedback signals for the speed and position control loops.

3.4 Tuning control loops using IMC technique

The literature reveals that there have been many control strategies for position control of BLDC motors over the years. PID controllers feature a number of advantages over other controllers, including simplicity of design and implementation, being widely used in many industrial applications. On the other way, the literature shows that there have been many methods for tuning the related coefficients. The best known method was proposed by Ziegler and Nichols, but as a function of the complexity of the controlled systems, various mechanisms were developed over time for tuning the PID and implementing it together with artificial intelligence methodologies. For example, researchers from Xi'an University of Technology designed and developed a new BLDC position servo system using a digital signal processor and fuzzy PID controller. The role of the fuzzy controller was to improve the robustness of the designed system.

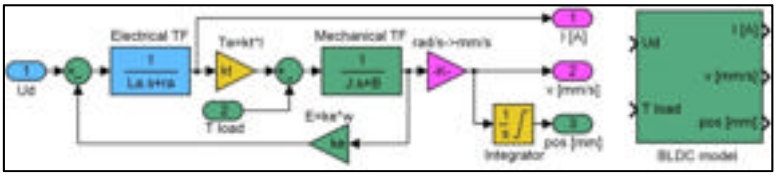

Figure 3.6 MATLAB/Simulink model of actuator.

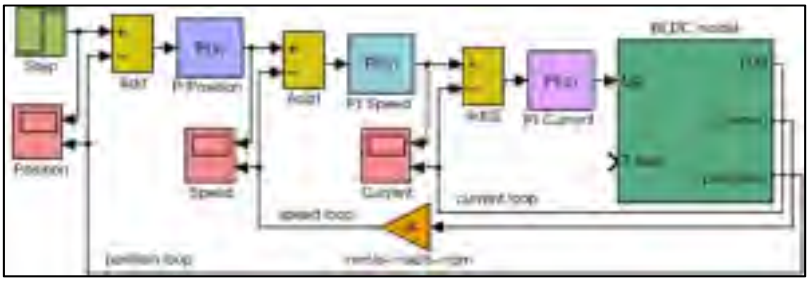

Figure 3.7 Three-loop control system for morphing actuator.

At Howard University in Washington, a smart position control system for brushless motor drives was developed, by combining the fuzzy logic techniques with the neural networks learning abilities(Rubaai A., 2003) . From another point of view, to obtain a controller with higher robustness, researchers from the National University of Singapore used the sliding-mode control method for a BLDC motor position controller (Tan Y-K, Panda S-K, 2004). In other application, developed at MSL R&D Center in Korea, a control system was designed for a missile actuator based on a BLDC motor and a DSP. The position controller was a classical PID one, while other two loops where used to control the electrical current, with PWM technique, and the speed, with an estimation algorithm with hall sensors, respectively. At the Institute of Space Technology in Pakistan, a three-phase BLDC motor was modelled and controlled using a PID controller optimized through a genetic algorithm(Ansari U, Alam S et al 2011) . The results highlighted more efficient position control for the motor using the proposed methodology instead of the traditional PID tuning method, which used the Ziegler-Nichols algorithm.

Starting from a previous study (Rivera DE, Morari M, Skogestad S, 1986) communicated in 1986, related to the tuning of PID controllers by using the Internal Model Control (IMC) method, Skogestad proposed in 2001 a new IMC tuning procedure(Skogestad S, 2001) . It provides poor disturbance response for integrating processes, but generally produces very good responses for set point changes (Postlethwaite I, Skogestad S, 2005).

The IMC methodology uses the philosophy according to that the control can be realized just if the designed controller includes a representation of the process which should be controlled. More specifically, if in the design process of the control system is taken into account the plant model, then a perfect control system may be obtained (Postlethwaite I, Skogestad S, 2005). As an example in the previous idea, it is considered that the process which needs to be controlled is $G_p(s)$, and one model for it has the form $\hat{G}_p(s)$. If the control law $G_c(s)$ is set to be equal with the inverse of the model,

$$G_c(s) = \widehat{G}_p^{-1}(s), \tag{3.19}$$

and the model equals the controlled process,

$$\widehat{G}_p(s) = G_p(s), \tag{3.20}$$

then the output will track perfectly the reference value set at input. If the plant associated transfer function $G_p(s)$ is minimum phase and invertible, meaning that it has no zeros in the right half-plane, then the controller can be written under the form $k(s) = w_c \cdot G_p^{-1}(s)/s,$ and the open loop transfer function is $k(s)G_p(s)=w_c/s$ (Postlethwaite I, Skogestad S, 2005). Therefore, the closed loop transfer function of the system has the expression $T(s)=k(s)\cdot G_p(s)/[1+k(s)G_p(s)]=w_c/(w_c+s)$, equating with an ideal first-order low-pass filter [42, 51].

Using the previous methodology, the following results were obtained successively for our BLDC motor control loops(Khan S, Botez RM, Grigorie, TL, 2015). At the first step, starting from the transfer function characterizing the electrical part of the actuator:

$$G_{Elect}(s) = \frac{1}{L_a \cdot s + r_a} = \frac{1}{0.000935 \cdot s + 1.715} \tag{3.21}$$

the expression of the control law resulted as:

$$k_{Elect}(s) = w_c \cdot \frac{G_{Elect}^{-1}(s)}{s} = 1500 \cdot \frac{0.000935 \cdot s + 1.715}{s} = \\ = \frac{1.4025}{s} + 2572.5 = K_{Ic} \cdot \frac{1}{s} + K_{Pc}. \tag{3.22}$$

The documentation associated to the controlled motor provided the next values for the parameters characterizing the motor phases: r_a=1.715 Ω for the resistance, and L_a=0.935 mH for the inductance. To obtain a suitable value for the coefficient w_c the trial and error method was applied, the very good step response being obtained for w_c=1500 . Therefore, the control law for the electrical current, as it results from Eq. (22), is a PI one, with the next gains :

$$K_{Pc} = 2572.5,\ K_{Ic} = 1.4025. \tag{3.23}$$

At the next step, the following values were obtained for the coefficients for the speed PI controller, based on the data flow in the block diagrams in Fig.3.6 and Fig 3.7 :

$$K_{Ps} = 1.3071,\ K_{Is} = 1.1203, \tag{3.24}$$

and the value of the proportional gain for the P controller used in position loop is:

$$K_{Pp} = 2. \tag{3.25}$$

According to the motor technical documentation, the used value for the torque constant was k_t=0.024 Nm/A, for the motor moment of inertia, J=3.5×10^{-6} Kg·m^2, and for viscous friction coefficient, B=3×10^{-6} N·m·s/rad.

In practice, the driving of a BLDC motor, equipped with three Hall-effect based sensors to have information related to the rotor position, is performed by using a general scheme as in Figure 3.8. The scheme includes an Insulated-Gate Bipolar Transistor (IGBT) driver and a three-phase inverter. The effective control is made by using Pulse Width Modulated (PWM) signals, which establish the average values of the driving coils voltages and currents. On the other way, based on SimPowerSystems toolbox blocks in Matlab, the Simulink model of the controlled BLDC motor can be organized as in Figure 3.9 (Keeping S, 2013).

According to the model, by using the right values for the proportional and integral gains in the electrical current control loop of the motor, as are, for example, the previously calculated gains K_{Pc} and K_{Ic} from Eq. (3.23), will be generated a duty cycle of high frequency PWM signals which allows for proper control in the speed and position channels.

The next loop considered in motor control achieving is reserved to the motor speed; the proportional-integral speed controller provides a reference value for the electrical current, which is actually the input value for the current controller. In the same time, the sign of this reference value dictates the rotation sense of the motor rotor, as it is used in the elaboration of the commutation signals in the block “Commutation table” together with the signals received from the Hall-effect based sensors. The last control loop, the outermost one, is reserved to the control of the position, and implements a proportional control law.

Using the simulation scheme in Figure 3.9, which implements the tuned controllers for all three loops, the results in Figure 3.10 were obtained for a position step input. The left-hand side of the Figure presents the desired (reference) and obtained positions for the linear actuation (expressed in mm), while the right-hand side of the Figure shows a comparative graphical exposure of the following speed signals (expressed in rpm): (A) the reference speed, collected as the output from the position controller block, and (B) the obtained speed, calculated starting from the obtained linear position. At the next step, the tuned controllers were tested with a more complex input signal in the form of a repeated sequence signal, with positive and negative ramps and actuation limits between –3 and 3 mm. The results depicted in Figure 3.11 were obtained. All numerical simulation results shown proper functioning of the obtained control scheme for the morphing actuator based on the BLDC motor, the used design approach providing a simplified method for tuning its control gains.

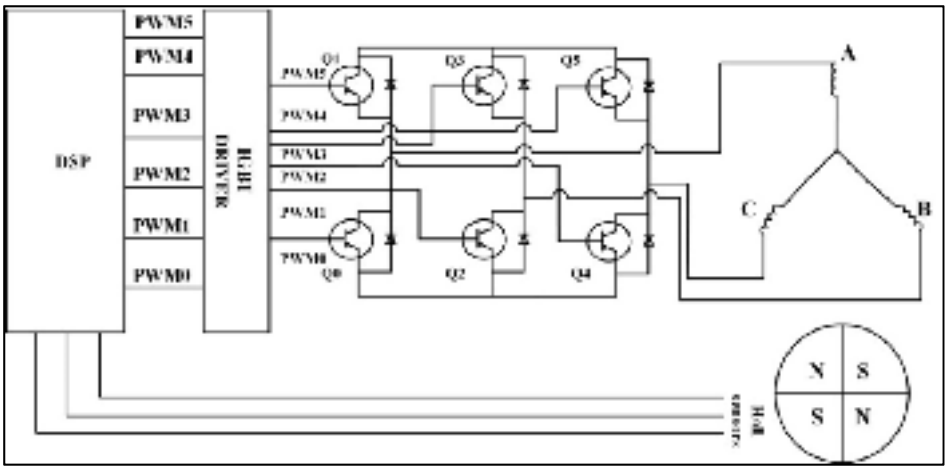

Figure 3.8 BLDC motor control using PWM

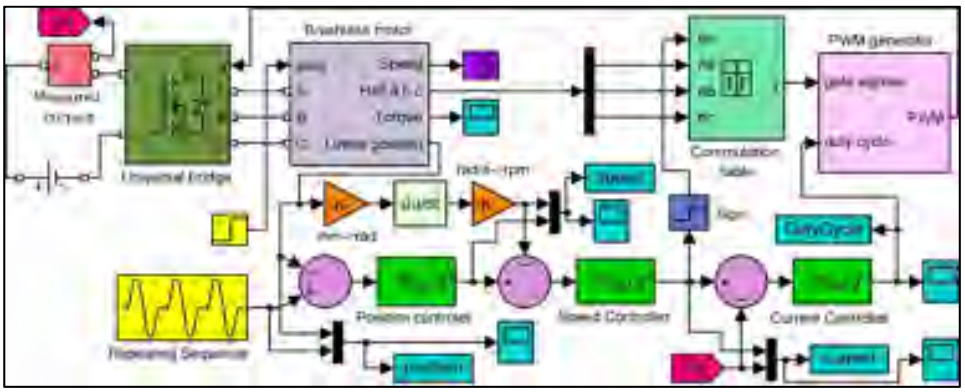

Figure 3.9 Actuator control by using SimPowerSystems toolbox in MATLAB.

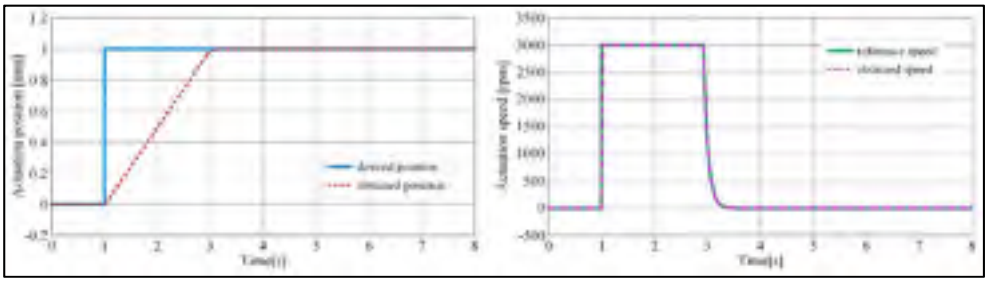

Figure 3.10 Results obtained from numerical simulation for a position step input as desired position.

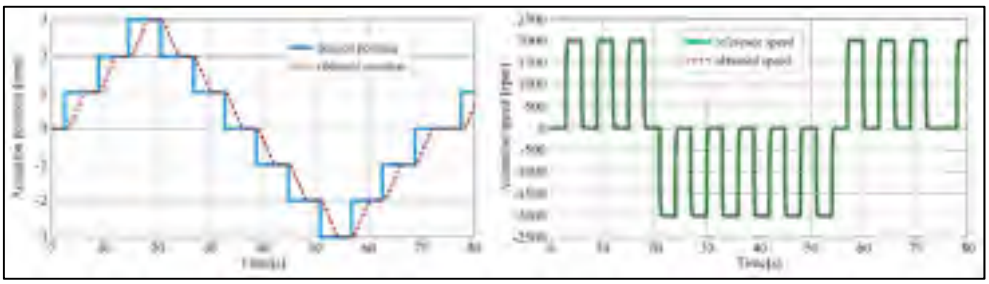

Figure 3.11 Results obtained from numerical simulation
for a repeated sequence input signal as desired position.

3.5 Bench testing of morphing wing control system

The developed experimental model for the deformable wing is tested both at the laboratory level, with no airflow, to evaluate the components integration and the whole system functioning, but also in the wind tunnel, in the presence of airflow, to evaluate its behavior and to validate the results predicted through numerical optimization from the aerodynamic point of view.

The control gains that were obtained were experimentally validated in bench tests for all of the four actuators used to morph the wing model. The whole bench testing operation was realized at ÉTS in the LARCASE laboratory. The architecture of the experimental testing system is presented in Figure 3.12, and was developed by using a Real Time (RT) Target from National Instruments (NI). As it can be easily observed, to have information related to the real values of the actuated distances (control feedback) for the morphing actuators four LVDT linear position sensors are used.

The bench test instrumentation is developed by using some programmable EPOS drives, produced by the Maxon Motor Company and dedicated for the BLDC motors integrated in the actuators, but also, by using the PXI technology from NI. Once performed the testing and validation of the control gains through numerical simulations, in order to develop the experimental model, it is necessary to performe a conversion before programming them into

the drives, according to the Maxon motors application notes (Maxon Motor Application notes). The following equations show how the gains from SI units (used in Simulink) are converted to EPOS units. For the electrical current control it results :

$$\begin{aligned} K_{\text{P\_EPOS}} &= K_{\text{P}}\,(\text{SI units})/(3.91\times10^{-3}), \\ K_{\text{I\_EPOS}} &= K_{\text{P}}\,(\text{SI units})/3.91, \end{aligned} \tag{3.26}$$

while, for the speed control:

$$\begin{aligned} K_{\text{P\_EPOS}} &= K_{\text{P}}\,(\text{SI units})/(2\cdot10^{-5}), \\ K_{\text{I\_EPOS}} &= K_{\text{P}}\,(\text{SI units})/(5\cdot10^{-3}), \end{aligned} \tag{3.27}$$

and for the position control:

$$K_{\text{P\_EPOS}} = K_{\text{P}}\,(\text{SI units})/(10^{-2}). \tag{3.28}$$

The flow of the design and bench testing of the control system can be summarized as in Figure 3.11.

After the conversion and implementation of the IMC tuned gains into the EPOS drives, various actuation commands were tested for the four actuators, both independently and simultaneously. The purpose of the independent actuator control was to assess whether it meets the mechanical requirements to which it is subjected when the wing is morphed.

When the actuators were simultaneously tested, firstly has been evaluated the behavior of the integrated morphing system in all optimized flight cases, and then the behavior of the morphing skin under various limit cases, where some of actuators pulled the skin and others pushed it, starting from the reference airfoil position. Figure 3.11 presents the control results for one actuator at a repeated step input signal as desired position. The first graphical window exposes the experimental obtained position versus the position obtained through numerical simulation and the required position, while the second graphical window shows the motor angular speed obtained during the experimental testing.

The graphical characteristics, drawn for position in the first window of Fig 3.14, prove that the obtained mathematical and software models reflect well the behavior of the experimental system. Therefore, the variant with a full bridge drive for the BLDC motor, operating in the two-phase conduction mode, was a good choice for the mathematical modelling step.

A short analyze of the characteristics shows that the rise times for numerical and experimental responses are approximately the same, but a small time delay in the command execution appears in the experimental situation. Few factors can generate and influence independently and/or cumulated the values of these delays, but also the allures of the time responses for position and speed: (A) the inherent differences between the obtained linear model and the nonlinear behavior of the actuation system in various actuation configurations; (B) the complex behavior of the morphed flexible skin, which generates a variable and hard to predict load when it is actuated (the load has been considered constant in the numerical simulations); (C) the behavior of the hardware equipment interfacing the control system with the real actuator (noise, time delays, etc.).

An important role is played by the experimental flexible skin equipping the model because it was attached on all four sides of the wing, attachment which increased its rigidity; the rigid structure, as well as, the flexible skin were specifically designed to meet aeronautical industry requirements. The time delays can be easily correlated with the angular speed profile in the second graphical window of Figure 3.14, observing that the speed transition from zero to the maximal value is made following various ramps with the slopes influenced by the changes in load.

Viewed in the context of the morphing wing project general aim, i.e. to extend the laminar flow regions on the wing surface, and thus to reduce the drag over an operating range of flight conditions, the discussed time delays are practically insignificant, taking into account the duration of a flight. Besides these delays, a more important aspect which can be noticed analyzing the curves in Figure 3.14 is that the controlled experimentally model does not have steady-state errors, which means that the designed control system meets the most important

condition to obtain a good experimental reproducibility of the numerical optimized wing shapes. Therefore, the experimental testing results demonstrated adequate functioning of the controlled morphing wing model, and recommended its preparation for the next series of experimental tests in a wind tunnel.

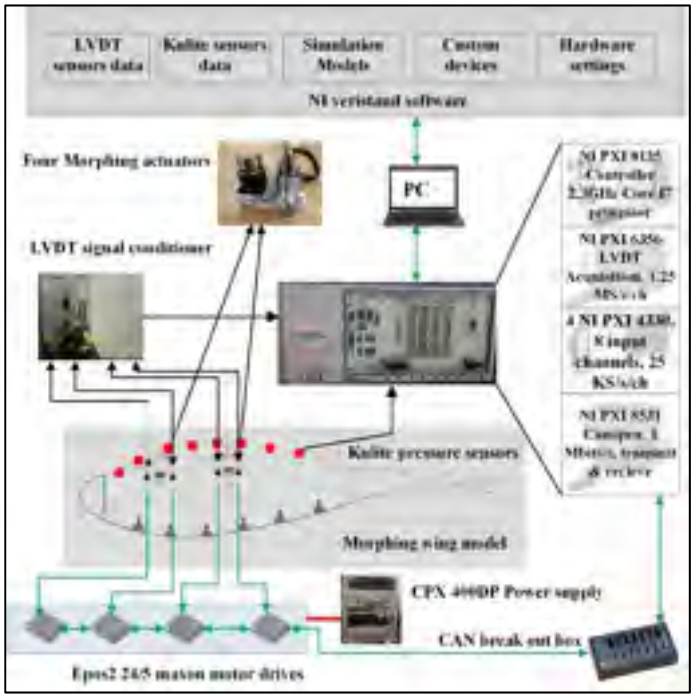

Figure 3.12 Architecture of experimental testing system.

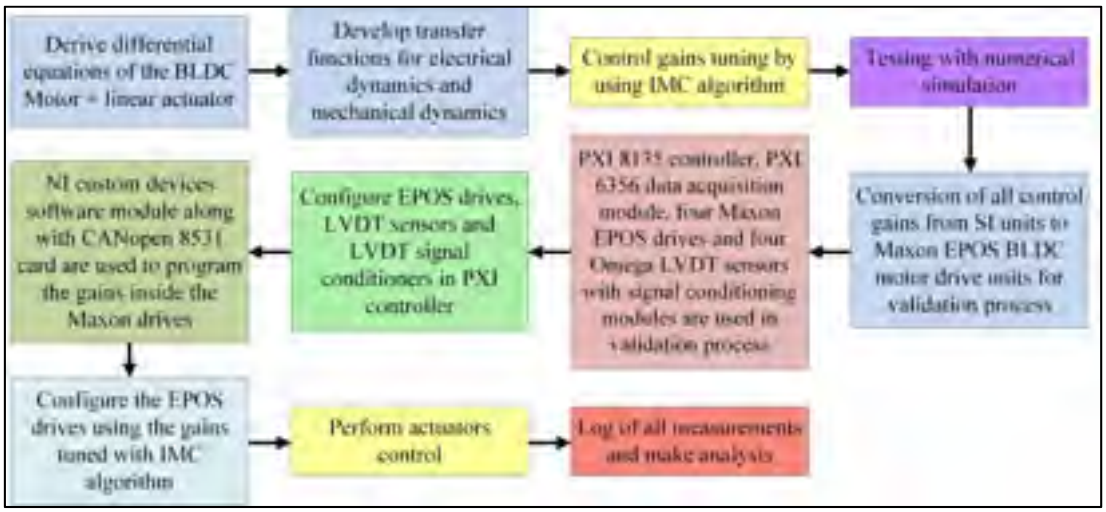

Figure 3.13 Flow of design and bench

testing of the control system.

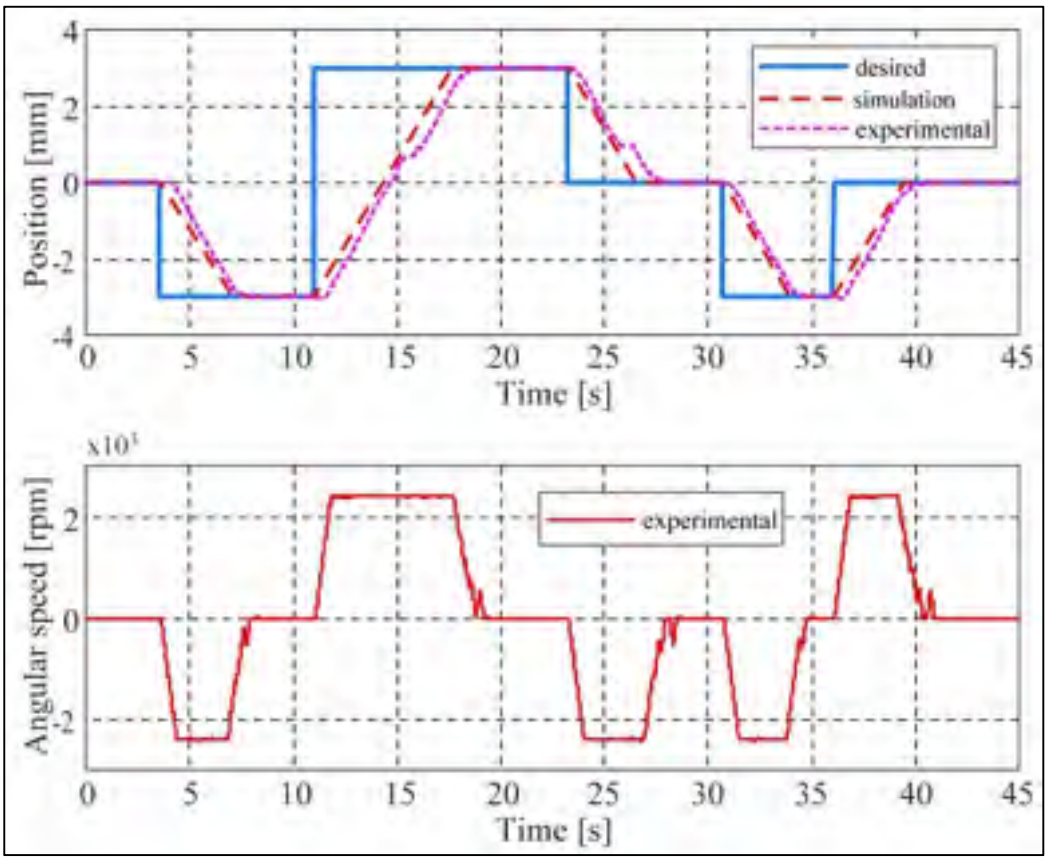

Figure 3.14 Bench test results

3.6 Evaluation of morphing wing experimental model through wind tunnel testing

For an assessment of the aerodynamic benefits provided by the morphing technology, the project research team tested the developed experimental model in the presence of airflow, in the National Research Council of Canada subsonic wind tunnel. The performed tests aimed also at the validation of the numerical study performed by the aerodynamic team and at the evaluation of the integrated morphing wing system behavior in various situations simulating a real flight, with different incidence angles, Mach numbers, aileron deflection angles and with

the inherent perturbations induced by the wind tunnel. Figure 3.15 presents the placement of the morphable wing experimental model in the IAR-NRC wind tunnel testing room; the wing position was a vertical one, which means that the variation of the incidence angle has been obtained by rotating the model around a vertical axis. The wind tunnel testing was performed for 97 flight cases, which were generated by combining various values of the incidence angle (nineteen values, between –3 and +3°), Mach number (three values: 0.15, 0.2 and 0.25) and aileron deflection angle (thirteen values, between –6 and +6°).

For an easiest interaction of the human operator with the experimental model a Graphic User Interface (GUI) has been conceived (see Figure 3.16); it allowed a safe testing and a complex evaluation of the experimental model in various situations. The GUI was organized to provide some functions, booth from the safety, but also from the testing needs points of view: emergency stop, mode selection (Manual, Flight case and Homing), flight case selection, real time displaying of the actuated distances by using the numerical indicators, real time plotting of the measured actuation distances and of the reference skin necessary actuation distances.

During all of the wind tunnel tests the Kulite sensors pressure data were real time processed to provide information related to the laminar-to-turbulent transition location; simultaneously with the control system survey based on the GUI, the Fast Fourier Transforms (FFT) for the acquired pressure data have been real time visualized on a parallel screen. Additionally, aiming at the evaluation of the laminar-to-turbulent transition location over the whole wing upper surface, not only on the Kulite sensors station, the Infra-Red (IR) thermography method was applied. Also, with the aim to get a further post-processing analyze, the Kulite data were acquired at 20 kHz rate for all of the tested flight cases, both for original (un-morphed) and optimized (morphed) airfoils.

Figure 3.15 exposes the results of the IR thermography for original and deformed airfoils in the flight case 19, generated for Ma=0.15, α=1.5˚ and δ=0˚; the air flows from the left to the right, booth pictures being views from the leading edge side of the morphable wing model, similar with the second picture presented in Fig 3.17. For both airfoils the NRC team estimated

the average transition line on the wing upper surface by using the gradient method; Figure 3.17 shows that the transition location depends by the chord-wise position. In the current flight case, the estimation of the transition position for whole wing provided the mean values of approximately 49%(±2%) of the chord (49.26%(±2%)) for original airfoil, and 52%(±2%) of the chord (51.72%(±2%)) for morphed airfoil, respectively. Also, on the span-wise station associated to the Kulite sensors (at 40% of the model span) the estimation of the transition position provided the values of 49.18% of the chord for original airfoil (somewhere between Kulite 13 and Kulite 14), and 52.08% of the chord for morphed airfoil (somewhere between Kulite 18 and Kulite 19). Therefore, the IR measurements revealed that, in this flow case, the use of the morphing technology produced an extension of the laminar region over the whole wing upper surface with a mean value of about 2.46% of the chord, while in the Kulites span-wise station the extension was approximately 2.90% of the wing chord.

The post-processing analysis, starting from the recorded pressure data, provided information related to the transition point position in the Kulite span-wise station by using two mechanisms: (A) the evaluation of the STandard Deviations (STDs) for the data collected from each of the 32 pressure sensors to obtain a graphical representation of the pressure fluctuations in the boundary layer of the flow; (B) the analyze based on the Fast Fourier Transforms (FFT) for the Kulites recorded data on each pressure channel to evaluate the noise magnitude in the air flow over the morphable wing upper surface.

The using of the first mechanism for the previous analyzed case (Ma=0.15, α=1.5˚ and δ=0˚ airflow conditions) provided the plot diagrams exposed in Figure 3.19, for both, original and deformed airfoils. According to that, the maximum value of the pressure data STD for original airfoil corresponds to the Kulite #14, and for the deformed airfoil to the Kulite #19. A big value for the pressure data STD on one pressure detection channel comparatively with the other channels suggests the presence of the turbulence influences in the acquired signal for that channel, which means that the turbulence started somewhere between the Kulite sensor associated with this channel and the previous Kulite sensor.

The second evaluation mechanism, based on the FFT decomposition, generated the graphics presented in Figure 3.20, for un-morphed airfoil, and in Figure 3.21, for morphed airfoil. If a turbulent airflow is present over a pressure sensor monitoring the flow on the morphable wing upper surface, then its associated FFT curve will be detached. For both mechanisms, the resolution for the laminar to turbulent transition position detection depends by the density of the sensors used to measure the pressure signals over the monitored surface. Because here have been used 32 pressure detection channels, which means a higher graphical data density, the FFT analyze was conducted step by step, depicting the associated curves for clusters of eight sensors counted successively beginning from the wing leading edge. Therefore, each of the Figure 3.20 and Figure 3.21 includes five graphical windows, the first four describing the FFT curves for the clusters of eight sensors, while, to have an image of the airflow on the whole Kulite station, the last one contains the FFT curves for all 32 detection channels. It can be seen from Figure 3.20 that the transition occurred between sensor#13 and sensor#14 for the unmorphed wing while Figure 3.21 shows that transition has occurred between sensor#18 and sensor#19.

As in the STD based analyze, the FFT results suggest that for the original airfoil the turbulent flow is present at the level of the pressure sensors #13 and #14 (second and fifth graphical windows in Figure 3.20), and for the deformed airfoil its maximum influence is at the level of the pressure sensors #18 and #19 (third and fifth graphical windows in Figure 3. 21).

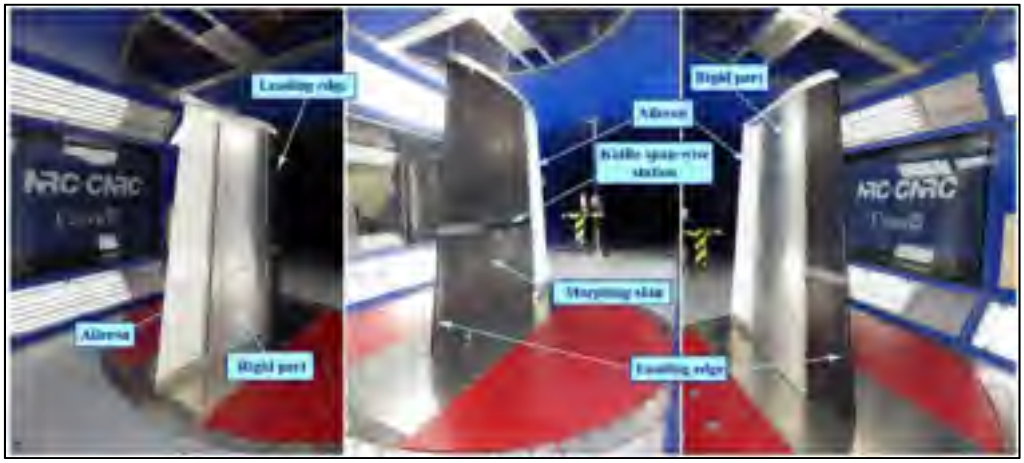

Figure 3.15 Positioning of morphable wing in the IAR-NRC

wind tunnel

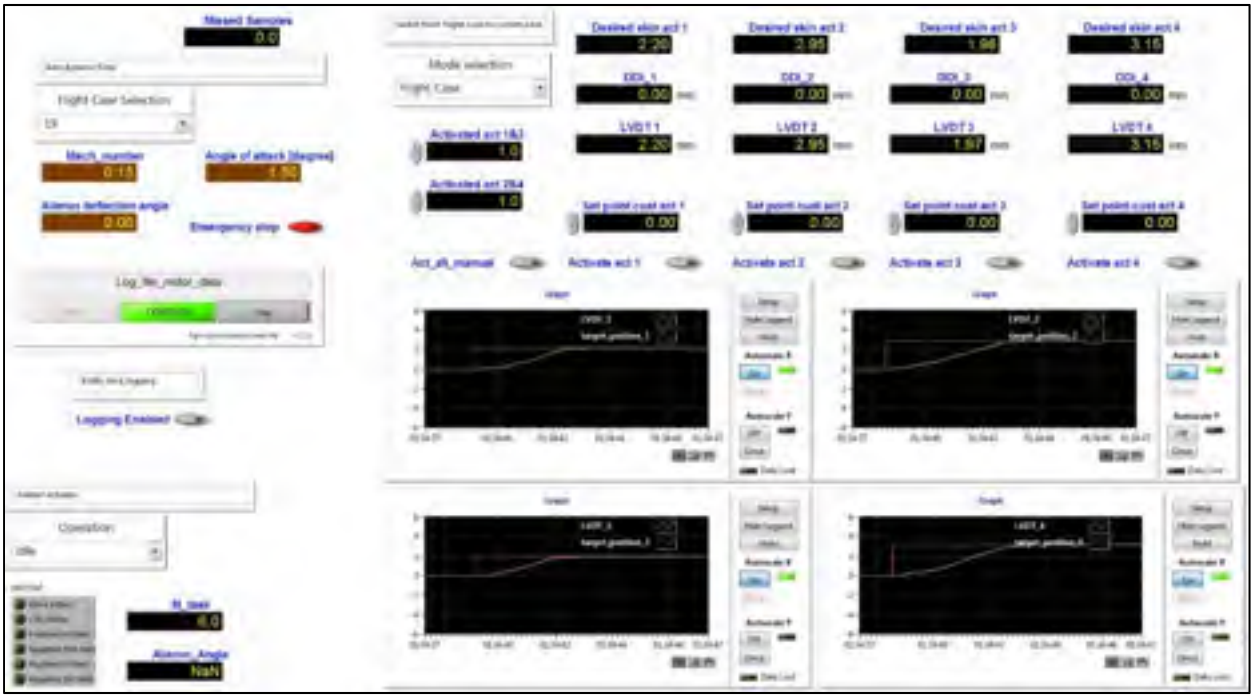

Figure 3.16 Experimental model associated GUI.

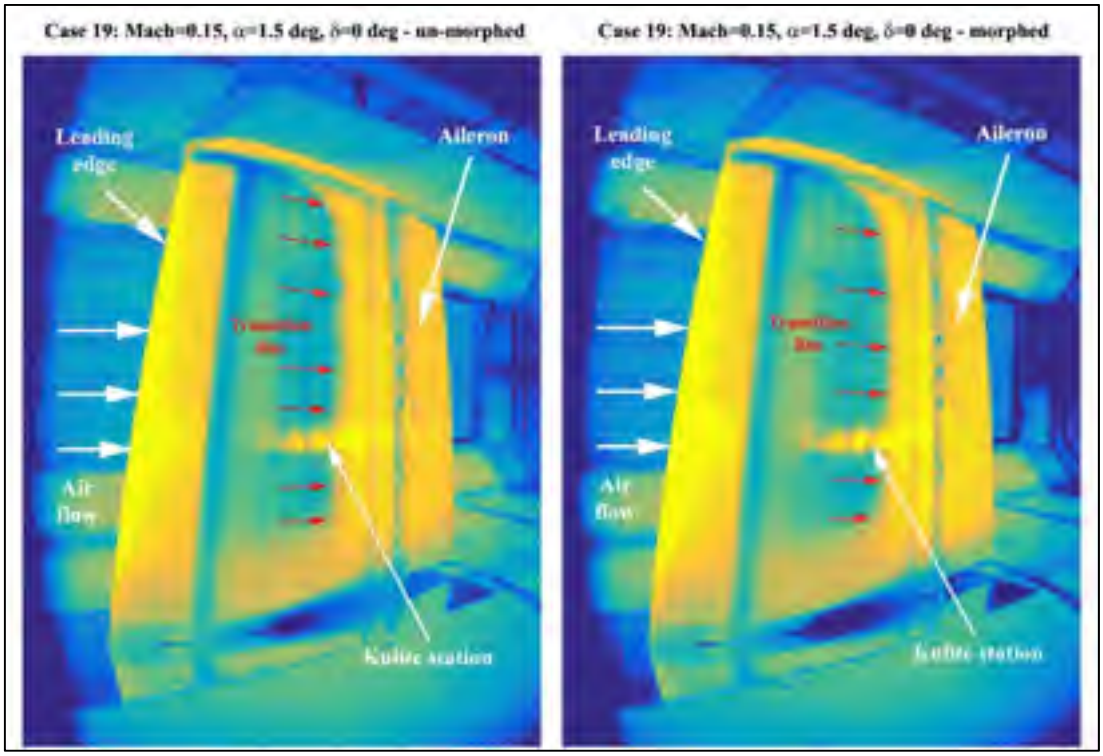

Figure 3.17 IR visualizations for *Ma*=0.15, α=1.5˚ and δ=0˚ airflow conditions.

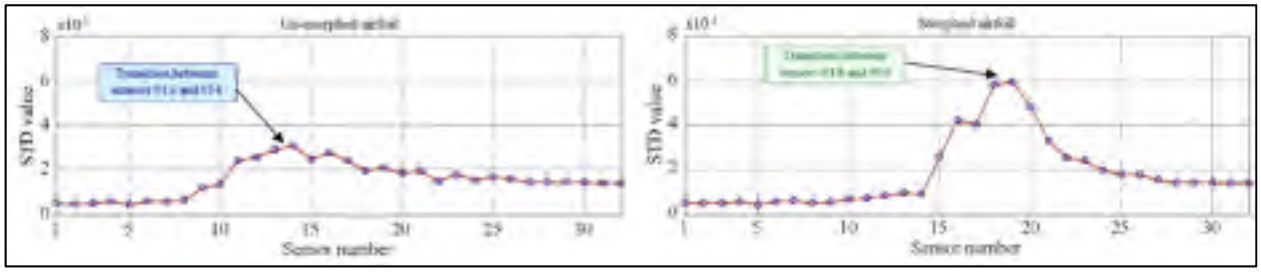

Figure 3.18 Standard deviations of pressure data recorded in

flow case 19 (*Ma*=0.15, α=1.5˚, δ=0˚).

It can be observed that all of the three techniques used to detect transition position provided similar results for the pressure sensors span-wise station both for original and morphed airfoils, validating in this way the IR thermography analyze of the flow performed for the whole wing. Also, for the great majority of the wind tunnel tested flight cases the research team of the project observed that the morphing technology improved the average position of the laminar to turbulent flow transition over the whole wing with more than 2.5% of the wing chord.

For the previous exposed flow case, the IR measurements proved that the morphed airfoil beneficiated by an expansion of the laminar region over the whole morphable wing upper surface with a mean value of about 2.46% of the chord, while in the Kulites span-wise station the extension was approximately 2.90% of the wing chord.

3.7 Conclusions

This paper presented the control tuning, instrumentation and experimental testing and validation for a morphable wing experimental model actuated using four miniature BLDC motors. The four used actuators were similar, and were required to produce a direct linear actuation of the flexible upper surface of the wing, manufactured from composite materials with elastic properties. The positions of the four actuation points were determined starting from the aerodynamically optimized shapes obtained for the deformable wing through numerical simulation in various flow cases. The structure of each actuator includes a BLDC motor and a mechanical part which converts rotation movement into linear movement. Due to limited space and the high actuation force requirements imposed by our application, the actuators were in house manufactured using miniature BLDC motors from the Maxon Motor Company.

The tuning of the three control loops included in the actuator control system was achieved using the Internal Model Control (IMC) methodology. The first testing step included a

numerical simulation, all results proving an adequate functioning of the obtained control scheme. Finally, the obtained control gains were validated in bench tests and wind tunnel tests experiments on all four morphing actuators incorporated by the morphable wing actuation mechanism. The experimental model was based on certain programmable EPOS drives, which were used for position control for the BLDC motors, and on the NI PXI technology. The bench testing results, with no aerodynamic load on the model, revealed a very good behavior of the controlled morphing wing model, recommending its preparation for the next series of experimental tests in a wind tunnel.

For an assessment of the aerodynamic benefits provided by the morphing technology, the project research team tested the developed experimental model in the presence of airflow, in the National Research Council of Canada subsonic wind tunnel. The performed testing actions aimed also at the validation of the numerical study performed by the aerodynamic team and at the evaluation of the integrated morphing wing system behavior in various situations simulating a real flight, with different incidence angles, Mach numbers, aileron deflection angles and with the inherent perturbations induced by the wind tunnel.

To estimate the laminar to turbulent transition location over the entire upper surface of the morphable wing the Infra-Red (IR) thermography method has been used. Also, to have information related to the transition point position in the Kulite span-wise station two mechanisms were applied: (A) the evaluation of the standard deviations (STDs) for the data collected from each of the 32 pressure sensors; (B) the Fast Fourier Transforms (FFT) decomposition of the acquired data on each pressure channel.

All of the three techniques used to detect transition position provided similar results for the pressure sensors span-wise station both for original and morphed airfoils, validating in this way the IR thermography analyze of the flow performed for the whole wing.

For the great majority of the wind tunnel tested flight cases the research team of the project observed that the morphing technology improved the average position of the laminar to

turbulent flow transition over the whole wing with more than 2.5% of the wing chord. On the other way, the results presented in the paper for the flight case 19, generated for Ma=0.15, α=1.5˚ and δ=0˚, shown that, according to the IR measurements, the morphed airfoil beneficiated by an expansion of the laminar region over the whole morphable wing upper surface with a mean value of about 2.46% of the chord, while in the Kulites span-wise station the extension was approximately 2.90% of the wing chord.

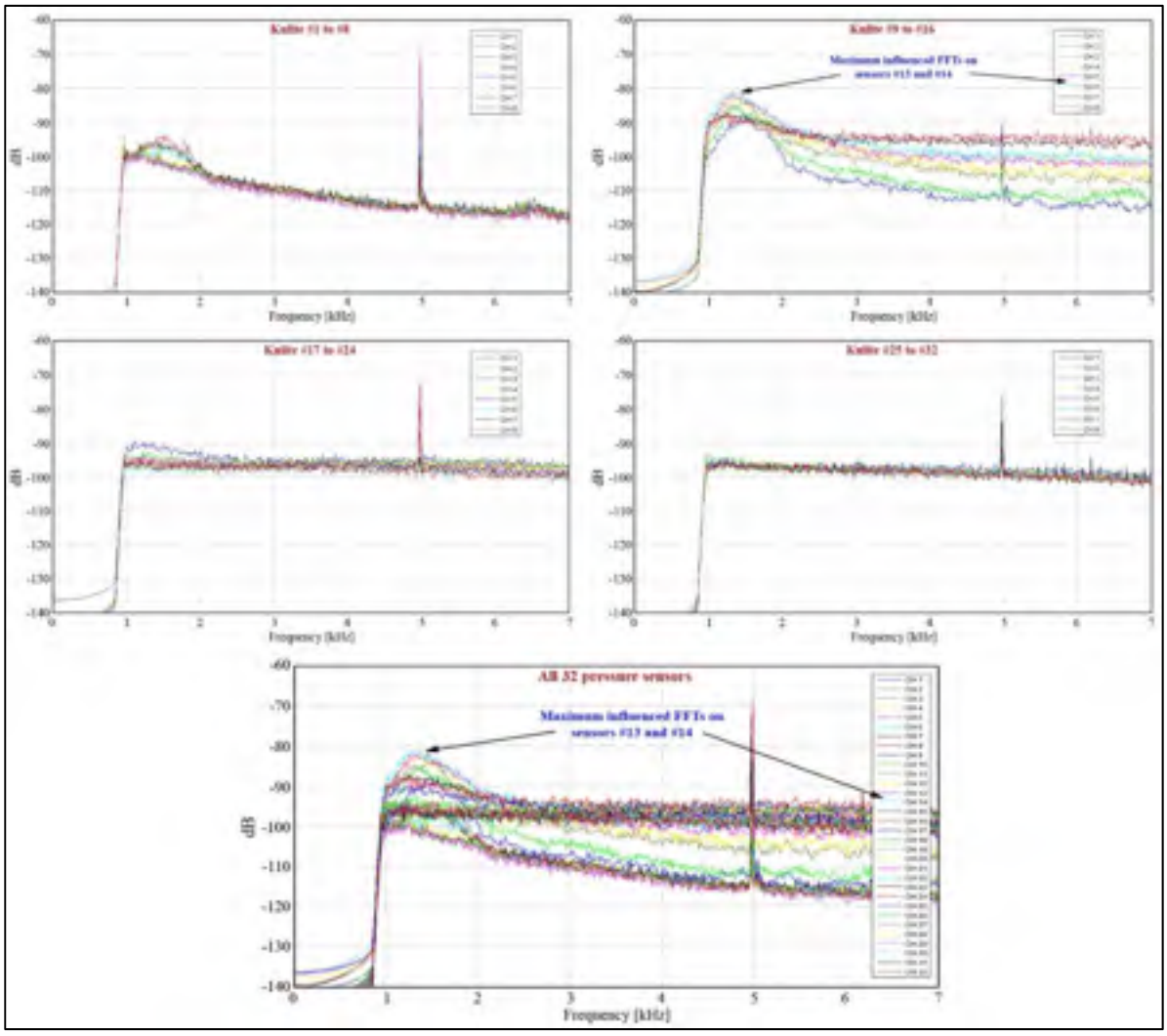

Figure 3.19 FFT results for original (un-morphed) airfoil

at Ma=0.15, α=1.5˚, and δ=0˚ (flow case 19).

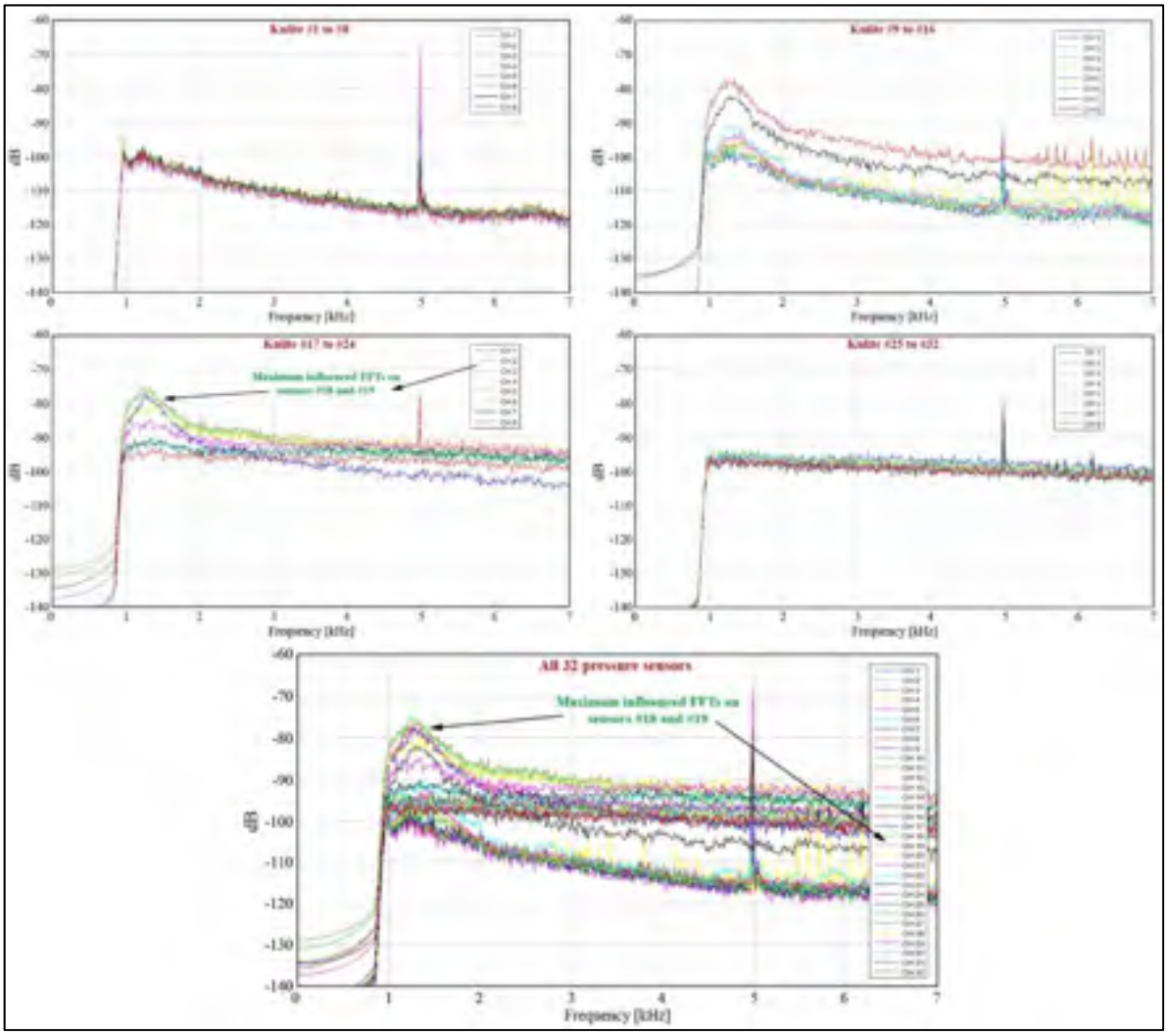

Figure 3.20 FFT results for the morphed airfoil at Ma=0.15, α=1.5˚,

and δ=0˚ (flow case 19).

3.8 Acknowledgements

The authors would like to thank the Thales team for their support, with special thanks to Mr. Philippe MOLARET, Mr. Bernard BLOUIN and Mr. Xavier LOUIS, and the Bombardier Aerospace team - Mr. Patrick GERMAIN and Mr. Fassi KAFYEKE for their help and fruitful discussions. We would also like to thank Bombardier Aerospace, Thales, and the Consortium for Research and Innovation in Aerospace in Quebec (CRIAQ) and the National Sciences and Engineering Research Council (NSERC) for the funding received in connection with the CRIAQ MDO 505 project.

CHAPTER 4 SECOND ARTICLE

Novel morphing wing actuator control based Particle Swarm Optimization

Shehryar Khan[1], Teodor Lucian Grigorie[1,2], Ruxandra Mihaela Botez[1]
Mahmoud Mamou[3], *Yousef* Mébarki[3]

[1]*École de Technologie Supérieure, Montréal, Québec H3C 1K3, Canada*
[2]*Military Technical Academy "Ferdinand I", Bucharest 050141, Romania*
[3]*National Research Council, Ottawa, Ontario K1A 0R6, Canada*

Proof of publication:

The paper was accepted in the "Aeronautical Journal", 2019.

RÉSUMÉ

L'article présente la conception et les essais expérimentaux d'un système de commande utilisé dans une nouvelle application d'aile déformable qui est à l'échelle d'une véritable aile d'avion. Le système d'actionnement de déformation utilise quatre moteurs BLDC miniatures similaires placés à l'intérieur de l'aile, qui agissent directement sur la surface supérieure flexible de l'aile fabriquee en matériaux composites. Le système de commande de chaque actionneur utilise trois boucles de régulation (courant, vitesse et position) caractérisées par cinq gains de régulation. Pour régler les gains de contrôle, la méthode PSO (Optimisation par essaim de particules) est utilisée. L'application de cette méthode supposait le développement d'un modèle Matlab/Simulink pour l'actionneur contrôlé, qui a utilise un sous-programme implémentant l'algorithme PSO pour trouver les meilleures valeurs pour les cinq gains de contrôle qui minimisent la fonction coût. Une fois les meilleures valeurs des gains de contrôle établies, le modèle de l'actionneur contrôlé est simulé numériquement afin d'évaluer la qualité du système de contrôle obtenu. Enfin, le système de commande conçu est validé expérimentalement lors d'essais sur banc et en soufflerie pour les quatre actionneurs miniatures intégrés au modèle expérimental de morphose. Les essais en soufflerie traitent le système dans son ensemble et comprennent, en plus de l'évaluation du système d'actionnement contrôlé, l'essai du modèle expérimental d'aile mobile intégré et l'évaluation des avantages aérodynamiques apportés par la technologie de deformation dans ce projet. Dans cette dernière perspective, le flux d'air sur

la surface supérieure deformable du modèle expérimental est surveillé à l'aide de diverses techniques, basées sur la collecte de données de pression avec des capteurs de pression Kulite, ou sur des visualisations par caméra thermographique infrarouge.

4.1 Abstract

The paper presents the design and experimental testing of the control system used in a new morphing wing application with a full-scaled portion of a real wing. The morphing actuation system uses four similar miniature BLDC motors placed inside the wing, which execute a direct actuation of the flexible upper surface of the wing made from composite materials. The control system of each actuator uses three control loops (current, speed and position) characterized by five control gains. To tune the control gains the Particle Swarm Optimization (PSO) method is used. The application of the method supposed the development of a Matlab/Simulink software model for the controlled actuator, which worked together with a software subroutine implementing the PSO algorithm to find the best values for the five control gains which minimize the cost function. Once the best values of the control gains established, the software model of the controlled actuator is numerical simulated in order to evaluate the quality of the obtained control system. Finally, the designed control system is experimentally validated in bench tests and wind tunnel tests for all four miniature actuators integrated in the morphing wing experimental model. The wind tunnel testing treats the system as a whole, and includes, besides the evaluation of the controlled actuation system, the testing of the integrated morphable wing experimental model, and the evaluation of the aerodynamic benefits brought by the morphing technology on this project. From this last perspective, the airflow on the morphable upper surface of the experimental model is monitored by using various techniques, based on pressure data collection with Kulite pressure sensors, or on infra-red thermography camera visualizations.

Keywords: Morphing Wing; Actuation system; BLDC Motor; Control Tuning; Particle Swarm Optimization; Experimental model; Wind tunnel testing

4.2 Introduction

The unpredictable variations in fuel prices and the annual increase in the number of passengers have heightened the concerns of the aeronautical industry, as the costs of operations increase dramatically. As immediate measures some airlines tried to reconFigure their fleets to increase the efficiency from the point of view of the fuel consumption, while other tried to reduce the in-flight aircrafts weights by using low-weight on-board items (UGAO, 2014). On the other way, these concerns have pushed the industry to collaborate with universities and research labs around the world in an effort to develop new technologies for fuel consumption reduction in aeronautics. One of the identified ways to limit the aircraft fuel consumption is morphing wing, being directly related to the optimization of the aircraft aerodynamics. Moreover, this aerodynamics optimization is real time realized, by changing the wing shape as a function of various flight parameters (for example, Mach number, angle of attack, …) (Popov,A-V., Grigorie, T.L et al, 2010).

The last decade revealed around the world many individual or collaborative studies related to morphing wing technology, in which were involved industrial entities, as well as research groups from universities and research institutes. Many projects were developed at the level of lab applications, by trying various optimization numerical algorithms for the wing shapes, but a lot of projects proved that the research subject is very hot, and, in very strong research consortiums, developed experimental morphing wing systems, with portions of real wings, and tested them in wind tunnel. The challenges were great both from the point of view of the numerical optimization of the wing shape, but especially from the point of view of the technologies used to develop and test the experimental models: materials for flexible skins, actuation systems, control systems, sensors and instrumentation.

In time, the wing shape design and optimization procedures used different cost functions and numerical algorithms, more or less complex, implying or not multi-objective criteria. In 2007

NASA published a report called “Modeling and Optimization for Morphing Wing Concept Generation”, which presented an approach to develop morphing wing weight equations, and an approach to size morphing aircraft (Skillen, M.D., Crossley, W.A, 2007). A research team from University of Bristol in UK developed a design procedure for aircraft fixed wing structures that incorporate morphing devices and exemplified it on a regional jet aircraft configuration (Yang, J., Sartor, P., 2015). A new approach for the synthesis of the internal structure of a morphing wing was proposed by a collaborative team from Thailand and Singapore; two design strategies were used: the first one applies design variables for simultaneous partial topology and sizing optimization while the second one includes nodal positions as design variables (Sleesongsom, S., Bureerat, S., 2013).

An optimization procedure coupled with a knowledge-based framework was developed at University of Milano, Italy, for the design of the shape of a morphing wing aircraft; the framework combined parametric geometry representation, multidisciplinary modelling, and a genetic algorithm, and was able to introduce morphing shape changes considering the presence of structural parts, the physical behavior of the morphing skins, and the effects of these changes on the aerodynamic performances (De Gaspari, A., Ricci, S, 2015). The aerodynamic performance benefits of a morphing trailing edge wing were analyzed by a research team from University of Michigan, USA, by using a gradient-based optimization algorithm (Zhoujie Lyu, Z, et al 2015). A multidisciplinary design optimization tool was developed by a collaborative research team from Portugal and Canada to design a morphing wing for a small experimental unmanned aerial vehicle; the tool coupled an aerodynamic shape optimization code with a structural morphing model to obtain a set of optimal wing shapes for minimum drag at different flight speeds (Gamboa, P., Vale, J. et al, 2009). Researchers from Swansea University, UK, designed a multi-objective optimization method for morphing airfoils, incorporating specific morphing systems into the optimization process (Fincham, J.H.S et al, 2015). In a similar way, at ETH Zurich, Switzerland, was performed an aero-structural optimization of morphing airfoils for adaptive wings; promising aerodynamic and structural morphing performances have been obtained by applying the method to a morphing concept using Dielectric Elastomers as actuators (Molinari, G., 2011).

From another perspective, the team from the Purdue University, USA, realized an aerodynamic optimization of a morphing airfoil by using energy as an objective; the relative strain energy used to pass from one airfoil shape to another was used as an additional design objective along with a drag design objective, while constraints were enforced on lift (Namgoong, H, 2007). As a result of the "Optimisation of Multi-scale Structures with Applications to Morphing Aircraft" grant, financed by the European Research Council, a new aircraft wing span morphing concept, named "Adaptive Aspect Ratio Wing", was introduced at Swansea University, UK; the concept realized a coupling between a compliant skin and a mechanism based internal structure to obtain a morphing wing able to provide significant changes in span and aspect ratio (Woods, B.K.S, 2015).

From the point of view of the mechanisms used to achieve the numerically optimized shapes of the morphing wings, many types of actuators were applied to control these shapes. Also, besides the classical actuation systems, in many morphing wing projects were proposed and tested actuation systems developed by using new materials, smart or less smart, but which allowed the users to obtain the desired deformations of the wings shapes with better performances.

In a research grand funded by NASA, and developed at California State University at San Bernardino, USA, piezoelectric microfiber composite (MFC) actuators were experimentally tested to control the surfaces of morphing wings; two different situations were experimented: a traditional flap configuration, where the MFCs have been bounded to each side of a metal substrate, and a configuration in which the MFCs have been bonded directly to the wing (Usher, T.D et al, 2013). A solid-state variable-camber morphing wing controlled with piezoceramic composite actuators was developed and wind tunnel tested for fixed-wing aircraft that operate in the low Reynolds number regime in a European research project; the tests revealed the feasibility of the design and comparable lift and drag response to the baseline wing (Bilgen, O et al, 2014). In a research sponsored by US Air Force Research Laboratory (AFRL),

has been experienced the use of morphing control surfaces, actuated with macro fiber composite (MFC) piezoelectric actuators, to replace traditional servo-actuated control surfaces in UAV applications; the evaluation of the aerodynamic performance starting from the experimental results indicated the increase of the sectional lift coefficients comparatively with a servo-actuated hinged flap airfoil (Ohanian III et al, 2011). In the same trend, the Experimental AeroScience Group from National University of Singapore developed a project related to "Airfoil morphing by MFC actuators" and used macro fiber composite piezoelectric actuators integrated into the skin of a wing for changing its shape (Debiasi, M., Bouremel et al, 2011). Another category of piezoelectric actuators, post-buckled precompressed piezoelectric actuators was tested in a morphing application by a collaborative research team from Delft University of Technology, Netherlands, and from University of Kansas, USA; the actuators equipped a morphing wing used to control the roll movement of an UAV - the flight testing shown a 38% increase in roll control authority and 3.7 times greater control derivatives vis-à-vis of the using of conventional ailerons (Vos, R., Barrett, R., 2007).

Another trend in the field is to use smart material actuators like shape memory alloy (SMA) to modify the wing shapes. With the aim to evaluate the applicability potential of SMA actuators in the small-sized and medium-sized unmanned air vehicles wings morphing, at RMIT University in Melbourne, Australia was developed an experimental morphing wing model, where the camber line of an airfoil section was modified using an SMA actuator; the model was also tested in the wind tunnel to investigate the effects on the aerodynamic behavior of the wing (Bil, C., Massey, K. et al, 2013). In a project supported by Korea Aerospace Research Institute, flexinol wires were used as SMA actuators in a flap morphing mechanism to operate a morphing wing model; the actuation performances were experimentally evaluated, while the aerodynamic performance of the morphed airfoils were analyzed by using the GAMBIT and FLUENT software (Kang, W.R., Kim, 2012). A similar study performed in Greece, aimed at the design, manufacturing and testing of an innovative actuation mechanism based SMA NiTiNol wires for the actuation and morphing of the flap's camber of a civil regional transportation aircraft's trailing edge (Karagiannis, D., Stamatelos et al, 2014). An Italian research study, supported and granted by Alenia Aeronautica S.p.A., realized the control of the

airfoil camber at the wing trailing edge on a full scale wing of a civil regional transportation aircraft by substituting the traditional split flap with a hingeless, smooth morphed flap; the basic element of the smart flap was an actuator device, made of a structural arc and an SMA active ribbon (Barbarino, S., Pecora, R., et al, 2011).

In this context, our team (Research Laboratory in Active Controls, Avionics and Aeroservoelasticity (LARCASE) of the Ecole de Technologie Supérieure (ETS) in Montréal, Canada) coordinated between 2006 and 2009 and a morphing wing project entitled “Laminar Flow Improvement on an Aeroelastic Research Wing”, developed in collaboration with Bombardier Aerospace, Thales Avionics, Ecole Polytechnique in Montréal and Institute for Aerospace Research at the National Research Council Canada (IAR-NRC) (Botez, R. M., Molaret, P et al 2007). The chosen wing model was a rectangular one, with a chord of 0.5 m and a span of 0.9 m; the model was equipped with a flexible skin made of composite materials (layers of carbon and Kevlar fibers in a resin matrix) morphed by two actuation lines using SMA wires as actuators. In the same time, some Kulite pressure sensors were disposed on the flexible skin in different positions along of the chord, allowing the real time detection and visualization of the laminar to turbulent transition point position. The project aimed at the drag reduction through the improvement of the laminar flow past aerodynamically morphing wing. Consequently, the project was finalized by developing an automatic system that, based on the information related to the pressure distribution along the wing chord, moved the transition point from the laminar to the turbulent regime closer to the trailing edge in order to obtain a larger laminar flow region. Based on the strong nonlinear behavior of the SMA actuators, but also in strong correlation with the project experimental model development phase, different control strategies were used, starting from the open loop architecture until a real time optimized closed loop architecture(Popov, A.V., Grigorie, T.L, 2010). After this big collaborative project our morphing wing experience continued with the design, optimization, manufacturing and testing in our proper wind tunnel at ETS in Montreal (Price-Païdoussis wind tunnel) of various deformable wings. During this period the team developed and tested various optimization algorithms for the wings shapes ([30], [31]), but also, in trend with the new concept in

aerospace engineering related to More Electric Aircraft, tried various morphing actuation systems with mechanisms based on DC miniature electrical motors (Kammegne Tchatchueng, M.J., Grigorie et al, 2014).

Based on previous experience, our research team initiated a second big project on morphing wing, this time at international level, involving strong research entities from Italy and Canada, as follows: Alenia, CIRA, and University Frederico II Naples from Italy, and Bombardier Aerospace, Thales, Ecole Polytechnique in Montréal, Institute for Aerospace Research at the National Research Council Canada (IAR-NRC) and Ecole de Technologie Supérieure (ETS) in Montréal (as coordinator) from Canada. The project aimed that, starting from a full-scaled portion of a real wing, an aerodynamically improved morphable wing-aileron prototype to be designed, optimized, manufactured, tested and validated using win tunnel tests at IAR-NRC. The here exposed work was performed during this project, and presents the design of the control system used for the morphing wing actuation system and the results obtained during the experimental testing of the morphing wing integrated model on the bench and in the wind tunnel. In the next sections of the paper are shown: 1) Architecture of the morphing wing experimental model integrating the controlled actuation system; 2) Control system tuning procedure based on Particle Swarm Optimization (PSO) method; 3) Testing results for the morphing wing experimental model in the wind tunnel, including here the evaluation of the aerodynamic benefits brought by the morphing technology on this project.

4.3 Architecture of the morphing wing experimental model

Called “Morphing architectures and related technologies for wing efficiency improvement” - CRIAQ MDO-505, the project has been funded by Bombardier Aerospace, Thales, CRIAQ (Consortium of Research in Quebec Aerospace Industries) and the NSERC (Natural Sciences and Engineering Research Council of Canada).

The designed and manufactured prototype resulted under the form of a technical demonstrator of a real aircraft wing tip, being based on a full-scaled portion of a real wing equipped with an

aileron. The entire internal structure of the demonstrator (including the spars and ribs) was designed and realized considering all structural constraints required by the original wing and imposed by industrial partners, while its dimensions were chosen to fit the dimensions of the IAR-NRC subsonic wind tunnel and force balance limitations (Figure 4.1); the model resulted with a 1.5 m span and a 1.5 m root chord, including the aileron, with a taper ratio of 0.72 and a leading-edge sweep of 8°. As can be easily observed from Figure 4.1 the wing box and whole internal structure is made from aluminum, while the upper surface of the wing was equipped with a flexible skin manufactured in carbon fiber reinforced composite and delimited by the front and rear spars placed between 20% and 65% of the wing chord. To measure the pressure distribution over the wing, but also to record the airflow wave frequencies, 32 Kulite pressure sensors were placed on the flexible skin. The final configuration included a morphable aileron designed and manufactured by the Italian team ([34], [35]).

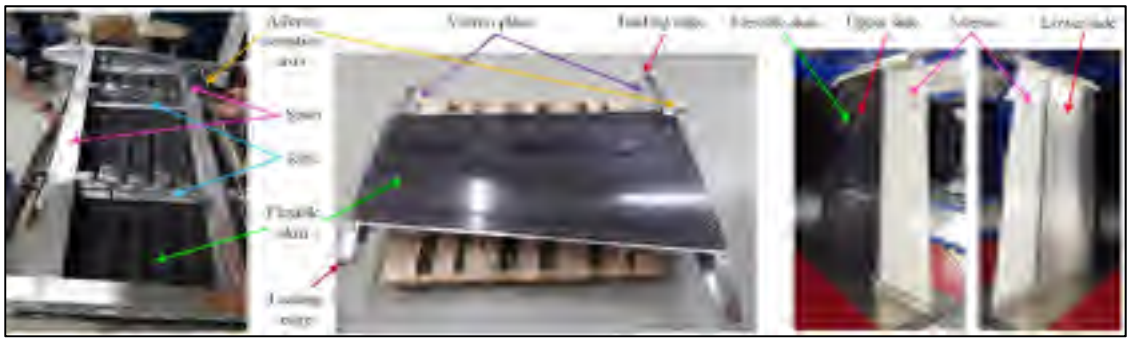

Figure 4.1 Structure of the morphing wing experimental model

An aerodynamic numerical study was subsequently performed with the aim to optimize the morphed airfoils for various flow cases, each one characterized by a Mach number (M), a wing angle of attack (α) and an aileron deflection angle (δ). In each flow case the optimum shape of the airfoil was searched by changing its local thickness in order to extend the laminar region of the upper surface flow (Koreanschi, A., Sugar-Gabor et al 2016). The team decided to use two actuation lines installed in the sections at 37% and 75% of the wing span, and, on each one, two actuation points placed at 20% and 65% of the local wing chord. Therefore, to morph

the upper surface of the wing the actuation mechanism was based on four similar actuators placed as in Fig. 2 and fixed to the two central ribs of the wing.

The actuators need to perform a direct actuation of the flexible skin by pushing or pulling it until their controlled displacements equal the desired ones provided by the aerodynamic study in each optimized flow case. The actuators were manufactured in our LARCASE laboratory at ETS, each of them including a Maxon BLDC motor and a mechanism which converts the rotational actuation into a translational one. The linear actuation position for each actuator is monitored by using a linear variable differential transformer (LVDT) sensor which communicates with the actuator control system.

4.4 Control system tuning procedure based on Particle Swarm Optimization (PSO) method

To realize the improvement of laminar flow over the wing, the BLDC motor based morphing actuator needs to be controlled in order to morph the wing until the skin displacements in the actuation points are the same with the aerodynamically predicted values for each studied flow case. As in all controlled systems design, after the understanding of the system behavior and the establishing of control objectives, a necessary step is the obtaining of a simplified model of it. In the current situation, when a software based design procedure was targeted, both mathematical and software models were desired. The model included both the BLDC motor model and the model of the mechanism converting the BLDC motor rotational output in a translational output (Figure 4.2) (Khan, S., Botez, R. M et al 2015); its inputs are the DC bus voltage “Ud” and the load torque “T load”, while as outputs it provided the electrical current “I”, the actuation speed “v” and the actuation linear position “pos”.

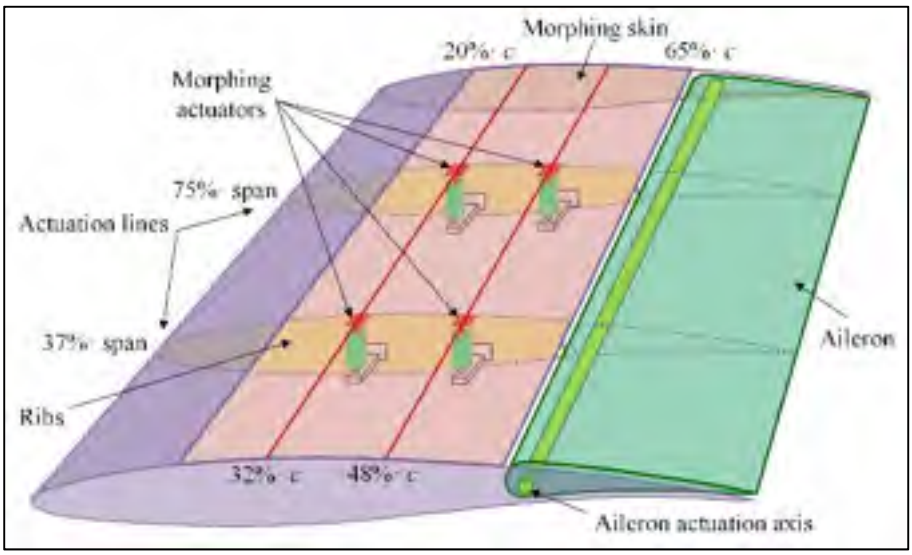

Figure 4.2 Position of the actuators in the wing box

The control of the actuation systems based BLDC motors can be performed in many ways, including here classical control strategies, intelligent control strategies and various combinations between them. Also, the literature provides a lot of methods to tune the coefficients of such control systems. In the current paper is shown the application of the Particle Swarm Optimization (PSO) method to tune the coefficients used in the control system of our morphing wing actuator at the level of all three implied control loops: current loop, speed loop and position loop. To simulate the behavior of the actuator, the "BLDC model" was integrated in the model in Figure 4.3 were are highlighted all three loops. Also, in the simulation model, a cost function has been defined by taking the integral of the sum of squares of the position, speed and current control errors.

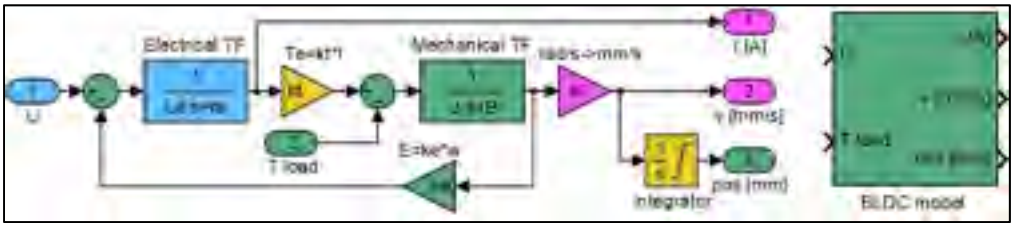

Figure 4.3 Model of the actuator

implemented in Matlab/Simulink

4.5 Particle Swarm Optimization algorithm

Particle swarm optimization (PSO) acts in a similar manner as the genetic algorithms, being a population based algorithm which has been born from the study of the social behavior of the insects swarming, bird flocking and fish schooling. Each individual of this population is called particle and, based on its own experience, it moves in steps with a specific speed in the direction of the location providing the best resources. In the same time these information are shared with the other members of the swarm, which are attracted by this location in a different degree. At the next step, based on the shared information between the members of the swarm, each particle reevaluates its speed and direction, mechanism which finally leads to the finding of the optimal location. From the PSO algorithm point of view, at each step a cost function is evaluated and the particle new speed and direction are decided. The technique was developed in 1995 by Dr. Eberhart and Dr. Kennedy (Kennedy, J., Eberhart, R, 1995) and further adapted and used in the optimization procedures for many applications in aerospace engineering field.

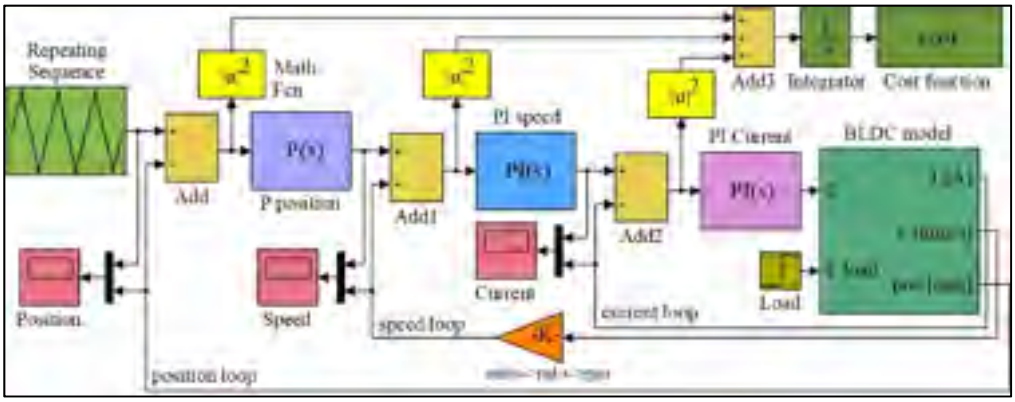

Figure 4.4 Simulation model used in the
control system tuning based PSO

A collaborative research team from NASA Langley Research Center and Vanderplaats Research and Development Inc., realized the optimization of a transport aircraft wing using particle swarm optimization; the optimization problem was a bi-level one, with severe

numerical noise and combining continuous and discrete variables, which restricted the use of gradient-based optimization algorithms (Venter, G., et al 2002). At University of Naples in Italy, was tested the PSO methodology application in the field of conceptual design, to define the preliminary configuration of an aircraft (Blasi, L et al, 2007). A very interesting application is related to the space trajectory optimization problems. A research team from University of Illinois, USA, used the PSO for the determination of periodic orbits in the context of the circular restricted three-body problem, and for the optimization of orbital transfers; the algorithm provided the optimal solutions with a very good numerical accuracy (Pontani, M. et al, 2010). Also, researchers from NASA Johnson Space Center in Houston, USA, applied this methodology to optimize the entry flight path angle and reference trajectory for a modified Apollo guidance during Mars entry (Grant, M.J. et al, 2007). Researchers from Concordia University in Montreal, Canada, applied the PSO in the path planning for team(s) of unmanned aerial vehicles (UAVs) in forest fires fighting applications (Ghamry, K.A, 2017), but also, in the cooperative control of the multiple wheeled mobile robots (Kamel, M.A., Yu, X. et al, 2016).

In a simplified approach, the mathematics of the algorithm can be described as follows. If the search space is *N*-dimensional, then each of the swarm particles has the form of a vector with *N* components

$$X = (x_1, x_2, \ ..., \ x_N), \tag{4.1}$$

with the speed expressed as

$$V = (v_1, v_2, \ ..., \ v_N). \tag{4.2}$$

At each discrete step time (k+1), the speed of the variable x_i characterizing the particle X is updated by using the formula (Blasi, L., Del Core et al 2007)

$$v_i(k+1) = w(k)v_i(k) + c_1\rho_1(k)[p_{l,i}(k) - x_i(k)] + c_2\rho_2(k)[p_{g,i}(k) - x_i(k)], \tag{4.3}$$

where w is the inertial weight, $p_{l,i}(k)$ is the value of the variable x_i reflecting the particle best position (local optimum), $p_{g,i}(k)$ is the value of the variable x_i reflecting the population best

position (global optimum), c_1 - the cognitive parameter, c_2 - the social parameter, and ρ_1 and ρ_2 are random variables generated with values between 0 and 1. The new value of the variable x_i results then with equation

$$x_i(k+1) = x_i(k) + v_i(k+1). \tag{4.4}$$

The choosing of the proper values for the c_1, c_2 and w parameters makes the algorithm more efficient. The literature survey suggested some limits for these values: $0 < c_1, c_2 \leq 2$ and $0.8 \leq w \leq 1.4$ (Poli, R., Kennedy, J., 2007). The velocity and position updates in PSO algorithm can be schematized as in Figure 4.5 (Hassan, R., Cohanim, B et al 2005), while, according to the exposed mechanisms, the flow chart of the PSO algorithm results as in Figure 4.6.

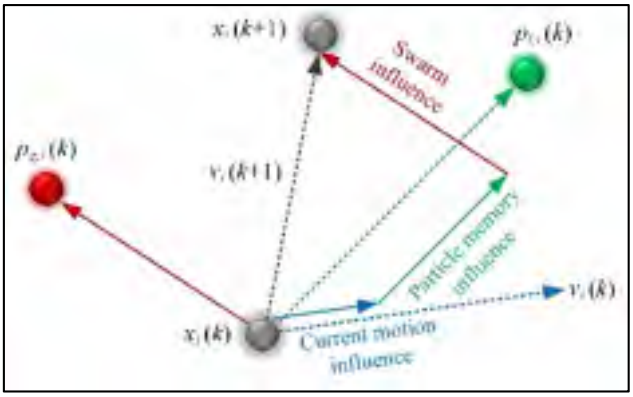

Figure 4.5 The velocity and
position updates in PSO algorithm

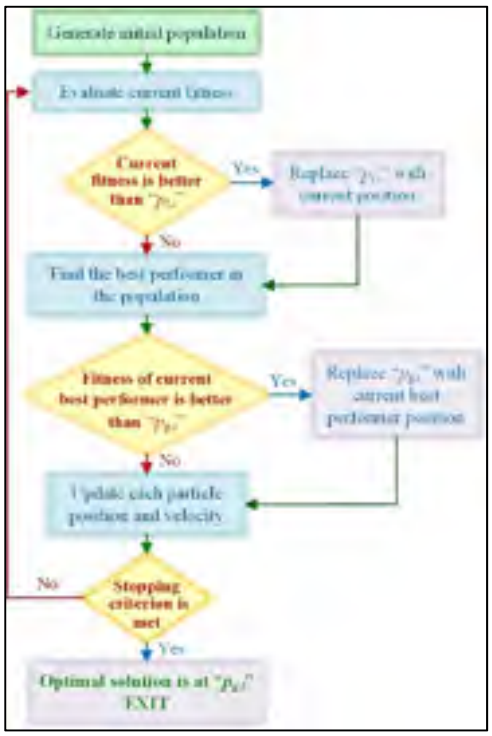

Figure 4.6.Flow chart of
the PSO algorithm

4.6 Control system tuning

According to the model presented in Figure 4.4, the control system desired to be tuned includes three loops (current loop, speed loop and position loop), which supposes the presence of five control coefficients, three proportional gains and two integral gains: K_{Pp} - proportional gain for Proportional (P) position controller; K_{Ps} - proportional gain and K_{Is} - integral gain for Proportional-Integral (PI) angular speed controller; K_{Pc} - proportional gain and K_{Ic} - integral gain for Proportional-Integral (PI) electrical current controller.

To tune the control system used for the morphing wing actuators the PSO algorithm has been implemented in a Matlab software subroutine which worked in conjunction with the simulation

model of the controlled actuation system presented in Figure 4.4. The code flow of the PSO algorithm for our system is shown in Figure 4.6.

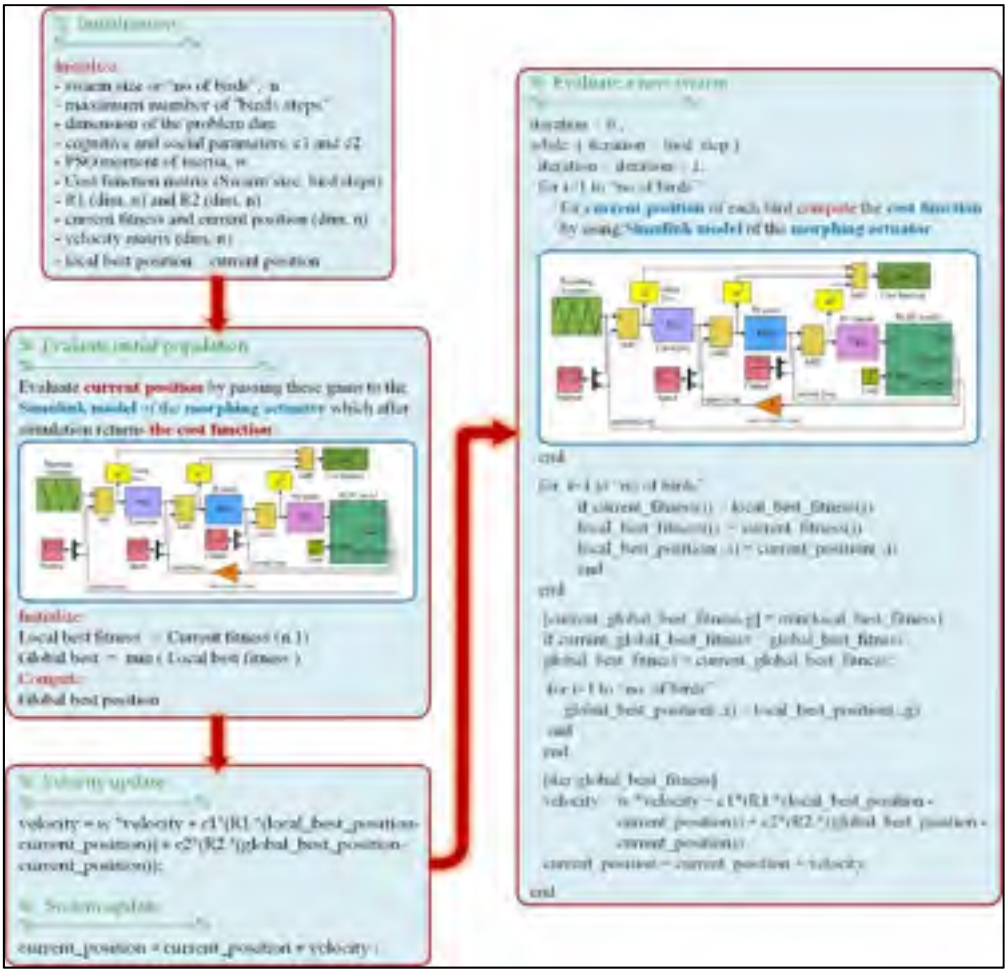

Figure 4.7 The PSO algorithm code
flow for our optimization case

The optimization procedure ran for various combinations of the three weight factors, w, c_1 and c_2, with values between 0.1 and 2.2 for c_1 and c_2, and between 0.1 and 1.9 for w, taken with a step of 0.1. Also, during the optimization, various values were considered for the swarm size ("number of birds"), 10 and 20, but also for the maximum number of "bird steps", between 10 and 100, taken with a step of 10. For the "initialization" of the control system five coefficients, two variants were used. In the first variant the initial coefficients were generated as random numbers in the vicinity of the gains derived by our team by using a classical tuning method

(Khan, S., Botez, R. M et 2015), while in the second variant the "randi" Matlab function has been used to generate the coefficients in the range of 1 to 40000. The best results were obtained for a swarm size of 20 "birds", with a number of 50 "bird steps", and with c_1=1, c_2=1.2 and w=0.9. The cost function has been found, in this case, with the value of $2.8424 \cdot 10^5$, while the optimized control gains were: K_{Pp}=42354, K_{Ps}=1.2, K_{Is} =0.005, K_{Pc}= 207, and K_{Ic}=34025.

Table 1 presents few cases evaluated during the optimization process, with the associated results, while Fig. 8 shows the variation of the cost function vs number of iterations for these cases; the Case #11 in the table presents the parameters of the optimal situation. The controlled actuator answers to a position step input as required signal, for the optimized values of the coefficients, position, speed and current loops. Also, a numerical simulation run for the optimal case, having as position input a complex signal with positive and negative ramps, connecting different horizontal levels considered between -3 mm and 3 mm, provided the results in Figure 4.10; shown are, also, the position, speed and current control results. Simulation results confirm that the actuator control system performed very well, with a rise time of approximately 2 s for a unitary step input in position, and with no overshoot.

Table 4.1 Parametric study of PSO for morphing wing actuator control

Case no.	PSO parameters					Final control coefficients					Cost function
						Position	Speed		Current		
	Birds no.	Steps	c_1	c_2	w	K_{Pp}	K_{Ps}	K_{Is}	K_{Pc}	K_{Ic}	
Control system coefficients initialized in the vicinity of the gains derived by using a classical tuning method ([37])											
1.	10	30	0.1	1.2	0.9	93070	8.2	90.4	14.4	135732	$3.7744 \cdot 10^5$
2.	10	30	0.3	1.2	0.9	96362	8.7	35.1	146	220226	$3.2286 \cdot 10^5$
3.	10	10	0.6	1.2	0.9	57920	4.5	50.3	50.6	71508	$3.7984 \cdot 10^5$
4.	10	30	0.8	1.2	0.9	93363	5.2	97.1	50.9	67510	$4.0816 \cdot 10^5$

Control system coefficients initialized in the range of 1 to 40000 by using the "randi" Matlab function											
5.	10	30	0.1	0.1	0.9	4435	7280	18502	24497	32696	$22.461 \cdot 10^5$
6.	10	30	0.1	1.2	0.9	48794	70	21.7	8489	49050	$7.5452 \cdot 10^5$
7.	10	30	0.3	1.2	0.9	85285	4.2	9313	415	930	$5.2845 \cdot 10^5$
8.	10	30	0.8	0.1	0.9	8221	10461	11445	3330	78242	$5.6007 \cdot 10^5$
9.	10	50	1.7	1.7	0.7	4820	7688	9490	21682	35755	$18.013 \cdot 10^5$
10.	10	100	0.9	1.5	1.5	4871	2585	24356	27095	37783	$24.351 \cdot 10^5$
11.	**20**	**50**	**1**	**1.2**	**0.9**	**42354**	**1.2**	**0.005**	**207**	**34025**	$\mathbf{2.8424 \cdot 10^5}$
12.	20	40	0.9	1.5	1.5	9629	7.2	11113	6388	65481	$4.9187 \cdot 10^5$

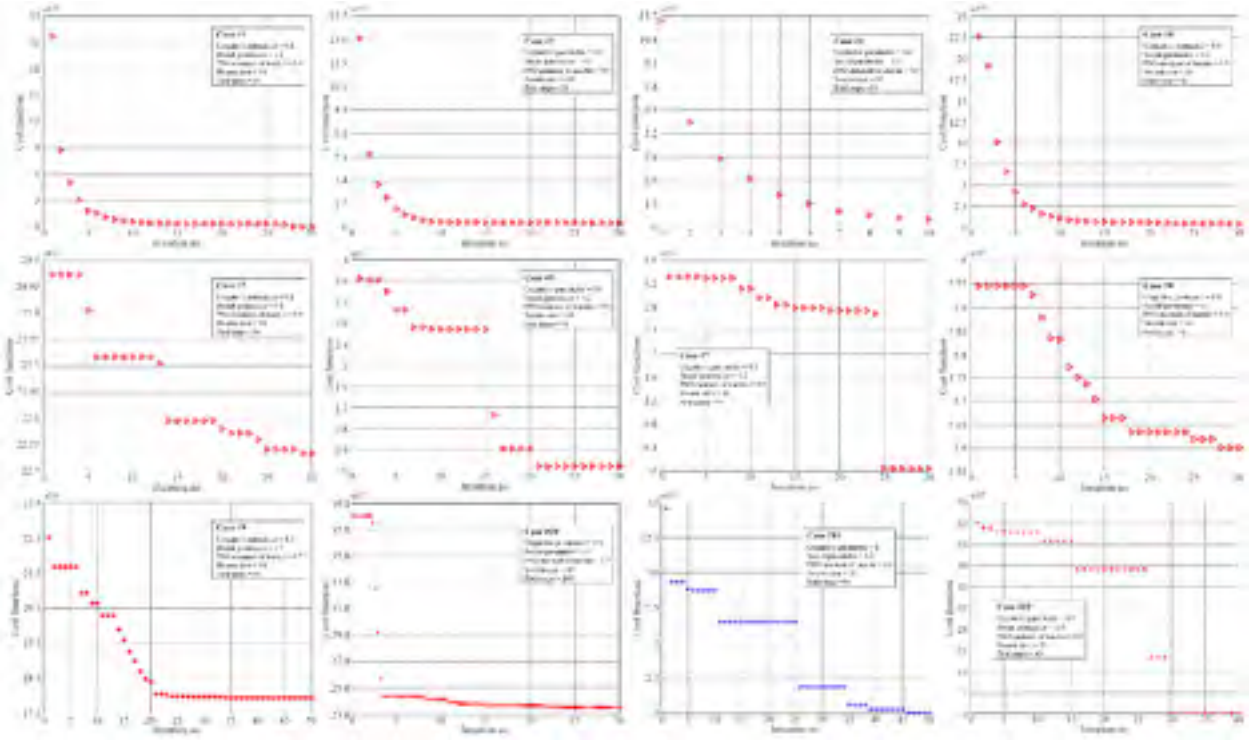

Figure 4.8 The variation of the cost function vs number of iterations table-1

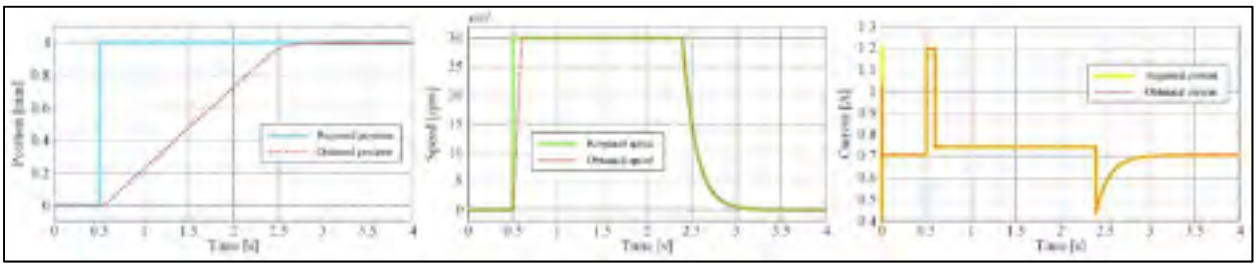

Figure 4.9 The controlled actuator answers to a position step

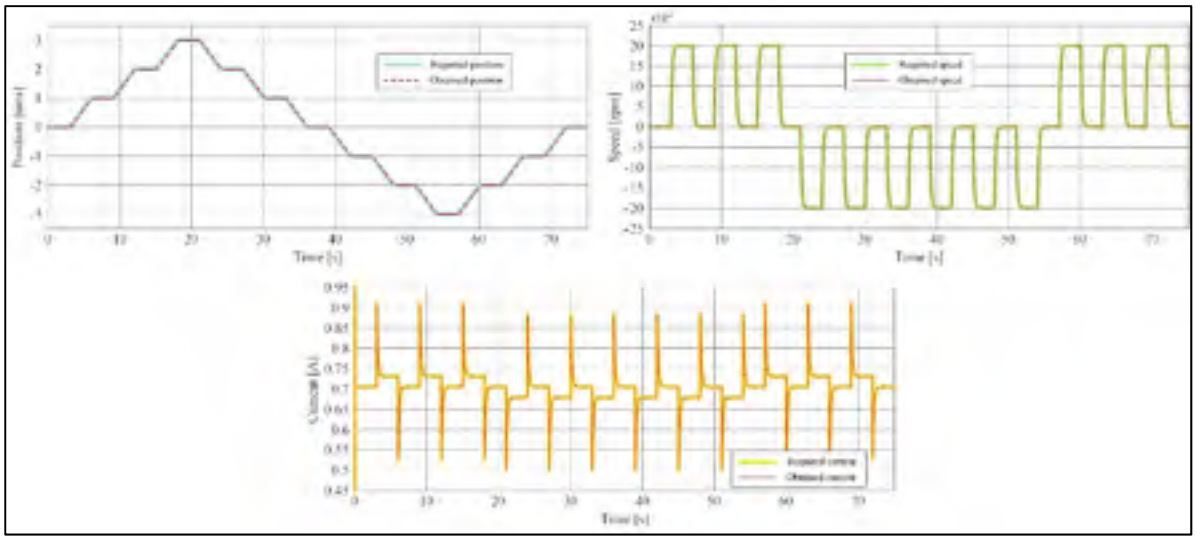

Figure 4.10 The controlled actuator answers to a complex signal

4.7 Experimental instrumentation of the morphing wing model and wind tunnel testing

The aim of the experimental instrumentation was to integrate the morphing wing system as a whole, with a well-controlled actuation system, but also with pressure sensors for airflow monitoring and corresponding software for data processing and decisions making. The equipment used to integrate all the equipment has been configured as shown in Figure 4.11.

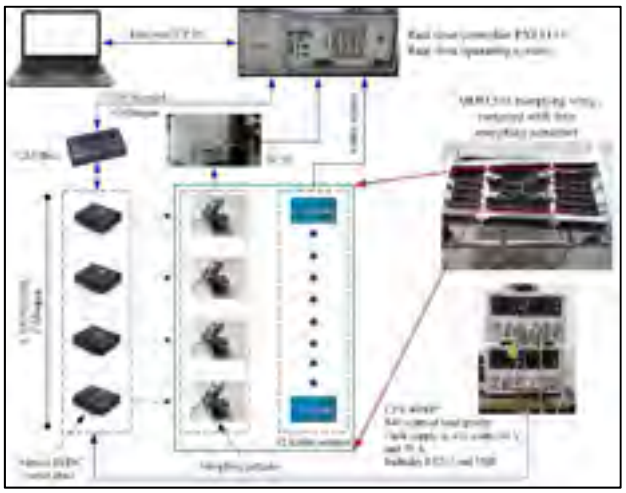

Figure 4.11 Equipment configuration

The *real time controller*, a PXI 8135 controller, with 2.3 GHz, is an Intel Core i7 embedded controller which runs a real time operating system, linked to the host through an Ethernet connection managed by a TCP/IP protocol. The controller was connected to various input output modules as shown in Fig. 11. The four morphing actuators were controlled by using some Maxon drives (EPOS2 24/5) connected to the PXIe controller via CAN breakout box, which in turn was connected to the CANopen interface module. This module is capable to transmit/receive process data objects and service data objects with a speed of up to 1 Mbits/s. The *EPOS 24/5 drives* are built with several communication interfaces both analog and digital, and can be connected as slaves in a CAN network via CAN interface on the device. The drives perform the electronic commutation of the brushless DC motor based on the feedback from Hall sensors. The regulation architecture is based on the current, speed and position loops, the devices allowing the programming of the control coefficients inside them through NI-Veristand CANopen custom devices. *NI-Veristand software* is used for the real time applications, being made up of three modules: project file, system file and the screen file. System definition file contains the configuration settings of the NI-Veristand engine which consist of target rate, hardware (DAQ, FPGA, ...), custom devices, models system mappings, etc. System explorer window of the system definition contains the target which user can add.

Once integrated, the controlled experimental morphing wing model was tested and calibrated

on bench, in the lab conditions, with no airflow load, and sent to the IAR-NRC subsonic wind tunnel for the final testing. The wind tunnel testing treated the system as a whole, and included, besides the evaluation of the controlled actuation system, the testing of the integrated morphable wing experimental model, and the evaluation of the aerodynamic benefits brought by the morphing technology on this project. From this last perspective, the airflow on the morphable upper surface of the experimental model was monitored by using various techniques, based on pressure data collection with Kulite pressure sensors, or on infra-red (IR) thermography camera visualizations. 97 flow cases, numerically optimized previously, were run and evaluated during the wind tunnel testing, both in original configuration (non-morphed), but also in optimized configuration (morphed), with the actuation system controlled in such a way that the controlled displacements equal the desired ones provided by the aerodynamic study in each optimized flow case.

Besides the real time monitoring and visualization of the airflow characteristics by using an in-house developed Graphical User Interface, for both configurations in each flow case a post-processing and analyze stage of the acquired data has been performed and conclusions drawn. The processing of pressure sensors aimed at the estimation of the position for the laminar to turbulent airflow transition in the pressure sensors station (a 2D estimation) based on Fast Fourier Transform (FFT) and on the Standard Deviation (SDT) evaluation. Also, a post-processing action and a detailed analysis has been performed for the infra-red captures in order to estimate the position for the laminar to turbulent airflow transition over the entire upper surface of the morphable wing (a 3D estimation).

As an example, Figure 4.12 exposes the results of the scanning performed in the LARCASE laboratory during the calibration of the integrated system for the case characterized by M=0.15, α=0.25˚ and δ=0˚ flow conditions. Shown is only the scan of the wing upper surface, without the aileron. The four required actuation distances were: -1.27 mm, 2.14 mm, -1.37 mm and 2.33 mm. Also, few calibration tests were performed in the National Research Council of Canada wind tunnel testing facility in Ottawa, when the model has been added in the testing

room (Figure 4.13). The corrections obtained during the calibration procedures were included in the application software component and taken into consideration during the wind tunnel tests.

From the developed Graphical User Interface it was obtained the picture in Figure 4. 14, describing the actuation results during the wind tunnel test for the morphed configuration of the wing in the same flow case. It can be easily observed that the controller performed very well in the wind tunnel conditions, with aerodynamic load. On the other way, the infra-red thermography technique provided the pictures in Figure 4.15, presenting the infrared captions for the un-morphed and morphed configurations and the 3D estimation for the position of the laminar to turbulent airflow transition over the entire upper surface of the morphing wing. The IR pictures were obtained during the first of the three wind tunnel tests.

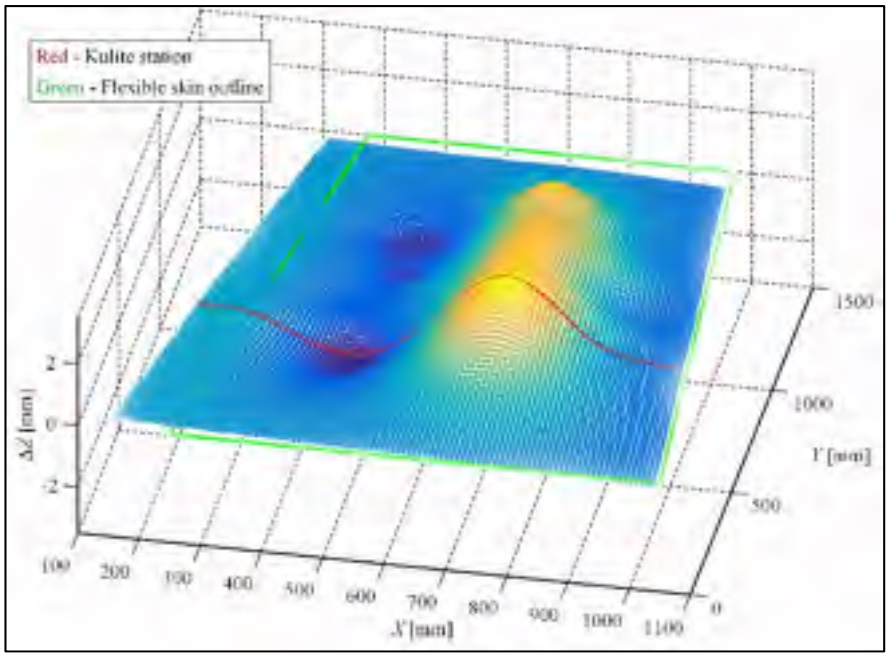

Figure 4.12 Calibration scanning on bench
for M=0.15, α=0.25˚ and δ=0˚ flow conditions

Figure 4.13 Model installation and calibration in the NRC wind tunnel

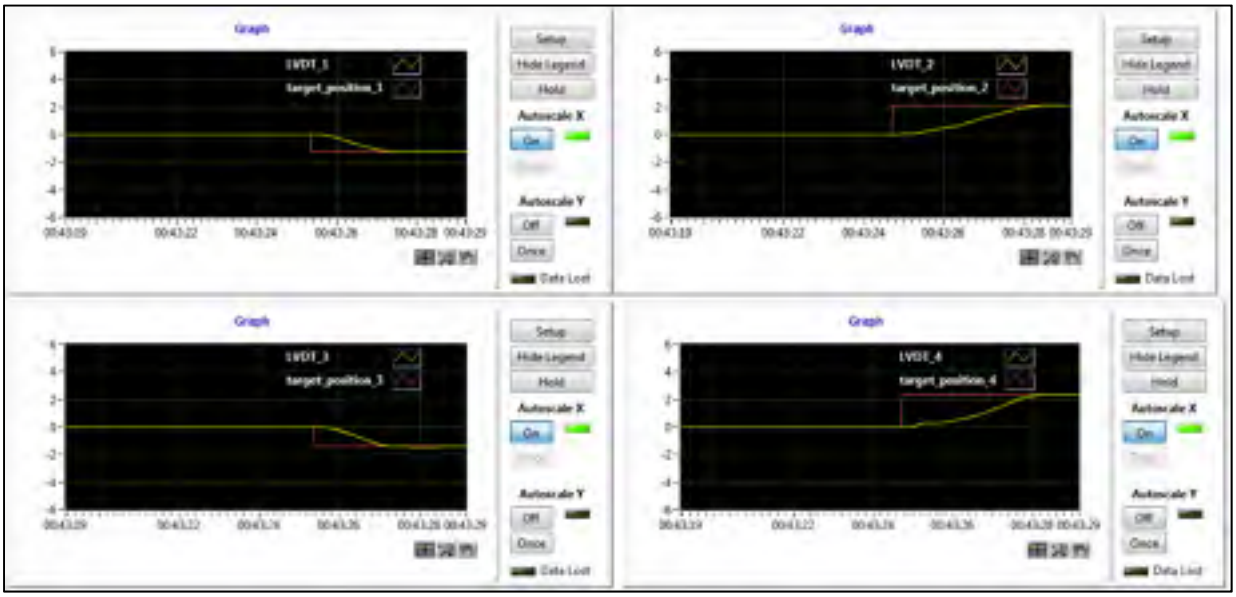

Figure 4.14 The actuation results during the wind tunnel
test for M=0.15, α=0.25˚ and δ=0˚ flow conditions

According to the results presented in the first picture of Figure 4. 15, the mean value estimated for the position of the laminar to turbulent airflow transition over the entire wing upper surface in original (un-morphed) configuration was 57.4% of the wing chord, with an error between -0.1% and +0.5%. The interpretation of the results exposed in the second picture

of Fig. 15, for the morphed configuration of the wing, locate the transition at 73.0% of the wing chord (with an error between -0.3% and +1.1%), in the area of the wing conjunction with the aileron.

Therefore, the improvement bring by the morphing technology in this flow case (M=0.15, α=0.25˚ and δ=0˚), calculated as the difference between the mean values estimated for the position of the laminar to turbulent airflow transition over the entire wing upper surface for the morphed and the original (un-morphed) configurations, is 73.0%-57.4%=15.6% of the wing chord.

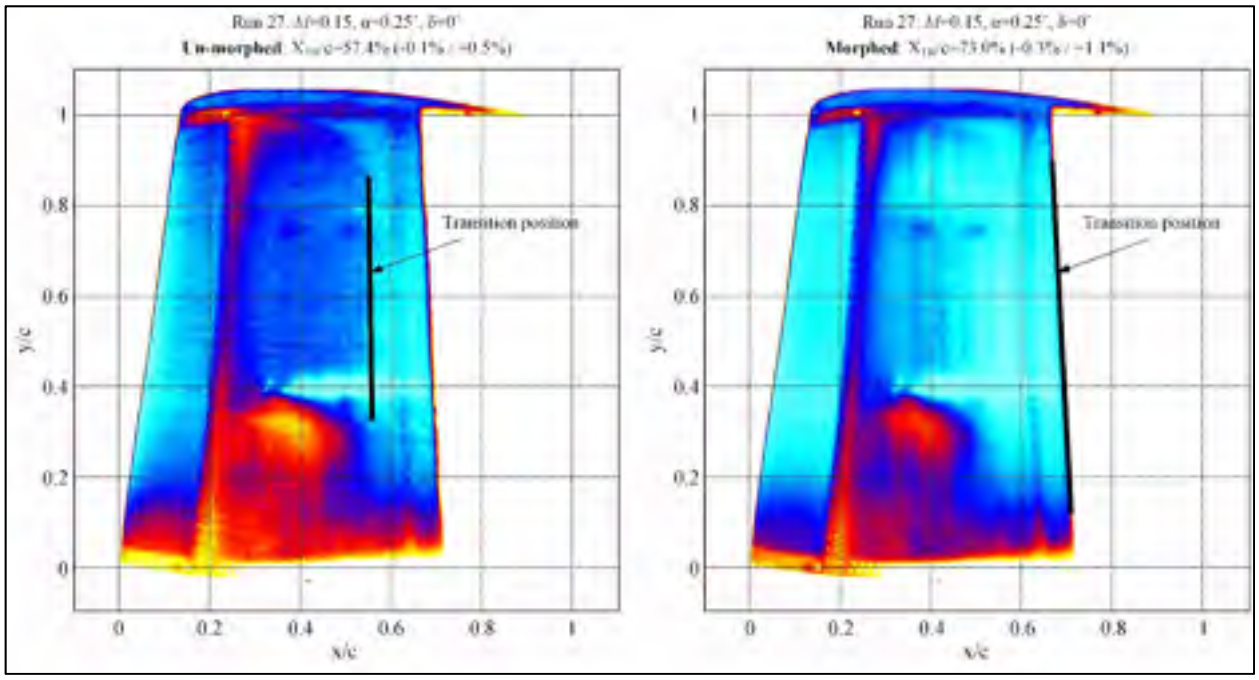

Figure 4.15 IR caption of the transition region
for M=0.15, α=0.25˚ and δ=0˚ flow conditions

During all three wind tunnel tests, the research team of the project observed that all three mechanisms used to estimate the airflow transition position (FFT, STD and IR) provided similar estimates related to the Kulite sensors span-wise station both for original (un-morphed) and morphed configurations, validating in this way the airflow's IR thermography analyze performed for the whole surface of the wing. Also, the team observed that the morphing technology improved the mean position of the laminar to turbulent flow transition over the whole wing (the difference between the mean values estimated for the position of the laminar

to turbulent airflow transition over the entire wing upper surface for the morphed and the original (un-morphed) configurations) with more than 2.5% of the wing chord for the great majority of the wind tunnel tested flight cases.

4.8 Conclusions

Shown here was a part of the work done during a major morphing wing research project exploring the improvement possibilities for the aerodynamics of a full-scaled portion of a real wing. The main presented contributions referred to the design of the control system used in the morphing wing application and to the experimental testing of the developed physical model for the morpable wing. The morphing actuation system included four similar miniature actuators placed inside the wing and based on four BLDC motors. The actuators were in house developed by the research team in such a way that they were able to execute a direct actuation of the flexible upper surface of the wing.

The tuning algorithm for the control system of this actuation system has been based on the Particle Swarm Optimization (PSO) method. In recent heuristic search methods PSO is one of the methods which takes inspiration from the collaborative behavior of the biological population or swarming. The obtained control coefficients were tested, with very good results, both through numerical simulations, but also experimentally, in bench tests and wind tunnel tests, together with all stuff included by the developed experimental model of the morphing wing. The wind tunnel testing supposed not only the evaluation of the controlled actuation system, but also, the testing of the integrated morphable wing experimental model, and the evaluation of the aerodynamic benefits brought by the morphing technology on this project.

The evaluation of the model from the perspective of the aerodynamics improvement implied the monitoring of the airflow on the morphable upper surface of the experimental model. Various techniques were used in this way: the acquisition of the pressure data provided by some Kulite pressure sensors, and theirs processing based on Fast Fourier Transform (FFT) and on Standard Deviation (SDT) evaluation, and infra-red (IR) thermography camera

visualizations. The FFT and STD techniques provided a 2D estimation of the position for the laminar to turbulent airflow transition in the pressure sensors station, while the IR technique provided a 3D estimation of this position.

The results obtained during the wind tunnel testing proved that the morphing technology is one of the most promising technologies for the improvement of the aircraft aerodynamics, providing in this way a fuel consumption reduction for the next generation of aircraft. The research team observed that the morphing technology improved the average position of the laminar to turbulent flow transition over the whole wing with more than 2.5% of the wing chord for the great majority of the 97 tested flight cases.

The research team observed that the morphing technology improved the mean position of the laminar to turbulent flow transition over the whole wing (the difference between the mean values estimated for the position of the laminar to turbulent airflow transition over the entire wing upper surface for the morphed and the original (un-morphed) configurations) with more than 2.5% of the wing chord for the great majority of the 97 tested flight cases.

4.9 Acknowledgments

The authors would like to thank the Thales team for their support, with special thanks to Mr. Philippe Molaret, Mr. Bernard Blouin and Mr. Xavier Louis, and the Bombardier Aerospace team - Mr. Patrick Germain and Mr. Fassi Kafyeke for their help and fruitful discussions. We would also like to thank Bombardier Aerospace, Thales, and the Consortium for Research and Innovation in Aerospace in Quebec (CRIAQ) and the National Sciences and Engineering Research Council (NSERC) for the funding received in connection with the CRIAQ MDO 505 project.

CHAPTER 5 THIRD ARTICLE

Fuzzy logic based control for a morphing wing-tip actuation system: design, numerical simulation and wind tunnel experimental testing

Shehryar Khan [1], Teodor Lucian Grigorie [1, 2, *], Ruxandra Mihaela Botez [1], Mahmoud Mamou [3] and Youssef Mébarki [3]

[1] École de Technologie Supérieure, Laboratory of Active Controls, Avionics and AeroServoElasticity LARCASE, Montreal H3C-1K3, Quebec, Canada; sherykhann@yahoo.com, Ruxandra.Botez@etsmtl.ca

[2] Military Technical Academy "Ferdinand I", Faculty of Aircraft and Military Vehicles, Center of Excellence in Self-Propelled Systems and Technologies for Defense and Security, Bucharest 040531, Romania; ltgrigorie@yahoo.com

[3] Aerodynamics Laboratory, NRC Aerospace, National Research Council Canada, Ottawa K1A0R6, Ontario, Canada; Mahmoud.Mamou@nrc-cnrc.gc.ca, Youssef.Mebarki@nrc-cnrc.gc.ca

Proof of publication:

The paper was accepted in "Journal of Biomimetics", 2019.

RÉSUMÉ

L'article présente la conception, la simulation numérique et les essais expérimentaux en soufflerie d'un système de commande basé sur ''une logique floue'' pour un nouveau système d'actionnement d'aile déformable équipé de moteurs à courant continu sans balais (BLDC), dans le cadre d'un projet international CRIAQ MDO 505. La déformation de l'aile est une préoccupation majeure de l'industrie aéronautique en raison des résultats prometteurs qu'on peut obtenir pour l'optimisation du carburant. Dans cette idée, un important projet international d'aile déformable a été réalisé par notre équipe universitaire du Canada, en collaboration avec des entités industrielles, de recherche et universitaires de notre pays, mais aussi d'Italie, en

utilisant une aile d'avion réelle équipée d'un aileron. L'objectif était de concevoir, fabriquer et tester un modèle expérimental d'aile pouvant être déformé de manière contrôlée et de fournir ainsi une extension de la zone d'écoulement laminaire sur sa surface supérieure, produisant une réduction de traînée avec un impact direct sur la consommation de carburant. Les travaux présentés dans cet article visent à décrire comment le modèle expérimental a été développé, contrôlé et testé afin de prouver la faisabilité de la technologie des ailes déformables pour la prochaine génération d'avions.

Abstract: The paper presents the design, numerical simulation and wind tunnel experimental testing of a fuzzy logic based control system for a new morphing wing actuation system equipped with Brushless DC (BLDC) motors, under the framework of an international project CRIAQ MDO 505. Morphing wing is a prime concern of the aviation industry due to the promising results it can give towards the fuel optimization. In this idea, a major international morphing wing project has been carried out by our university team from Canada, in collaboration with industrial, research and university entities from our country, but also from Italy, by using a full scaled portion of a real aircraft wing equipped with an aileron. The target was to conceive, manufacture and test an experimental wing model able to be morphed in a controlled manner and to provide in this way an extension of the laminar airflow region over its upper surface, producing a drag reduction with direct impact on the fuel consumption economy. The work presented in the paper aims to describe how the experimental model has been developed, controlled and tested in order to prove the feasibility of the morphing wing technology for the next generation of aircraft.

Keywords: morphing wing; experimental model; control system; fuzzy logic; BLDC motors; wind tunnel testing; pressure data processing; infrared thermography.

5.1 Introduction

Rising environmental concerns, fuel prices and ever increasing operational cost has raised the concerns of aviation industry. Last two decades industry has increased its collaboration

with academia and research institutes around the world in an effort to accelerate the technological advancements of aircraft systems with an ultimate aim of reducing the overall operating cost. On these lines several initiatives were started by industry around the world.

Among these research initiatives NOVEMOR project targeted the development of new concepts related to structures, aerodynamics, aero elasticity, adaptive morphing wing, noise impact reduction, loads reduction (Novel air vehicle configuration, 2019). A similar initiative is SARISTU, which was launched with the objectives of fuel optimization and consequently low passenger fares (SARISTU, 2019). In another collaboration between academia and industry, FutureWings project, funded research objective were to develop a wing having an ability to change their shape by them self-using piezoelectric fibers embedded into composite materials (FUTUREWINGS, 2019). LeaTop project focused on the development of Leading Edge Actuation Topology and identified important bottle necks in the design of leading edge morphing actuation (LeaTop, 2019). FlexSys in its collaboration with Air Force Research Laboratory developed variable geometry trailing edge structures which were composed of three wind tunnel models and a flight test specimen (Kota, S.; Osborn, 2009).

Within Joint European Initiative on Green Regional Aircraft frame, the researchers from CIRA in cooperation with the University of Naples, Department of Aerospace Engineering, used the Shape Memory Alloy (SMA) technology in the development of morphing wing architectures (Ameduri, S.; Brindisi et al, 2012). Morphing wings are in demand due the fact that they can reduce the drag on the aircraft wings and which results in fuel optimization. Additionally they can reduce the weight of the aircraft by eliminating the need for conventional flaps and ailerons. At Texas A&M University-Kingsville a morphing wing was developed by using elastomeric composites as skins and actuators (Peel, L.D.; Mejia, J. et al,2008). Various studies related to this trend were performed also in Military Technical Academy in Romania (Larco, C.; Constatin, 2018). A review related to the development of pneumatic artificial muscles has been realized by the American researchers from the University of Maryland (Wereley, N.M.; Kothera et al, 2009); the target was to highlight theirs applications in the morphing wing field.

DARPA in collaboration with NASA and AFRL completed a morphing wing project where the objectives were to replace the conventional control surfaces with the hinge less morphing variable geometry control surfaces (Kudva, J.N., et al 2004). An international collaborative team, with researchers from Politecnico di Torino. Italy, and from RMIT University, Australia, realized the design, analysis and experimental testing of a morphing wing with the aim to obtain a new wing concept not to be affected by aerodynamic losses due to geometrical discontinuity typical of wing-flap assembly (Martinez, J.M.; Scopelliti et al 2017). The Indian Institute of Technology performed also some structural and aerodynamics studies on various wing configurations for morphing (Kumar, D.; Faruque Ali,et al 2018). A collaboration between the University of Tokyo and the Japan Aerospace Exploration Agency was concretized in the design, manufacturing and wind tunnel testing of a of variable camber morphing airfoil using corrugated structures (Yokozeki, T.; Sugiura, 2014). A research team from ONERA in France studied morphing winglet concepts with the aim to improve the load control and the aeroelastic behavior of civil transport aircraft (Liauzun, C.; Le Bihan, 2018).

In this international context, our team from Research Laboratory in Active Controls, Avionics and Aeroservoelasticity (LARCASE), Ecole de Technologie Supérieure (ETS) in Montréal, Canada, successfully fabricated and tested a morphing wing demonstrator, equipped with Shape Memory Alloys actuators, during a major morphing wing project financed by the Consortium for Research and Innovation in Aerospace in Quebec and called CRIAQ 7.1 - *Improvement of laminar flow on a research wing*. Key objectives were in-flight fuel economy, replacement of conventional control surfaces, reduction of drag to improve range and reduce flutter risk and vibrations. The experimental model of the morphing wing was a rectangular one, with 0.5 m of chord and 0.9 m of span, and has been manufactured starting from a reference airfoil WTEA-TE1. The upper surface of the model was a flexible skin from a composite material which include a resin matrix, Kevlar fibers and layers of carbon. Two actuation lines based on the Shape Memory Alloys have been used to morph the skin towards the optimized profile, being controlled in the “open loop” architecture by using both conventional and intelligent control methods. Also, few methodologies for laminar to turbulent flow detection have been experimentally demonstrated, together with a closed loop morphing

wing control method based on the feedback provided by some pressure sensors fixed on the flexible upper surface of the wing (Popov, A.V.; Grigorie, T.L., et al 2010).

Recently, aircraft systems are going under a major change where many of the mechanical, pneumatic and hydraulic systems are being replaced by the electrical systems. Boeing 787 and A-380 have comparatively greater number of electrical systems as compared to the conventional aircrafts (Wheeler, P.W.; Clare, J.C et al 2013). Electrical systems come with the benefits that they are light weight, lot quieter and efficient as compared to the hydraulic and pneumatic counterparts. The enabling technology for More Electrical Aircraft (MEA) is power electronics without which it cannot be realized. However, aerospace applications still present challenges to the field of power electronics from the perspective of volume, weight and size (Madonna, V.; Giangrande, 2018). Advisory council for aeronautics research in Europe has set a target to reduce aircraft CO2 emission, fuel optimization and weight reduction of the aircraft. In order to achieve this target aircraft manufacturers are focusing on the development of the MEA technology (Sun, J.; Guan, Q.; Yanju et al, 2016).

In this trend of the green aircraft technologies growth, correlated with the replacement of the conventional pneumatic/hydraulic/mechanical actuators with the electrical ones, our team developed a second major morphing wing project on a real aircraft wing equipped with an aileron and morphed with an actuation system equipped with Brushless DC (BLDC) motors. The here presented work was performed under this project, called CRIAQ MDO-505 - *Morphing architectures and related technologies for wing efficiency improvement*.

5.2 Short Description of the Morphing Wing Project

The project was developed in Canada and Italy, having as leader the École de Technologie Supérieure (ETS) in Montreal, as Canadian partners, École Polytechnique in Montreal, Institute for Aerospace Research of the National Research Council Canada (IAR-NRC), Bombardier Aerospace, Thales Avionics, and as Italian partners, University of Naples

Frederico II, CIRA and Alenia. The project calls for both aerodynamic modeling as well as conceptual demonstration of the morphing principle on real models placed in the wind tunnel, i.e. of a full scaled portion of a real aircraft wing equipped with an aileron (morphing wing-aileron). The project objective is to obtain a morphing wing-aileron experimental model able to be morphed in a controlled manner and to provide in this way an extension of the laminar airflow region over its upper surface, producing a drag reduction with direct impact on the fuel consumption economy. The physical model developed is shown in Figure 5.1, where four BLDC motor based actuators are mounted under the morphable wing along with 32 Kulite pressure sensors used to monitor the transition point.

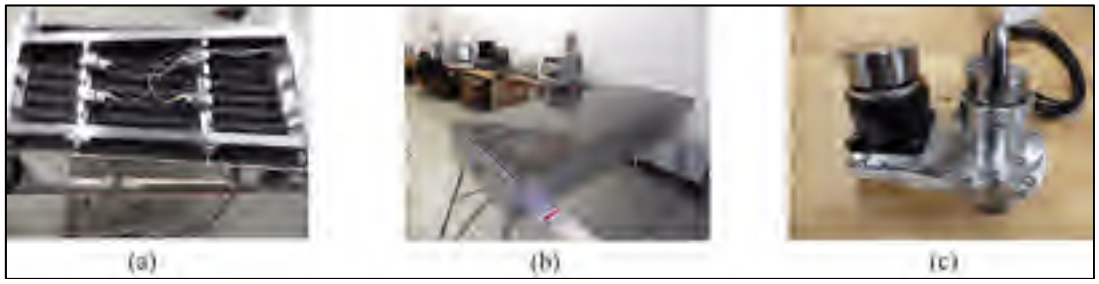

Figure 5.1 Morphing wing and BLDC motor based actuator.

Our team working at LARCASE is focusing on two main objectives: a) To sense and monitor the pressure over the flexible skin using pressure sensors; b) To develop an actuator control system which can move the laminar to turbulent transition point towards the trailing edge and hence result in large laminar flows.

In initial aerodynamic studies some optimized airfoils were computed for 97 flow cases generated as combinations of nineteen values for the angle of attack α (between –3° and +3°), three values for the Mach number *M* (0.15, 0.2 and 0.25) and thirteen values for the aileron deflection angle δ (between –6 and +6°). Computational Fluid Dynamics software in combination with optimization algorithms was used to compute the optimum airfoils shapes. For all of the 97 studied flow cases the optimum airfoil shape was searched by changing its local thickness in order to extend the laminar region of the upper surface flow (Koreanschi, A.; Sugar-Gabor et al, 2016).

At the requirement of the industrial partners involved in the project the wing structure was kept unchanged, similar to the real-life version of the aircraft, except for its upper surface which was replaced by a flexible skin, made from composite material. The model resulted with a 1.5 m span and a 1.5 m root chord, including the aileron, with a taper ratio of 0.72 and a leading-edge sweep of 8°. As shown in Figure 1, the experimental wing model is composed of three parts: a) unmodified metal structure, b) flexible upper skin, and c) actuation system. The flexible skin placed on the upper surface of the wing was delimited by the front and rear spars placed between 20% and 65% of the wing chord. The metal part is composed of four ribs, two of them are in the mid (Rib#2 and Rib#3) and two of them are on the edges (Rib#1 and Rib#4). The actuation system used to morph the wing used four in house developed miniature electrical actuators based on BLDC motors, which performed a direct actuation of the flexible skin. The four identical actuators are placed on the two actuation lines as shown in Figure 5.2, installed in two sections considered at 37% and 75% of the wing span. Each of the two actuation lines includes two actuators placed at 20% and 65% of the local wing chord.

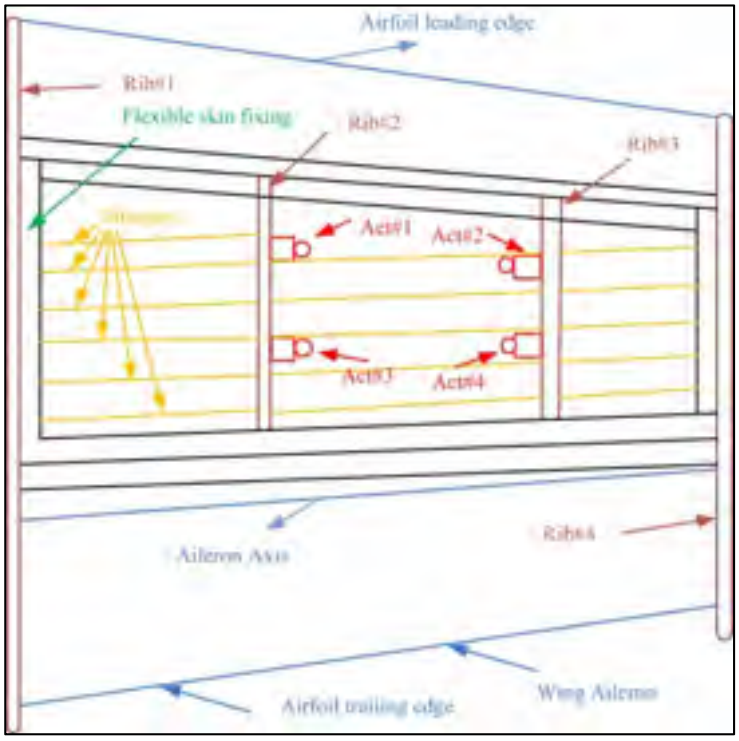

Figure 5.2 Morphing wing layout.

Subject wingtip is the demonstrator for the morphing wing of the regional aircraft as shown in Figure 5.3. The final configuration of the wing-aileron model included a morphable aileron designed and manufactured by the Italian team (Amendola, G.; Dimino et al 2016).

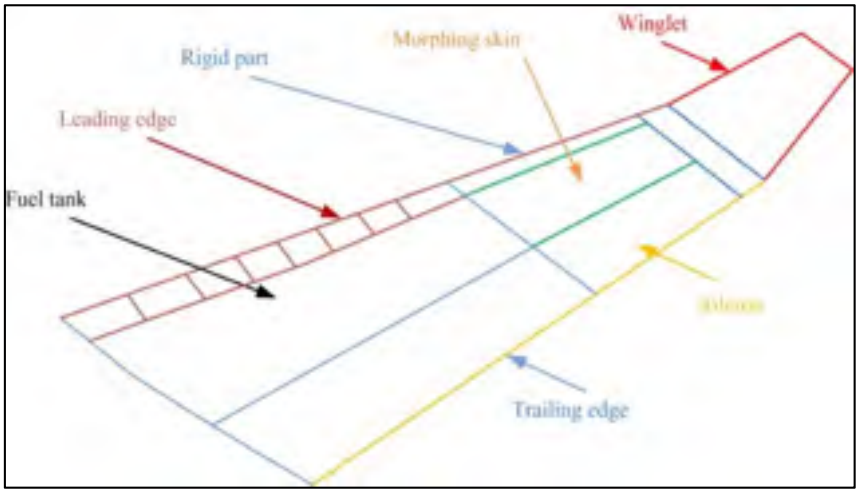

Figure 5.3 The demonstrator for the morphing wing of the regional aircraft.

To evaluate the added value of the morphing technology on our project, the developed experimental model of the morphable wing-aileron system has been tested in the subsonic wind tunnel of the National Research Council of Canada. This testing phase was a complex one because the team aimed also to validate the results obtained after the numerical optimization of the airfoil shape for all 97 studied flow cases, and to observe the behavior of the experimental model as a whole in various testing conditions similar to the ones found in a real flight, both from the point of view of the flow parameters, but also from the point of view of the perturbations, which in this situation were induced by the wind tunnel.

The here presented work refers to the design, numerical simulation and experimental testing of an intelligent control method, based on fuzzy logic technique for a new morphing wing actuation system equipped with BLDC motors. The paper aims also to describe how the experimental morphing wing model has been developed, controlled and tested in order to prove the feasibility of the morphing wing technology for the next generation of aircraft.

5.3 Physical architecture and simulink model of the controlled actuator

Over the last decades, BLDC motors have gained much reputation and they have many applications in aerospace, automotive industry, medical instruments and industrial automation. The choice between Brush DC motor and BLDC motor really depends on many factors, the difference becomes clearer when the motor has to operate in high temperatures. Due to the absence of carbon brushes the BLDC has much less wear and tear and more time between the maintenance. On the other way, the BLDC motors are electronically commutated, and has an improved torque to size ratio which means that they are more useful in the applications where space and weight are critical. Between the advantages of the BLDC motors with respect to DC motors may be specified: better speed ranges than DC motors, improved torque efficiency, less noise, improved efficiency, long operating life, better weight to size ratio (Allied Motion Technologies, 2019). Having in mind that reasons, but also the structural particularities of our application which required a higher torque to size ration due to the direct actuation in a small space, the team decided to use some actuators based on BLDC motors. Because the market did not offer a convenient solution our team resorted to manufacturing its own actuators by using some BLDC motors provided by the Maxon Company (Maxon Motor Inc et al, 2019).

The novel morphing actuator used in CRIAQ MDO 505 morphing wing project is composed of BLDC motor coupled to the linear actuator through gears (Figure 5.4). The shaft of the motor is coupled to the gears which in turn are coupled to the screw through gears, in this way the rotational motion of the gear is converted to the linear motion as shown in Figure 4e. Figure 4a and Figure 4b shows the actuator piston and housing. Figure 4b exposes the mechanical structure which is mounted on the linear screw and is moved up and down either to push the skin of the wing up or down based on the various flight conditions. Figure 4c depicts the LVDT (Linear Variable Differential Transformer), which is coupled via gears to the linear screw of the actuator to measure the linear displacement travelled by the actuator, and to provide in this way the feedback signal for the position control loop. The relationship between the rotational speed of the BLDC motor and the linear screw is such that for each 100

revolutions of motor the linear screw would move 1mm. Figure 4d represents the actuator placement under the morphing skin.

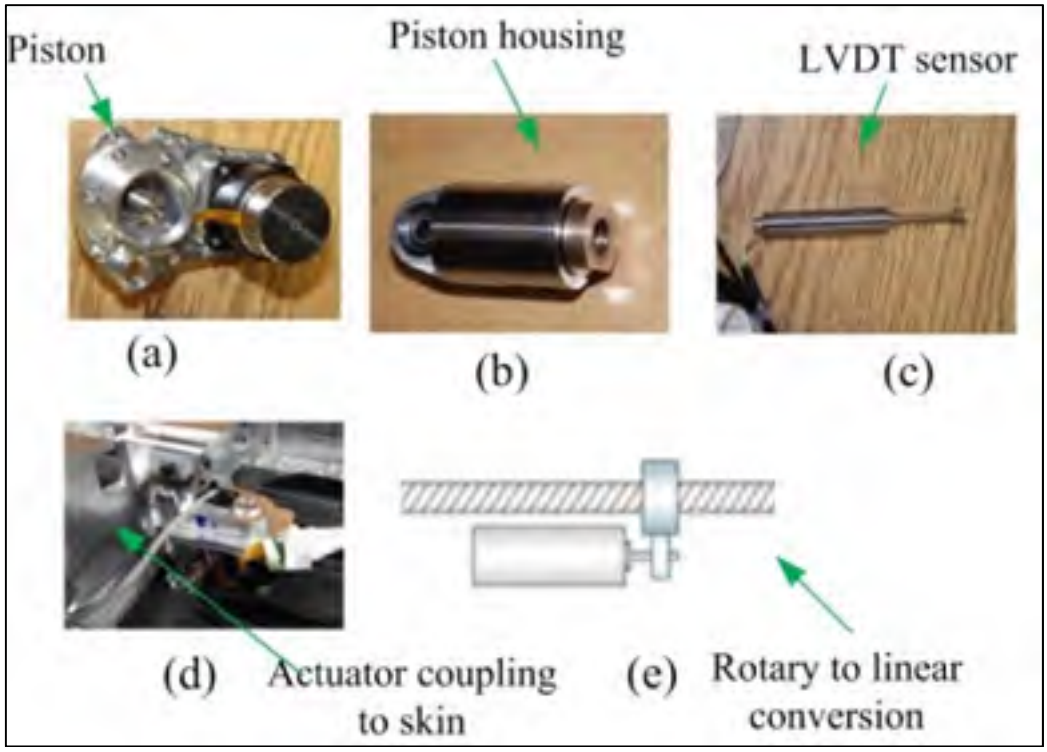

Figure 5.4 The demonstrator for the morphing wing of the regional aircraft.

The morphing actuator: (**a**) Piston; (**b**) Piston housing; (**c**) LVDT sensor; (**d**) Actuator coupling with wing skin; (**e**) Principle of rotary to linear conversion.

The control model of the actuators used in CRIAQ MDO 505 project has been presented in (Khan, S.; Botez, R. M et al, 2015). This section will explain the major blocks which were used in the actuator modeling. Major component driving the actuator is the BLDC motor, acquired from Maxon Motor Inc., with nominal voltage of 12 volts, nominal current of 1 ampere and nominal torque of 25 mN-m. With these characteristics the motor was considered capable enough to provide the necessary torque to push the skin of the morphing wing. The Matlab/Simulink software model obtained for the linear model of the motor, which was used in the design of the actuator control, looks as in Figure 5.4 ; it has been called “BLDC model”. The software includes three main parts: the electrical model of the motor, the mechanical model of the motor, and the model of the mechanism converting angular actuation to linear actuation. The “BLDC model” block inputs are the DC bus voltage “Ud” and the load torque

“T load”, while it provides as outputs the actuation speed “v” (expressed in mm/s), the actuation linear position “pos”, (expressed in mm) and the electrical current “I” (expressed in A).

As shown in Figure 5.5, the linear position of the actuator can be obtained after incorporating the appropriate gains representing the operation of the gears converting the rotary motion into the linear motion. Since the morphing actuator has to push against the load offered by the skin of the wing, there is a need to control the amount of current flowing in the coils of the BLDC motor, which in turn controls the torque produced by the motor. Current control loop is also required for the speed and position control loops as the amount of current decides the speed and torque with which the actuator will acquire the required skin displacement for each flight case. To design the control system of the actuator at the level of its three control loops (for actuation position, actuation speed and electrical current), the “BLDC model” block was integrated into the model in Figure 5.5. According to the model in Figure 5, the electrical current results as output of the “Electrical TF” transfer function, while the actuation speed expressed in rad/s is the output of the “Mechanical TF” transfer function, which is further converted in mm/s, but also provides the actuation linear displacement expressed in mm. All three parameters obtained as outputs of the “BLDC model” block are used as feedbacks for the three control loops of the electrical actuator, as it is presented in Figure 5.6.

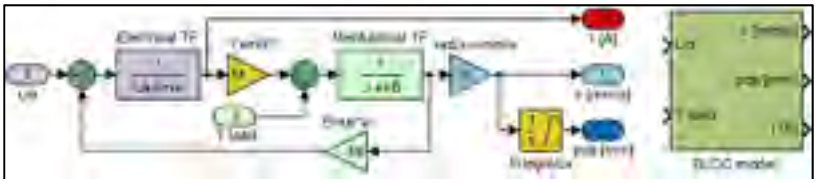

Figure 5.5 MATLAB/Simulink model of BLDC motor.

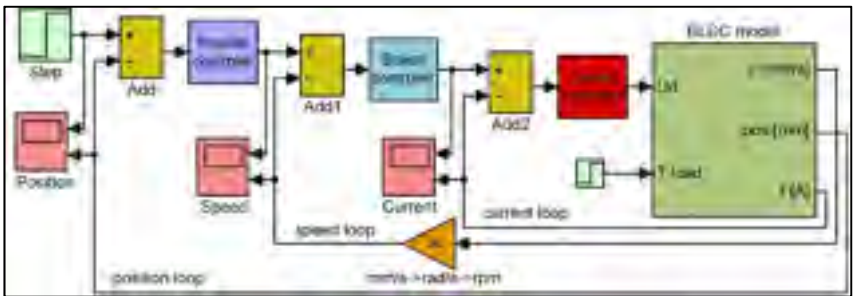

Figure 5.6.Control system of the morphing

actuator based on three control loops**.**

5.4 The control system design and numerical validation results

A short literature review show that the position control of the BLDC motors can be performed in many ways, the simplest one being based on the classical PID controllers with or without all control components inside. Due to the nonlinear character of the system as a whole, generated especially by the complex behavior of the morphed flexible skin interacting with actuators and with the aerodynamic loads appearing in the wind tunnel testing, the team decided to develop an intelligent control variant for the morphing actuation system. Therefore, the system controlling the morphing actuators, which is here shown, is a nonlinear one, being based on the fuzzy logic technique for all of the three control loops used for each of the four actuators.

Fuzzy controllers are based on fuzzy inference systems (FIS's), which is composed of several steps. Firstly, the inputs are mapped into appropriate membership functions, following which IF-THEN logic rules are created. The IF's are known as "antecedents", while the THEN's are known as "consequents". Based on the membership grades all the rules which are invoked are combined. In the final stage the combined result from all the rules is converted into a specific output control value.

The numerical simulations achieved in the design phase provided a fuzzy logic Proportional-Derivative architecture for the position control loop, with the schema in Figure

5.7a, a fuzzy logic Proportional-Integral-Derivative architecture for the speed control loop, with the schema in Figure 5.7b, and a fuzzy logic Proportional-Integral architecture for the electrical current control loop, with the schema in Figure 5.7c. The obtained FISs were called "PositionFIS" (for the position controller), "SpeedFIS" (for the speed controller), and "CurrentFIS", for the electrical current controller. The elements in Figure 5.7 are: Kp_p - proportional gain in position control loop, Kd_p - derivative gain in position control loop, K_p - change in output gain in position control loop, Kp_s - proportional gain in speed control loop, Kd_s - derivative gain in speed control loop, Ki_s - integral gain in speed control loop, K_s - change in output gain in speed control loop, Kp_c - proportional gain in current control loop, Ki_c - integral gain in current control loop, and K_c - change in output gain in current control loop. With the three controllers structures presented in Figure 5.7 the Matlab/Simulink model for the morphing actuator control system resulted as in Figure 5.8.

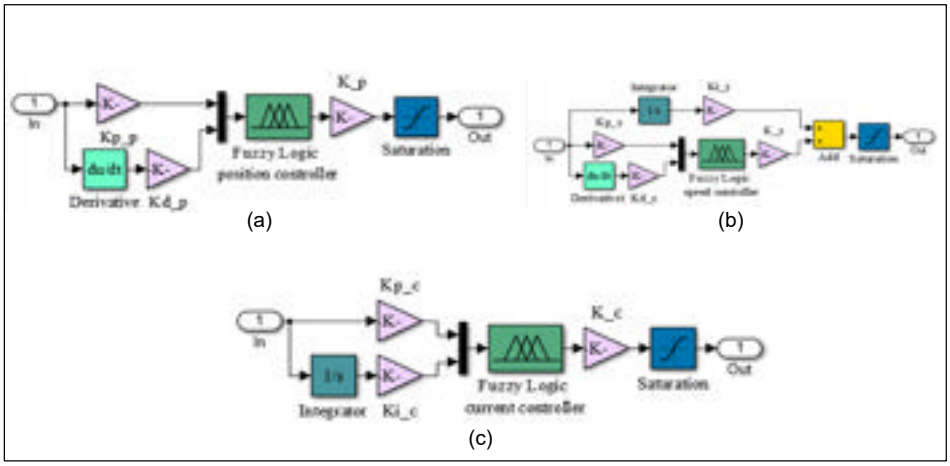

Figure 5.7 Structures of the controllers used in the three loops:

(**a**) Position; (**b**) Speed; (**c**) Current.

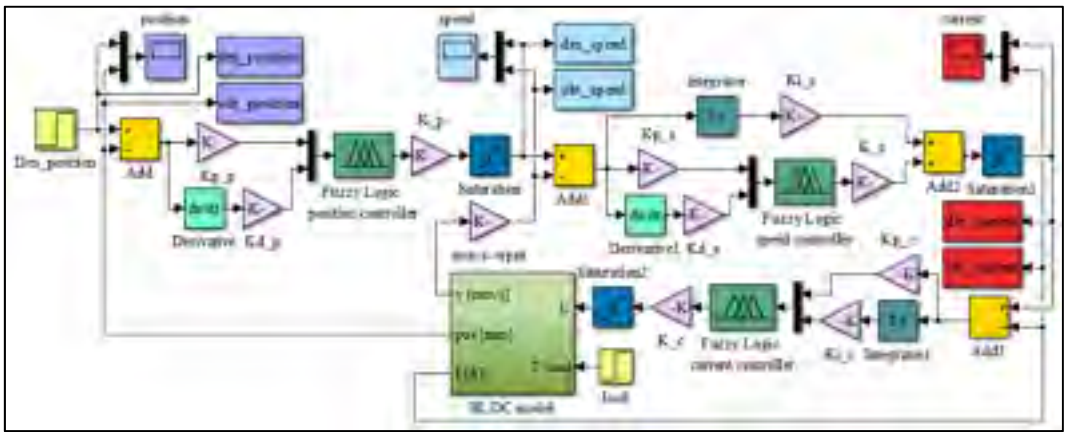

Figure 5.8 Matlab/Simulink model for the morphing actuator control system.

Considering [-4, 4] interval as universe of discourse for the first input of the "PositionFIS", and [-5×10^4, 5×10^4] interval as universe of discourse its second input, six membership functions (*mf*) were chosen for each of the two inputs (A_1^1 to A_1^6, respectively A_2^1 to A_2^6). The linguistic terms for both inputs, but also for the output, were NB (negative big), NM (negative medium), NM (negative small), PS (positive small), PM (positive medium) and PB (positive big). The considered shapes for the first input membership functions were *z*-functions (*mf*1), π-functions (*mf*2 to *mf*5), respectively *s*-functions (*mf*6), while for the second input membership functions shapes was a triangular one.

From the perspective of the "SpeedFIS" fuzzy inference system, [-150, 150] interval was chosen as universe of discourse for the first input, and [-1.5×10^4, 1.5×10^4] interval as universe of discourse for its second input. This time, seven membership functions (*mf*) were chosen for each of the two inputs of the FIS, while, from the linguistic terms point of view, for both inputs, but also for the output, a new one has been added (Z (zero)) comparatively with the "PositionFIS". The considered shapes for the both inputs membership functions were *z*-functions (*mf*1), π-functions (*mf*2 to *mf*6), respectively *s*-functions (*mf*7).

A simplified situation was for the "CurrentFIS" fuzzy inference system, where each of the two inputs were used with two membership functions, with *z*-function (*mf*1), respectively *s*-function shapes (*mf*2). [-3, 3] and [-0.01 0.01] intervals were chosen as universes of discourse

for the first input, and for the second input, respectively. In this case, the linguistic terms for both inputs were N (negative) and P (positive), while for the output were N (negative), Z (zero) and P (positive).

An *s*-function shaped membership function can be implemented using a cosine function :

$$s(x_{left}, x_{right}, x) = \begin{cases} 0, & \text{if } x < x_{left} \\ \frac{1}{2}\left[1 + \cos\left(\frac{x - x_{right}}{x_{right} - x_{left}}\pi\right)\right], & \text{if } x_{left} \le x \le x_{right}, \\ 1, & \text{if } x > x_{right} \end{cases} \tag{5.1}$$

a *z*-function shaped membership function is a reflection of a shaped *s*-function (Grigorie, T.L.; Popov, A.V.et al, 2011):

$$z(x_{left}, x_{right}, x) = \begin{cases} 1, & \text{if } x < x_{left} \\ \frac{1}{2}\left[1 + \cos\left(\frac{x - x_{left}}{x_{right} - x_{left}}\pi\right)\right], & \text{if } x_{left} \le x \le x_{right}, \\ 0, & \text{if } x > x_{right} \end{cases} \tag{5.2}$$

and a π -function shaped membership function is a combination of both functions (Grigorie, T.L.; Popov, A.V.et al, 2011):

$$\pi(x_{left}, x_{m1}, x_{m2}, x_{right}, x) = \min[\, s(x_{left1}, x_{m1}, x),\ z(x_{m2}, x_{right}, x)], \tag{5.3}$$

with the peak flat over the [x_{m1}, x_{m2}] middle interval. x is the independent variable on the universe of discourse, x_{left} is the left breakpoint, and x_{right} is the right breakpoint (Grigorie, T.L.; Popov, A.V.et al, 2011). On the other way, the triangular shape can be expressed as follows ([34]):

$$f_{\Delta}(x; a, b, c) = \begin{cases} 0, & \text{if } x \le a, \\ \frac{x-a}{b-a}, & \text{if } a < x < b, \\ \frac{c-x}{c-b}, & \text{if } b \le x < c, \\ 0, & \text{if } c \le x, \end{cases} = \max\left[\min\left(\frac{x-a}{b-a}, \frac{c-x}{c-b}\right), 0\right]. \tag{5.4}$$

Similarly, x is the independent variable on the universe of discourse, while the parameters a and c locate the feet of the triangle and b gives its peak.

In accordance with the expressions given in Eqs. (5.1) to (5.4), the parameters characterizing the membership functions for the first input of the “PositionFIS” and for both

inputs of the "CurrentFIS" are given in Table 5.1, the parameters characterizing the membership functions for both inputs of the "SpeedFIS" are given in Table 5.2, while the parameters characterizing the membership functions for the second input of "PositionFIS" are listed in Table 5.3.

Table 5.1 Parameters of the *mf* for the "PositionFIS" first input and for the "CurrentFIS" both inputs.

	PositionFIS/Input1						**CurrentFIS/Input1**		**CurrentFIS/Input2**	
Param.	***mf*1**	***mf*2**	***mf*3**	***mf*4**	***mf*5**	***mf*6**	***mf*1**	***mf*2**	***mf*1**	***mf*2**
x_{left}	-4	-4	-3	-1	0	2	-3	-2.4	-0.01	-0.008
x_{m1}	-	-2	-1	1	2	-	-	-	-	-
x_{m2}	-	-2	-1	1	2	-	-	-	-	-
x_{right}	-2	0	1	3	4	4	2.4	3	0.008	0.01

The rules for all three fuzzy inference systems involved in the control loops were defined by using the Sugeno fuzzy model, which was proposed by Takagi, Sugeno and Kang ([35]). According to this model, a fuzzy rule for a two input-single output system can be expressed as follows:

$$\text{"if } (x_1 \text{ is } A) \text{ and } (x_2 \text{ is } B) \text{ then } y = f(x_1, x_2)\text{"}, \tag{5.5}$$

where A and B are fuzzy sets in the antecedent, $y = f(x_1, x_2)$ is a crisp function in the consequent, and f is a polynomial function (Grigorie, T.L.; Popov, A.V et al, 2011). If f is a constant, then the Sugeno fuzzy model is a zero-order model. Considering [-3000, 3000] interval as universe of discourse for the "PositionFIS" output and a zero-order Sugeno fuzzy model, the output *mf* were chosen as constants with the values: NB=-3000, NM=-2500, NS=-1000, PS=1000, PM=2500 and PB=3000. Also, for the output of the "SpeedFIS" the [-120, 120] interval was used as universe of discourse and the *mf* resulted with the values NB=-120, NM=-60, NS=-30, Z=0, PS=30, PM=60 and PB=120, while for the "CurrentFIS" output the [-1.5, 1.5] interval was used as universe of discourse and the *mf* taken with the values N=-1.5, Z=0, P=1.5.

Table 5.2 Parameters of the *mf* for the both inputs of the "SpeedFIS".

	SpeedFIS/Input1							SpeedFIS/Input2						
Param.	***mf*1**	***mf*2**	***mf*3**	***mf*4**	***mf*5**	***mf*6**	***mf*7**	***mf*1**	***mf*2**	***mf*3**	***mf*4**	***mf*5**	***mf*6**	***mf*7**
x_{left}	-150	-150	-100	-50	0	50	100	$-1.5\cdot10^4$	$-1.5\cdot10^4$	$-1\cdot10^4$	$-5\cdot10^3$	0	$5\cdot10^3$	$1\cdot10^4$
x_{m1}	-	-100	-50	0	50	100	-	-	$-1\cdot10^4$	$-5\cdot10^3$	0	$5\cdot10^3$	$1\cdot10^4$	-
x_{m2}	-	-100	-50	0	50	100	-	-	$-1\cdot10^4$	$-5\cdot10^3$	0	$5\cdot10^3$	$1\cdot10^4$	-
x_{right}	-100	-50	0	50	100	150	150	$-1\cdot10^4$	$-5\cdot10^3$	0	$5\cdot10^3$	$1\cdot10^4$	$1.5\cdot10^4$	$1.5\cdot10^4$

Table 5.3 Parameters of the *mf* for the second input of the "PositionFIS".

	PositionFIS/Input2					
Param.	***mf*1**	***mf*2**	***mf*3**	***mf*4**	***mf*5**	***mf*6**
a	$-7\cdot10^4$	$-5\cdot10^4$	$-3\cdot10^4$	$-1\cdot10^4$	$1\cdot10^4$	$3\cdot10^4$
b	$-5\cdot10^4$	$-3\cdot10^4$	$-1\cdot10^4$	$1\cdot10^4$	$3\cdot10^4$	$5\cdot10^4$
c	$-3\cdot10^4$	$-1\cdot10^4$	$1\cdot10^4$	$3\cdot10^4$	$5\cdot10^4$	$7\cdot10^4$

According to the values in the Table 5.1 to Table 5.3, the membership functions associated to the inputs of the "PositionFIS", "SpeedFIS" and "CurrentFIS" are by the forms exposed in Figure 5.5.

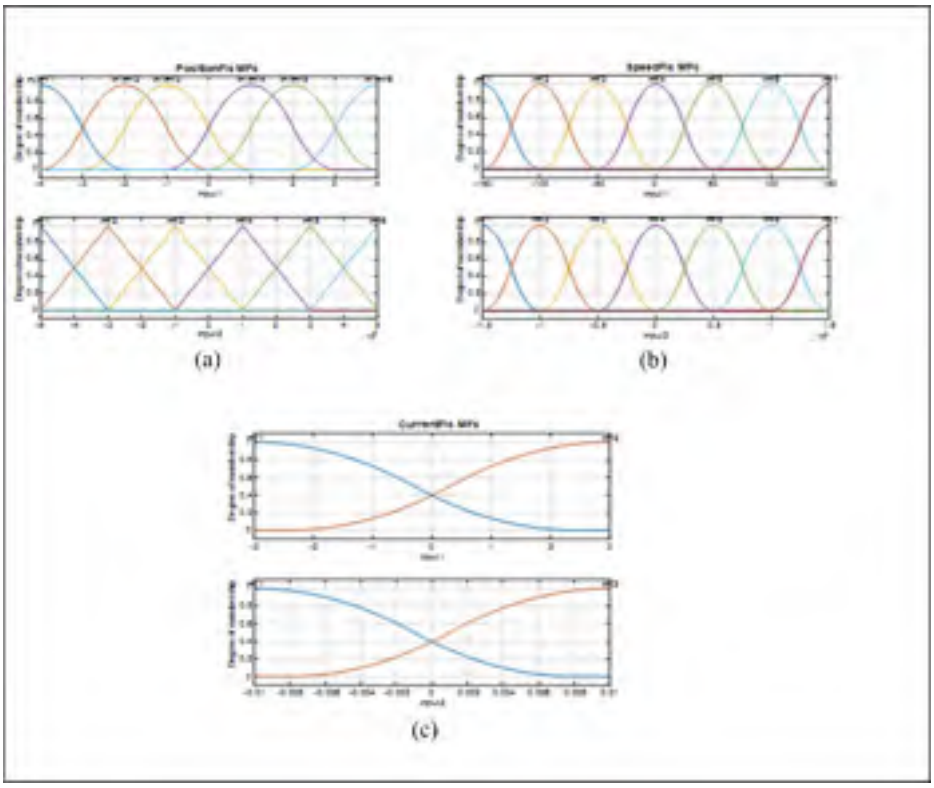

Figure 5.9. Membership functions for the FISs inputs: (**a**) PositionFIS; (**b**) SpeedFIS; (**c**) CurrentFIS.

Starting from the inputs' and output's membership functions of the three FISs, a set of 6 inference rules were obtained for the "PositionFIS":

$$\begin{aligned}
&\text{Rule 1: If } in1 \text{ is } A_1^1 \text{ and } in2 \text{ is } A_2^1, \text{ then } y^1(in1,in2) = -3000,\\
&\text{Rule 2: If } in1 \text{ is } A_1^2 \text{ and } in2 \text{ is } A_2^2, \text{ then } y^2(in1,in2) = -2500,\\
&\text{Rule 3: If } in1 \text{ is } A_1^3 \text{ and } in2 \text{ is } A_2^3, \text{ then } y^3(in1,in2) = -1000,\\
&\text{Rule 4: If } in1 \text{ is } A_1^4 \text{ and } in2 \text{ is } A_2^4, \text{ then } y^4(in1,in2) = 1000,\\
&\text{Rule 5: If } in1 \text{ is } A_1^5 \text{ and } in2 \text{ is } A_2^5, \text{ then } y^5(in1,in2) = 2500,\\
&\text{Rule 6: If } in1 \text{ is } A_1^6 \text{ and } in2 \text{ is } A_2^6, \text{ then } y^6(in1,in2) = 3000,
\end{aligned} \tag{5.6}$$

49 rules for the "SpeedFIS" (Figure 10), and 4 rules for the "Current FIS":

$$\begin{aligned}
&\text{Rule 1: If } in1 \text{ is } A_1^1 \text{ and } in2 \text{ is } A_2^1, \text{ then } y^1(in1,in2) = -1.5,\\
&\text{Rule 2: If } in1 \text{ is } A_1^1 \text{ and } in2 \text{ is } A_2^2, \text{ then } y^2(in1,in2) = 0,\\
&\text{Rule 3: If } in1 \text{ is } A_1^2 \text{ and } in2 \text{ is } A_2^1, \text{ then } y^3(in1,in2) = 0,\\
&\text{Rule 4: If } in1 \text{ is } A_1^2 \text{ and } in2 \text{ is } A_2^2, \text{ then } y^4(in1,in2) = 1.5.
\end{aligned} \tag{5.7}$$

In1 / In2	NB	NM	NS	Z	PS	PM	PB
NB	NB	NB	NB	NB	NM	NS	Z
NM	NB	NB	NB	NM	NS	Z	PS
NS	NB	NB	NM	NS	Z	PS	PM
Z	NB	NM	NS	Z	PS	PM	PB
PS	NM	NS	Z	PS	PM	PB	PB
PM	NS	Z	PS	PM	PB	PB	PB
PB	Z	PS	PM	PB	PB	PB	PB

Figure 5.10. The inference rules for the "SpeedFIS".

Starting from the characteristics previously specified for the three fuzzy inference systems theirs control surfaces have been obtained with the shapes presented in Figure 5.11.

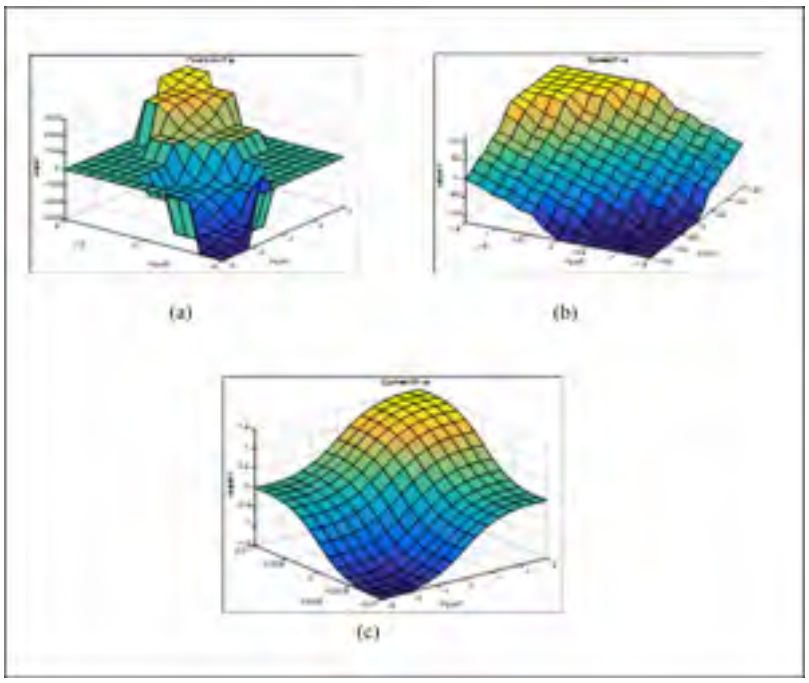

Figure 5.11 The fuzzy control surfaces for the three FISs:

(**a**) PositionFIS; (**b**) SpeedFIS; (**c**) CurrentFIS.

Following a tuning procedure, the best values of the controllers' gains were established, and further used in the control system Matlab/Simulink model in order to test is through

numerical simulation by using various signals as desired inputs. In a first numerical simulation test, a step input was applied as desired signal for the actuation position. The obtained results are shown in Figure 5.12 for all of the three controlled parameters: position, speed and electrical current. It can be easily observed that the designed control system worked very well in all of the three control loops. Moreover, in Figure 5.12a, which depicts the controlled actuation position, are presented together the results obtained by using the here design controller, but also the curve obtained if it is used a classical variant for the control system, designed also by our team research team (Khan, S.; Botez, R. M et al 2015). A short analyze of the two answers proves that the fuzzy logic based control system provides a small settling time comparatively with the classical control system.

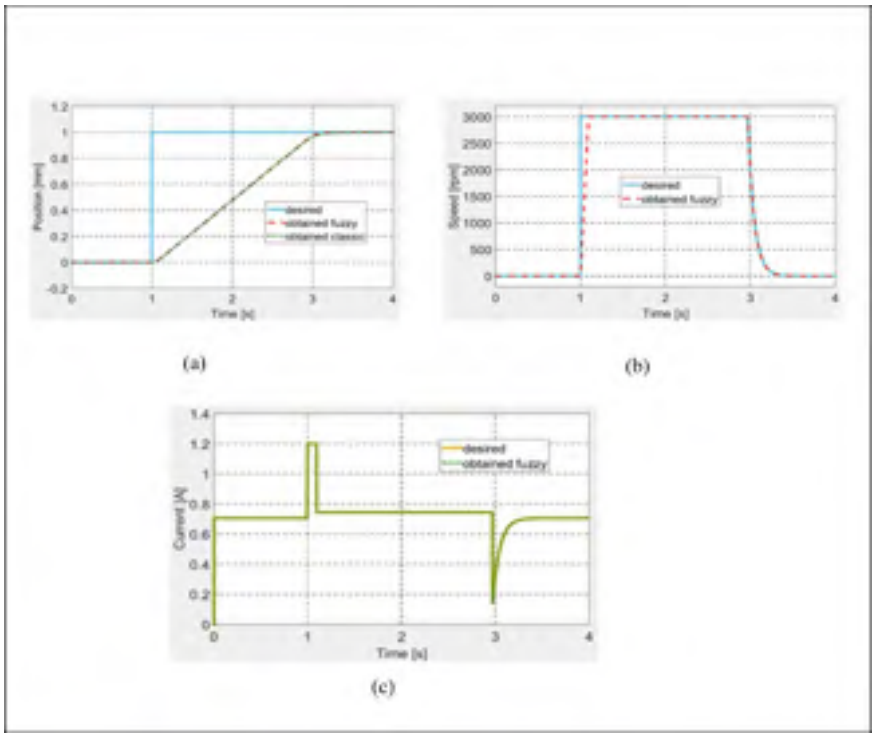

Figure 5.12. The control results for a step input as desired position:

(**a**) Position; (**b**) Speed; (**c**) Current.

Another important test required to the actuator to follow a desired position signal under the form of successive steps, in order to test the ability of the actuation system to switch

between positive and negative positions, similarly with the actuation situations resulted from the numerical optimization performed for the 97 flow cases. The results for this test are exposed in Figure 5.13, confirming once again a very good operation of the control system in all of the three control loops.

Once completed the design and testing through numerical simulation for the control system, the research team sent the morphing wing project at the next level, performing the integration of all components in the experimental model and preparing it for the wind tunnel tests.

5.5 Wind tunnel experimental testing of the wing-aileron morphing system

To evaluate the impact of the morphing technology on our experimental model the set of the 97 flow cases were studied both from numerical and experimental points of view. During the experimental evaluation, performed in the wind tunnel testing facility of the Canadian National Research Council in Ottawa, the airflow over the upper surface was monitored for all studied flow cases by using two techniques: 1) the real time processing of the pressure data in a section along the wing chord, which were collected by using 32 Kulite pressure sensors; 2) the Infrared (IR) thermography based on a Jenoptik camera, which provided captions for the airflow over the entire upper surface of the wing. Beside the real time monitoring, a post processing phase of the pressure data has been done; 20 kSamples/s was the rate for the pressure data recording in all of the 32 detection channels, both for original (un-morphed) and optimized (morphed) airfoils tested in the 97 flow cases. The main instruments in both pressure data processing phases were the Fast Fourier Transform (FFT) and the Standard Deviation (STD), which, together and based on different scientific arguments, served at the estimation of the laminar-to-turbulent airflow transition point position in the monitored section (2D estimation of this position). On the other way, the IR captions validated the technique based on the pressure data processing, but, more important, having in mind that the tested morphing wing has a complex structure, allowed the researchers to evaluate the global aerodynamic gain

produced by the morphing technology. This was possible because the IR technique provided captions with the whole upper surface of the wing, which facilitated the estimation of the position for the laminar-to-turbulent airflow transition region along the whole wing span (3D estimation of this position).

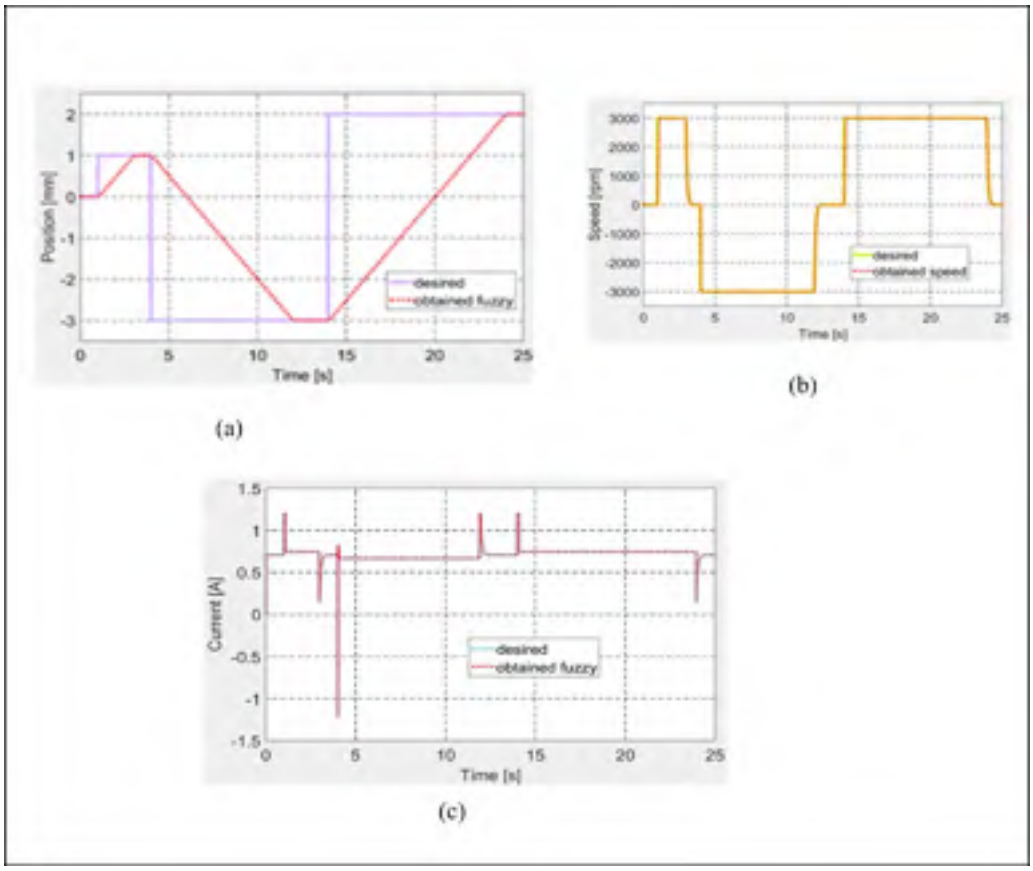

Figure 5.13 Control for successive steps signal as desired position:

(**a**) Position; (**b**) Speed; (**c**) Current.

As a preparatory step for the wind tunnel tests, some calibrations were performed, both in the LARCASE laboratory, with no airflow, but also when the model was fixed in the wind tunnel testing room. To evaluate the morphed shape of the wing, a laser scanning was realized in the LARCASE laboratory with the actuation system controlled for all of the 97 studied flow cases. For example, in the flow case characterized by the M=0.2, α=2˚ and δ=4˚ the laser

scanning of the wing upper surface provided the picture shown in Figure 5.14; there is Figured just the scan of the wing, without the aileron. The actuation distances obtained from the numerical optimization of this flow case were: 2.89 mm, 2.95 mm, 2.71 mm and 3.44 mm.

During the wind tunnel tests the morphing wing-aileron experimental model has been fixed in vertical position in the IAR-NRC wind tunnel testing room (Figure 5.15). Once fixed on the testing position, the model has been subjected to a new set of calibrations, this time by using some absolute digimatic indicators. The estimated corrections completed the final version of the application software, working with the control system during the wind tunnel tests. The software component developed by the team included also a Graphic User Interface (GUI) containing some graphical windows and some buttons which allowed the users to monitor and control the experimental model during testing, but also to visualize what's happen at the level of the laminar to turbulent transition point position in the Kulite pressure sensors station (2D estimation of the transition position). Figure 5.16 shows a part of the GUI monitoring in real time the controlled actuation positions for all of the four actuators in the morphed configuration of the wing, for the flow case characterized by M=0.2, α=2˚ and δ=4˚ conditions.

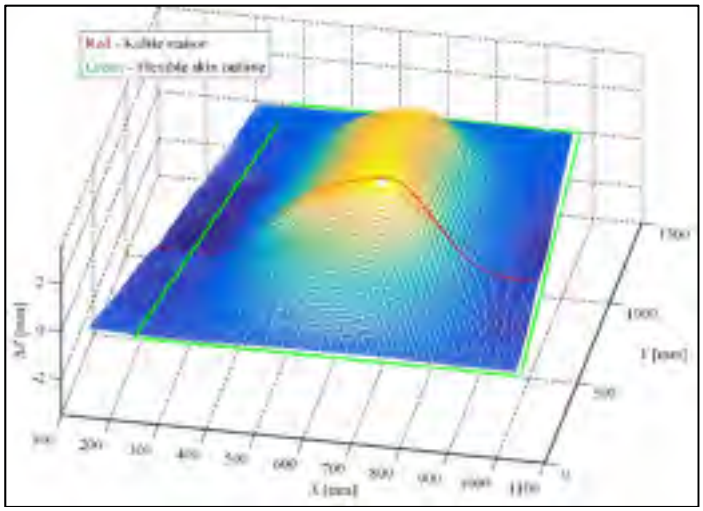

Figure 5.14. Laser scan of the morphed wing shape for M=0.2, α=2˚, δ=4˚ flow case.

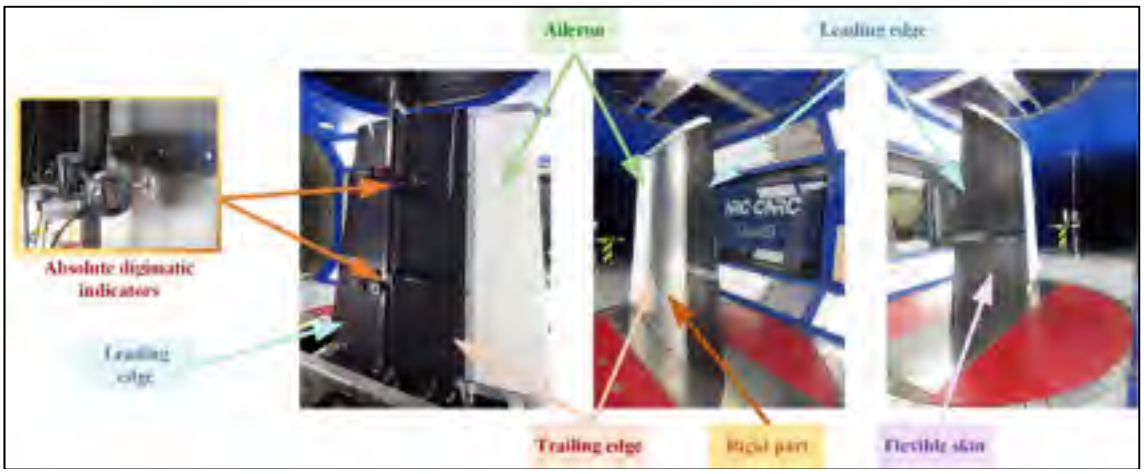

Figure 5.15. Morphing wing-aileron experimental model

in the IAR-NRC wind tunnel testing room.

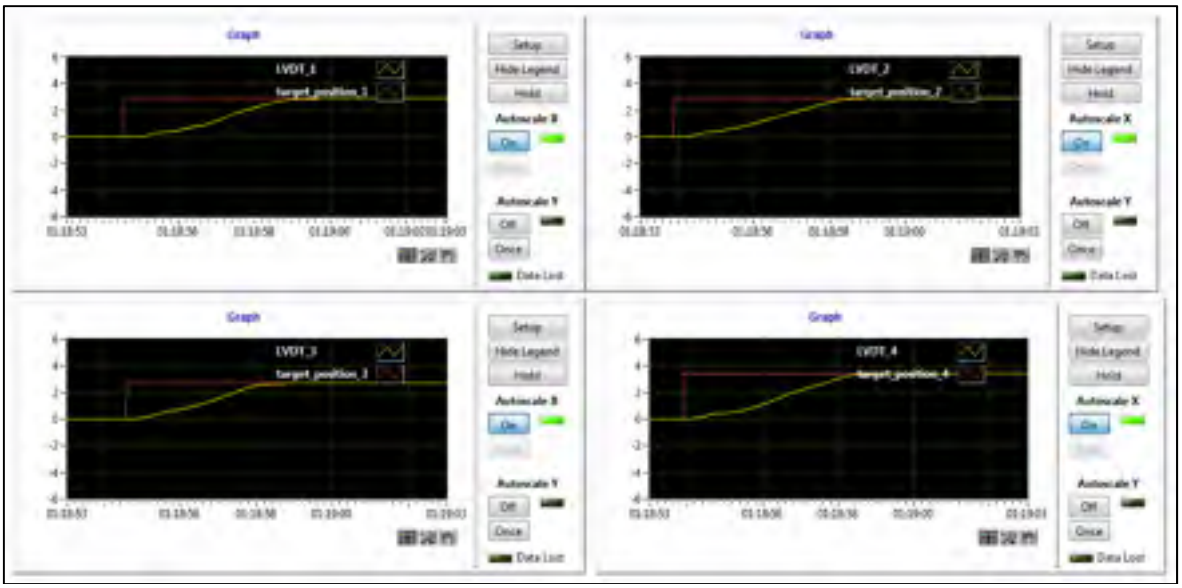

Figure 5.16. Actuators real time monitoring

for M=0.2, α=2˚, δ=4˚ flow case with the wing morphed.

As was already mentioned, in the Kulite sensors station it was performed a 2D evaluation of the airflow laminar to turbulent transition point position based on the pressure data processing by using the Fast Fourier Transform (FFT) and the Standard Deviation (STD). Figure 5.17 and Figure 5.18 describe the FFT characteristics obtained for un-morphed and

morphed airfoils when the flow conditions were M=0.2, α=2˚ and δ=4˚, while Figure 5. 19 presents the results for the STD evaluation for both airfoils in the same flow case. It can be observed that FFTs and STDs curves suggest the same regions for the transition location in the un-morphed configuration, but also in the morphed one. Therefore, for the un-morphed airfoil both FFT and STD indicated that the passing from laminar to turbulence was made somewhere in the area of the 10^{th} Kulite sensor, i.e. at 42.45% of the wing chord, while for the morphed airfoil was made somewhere in the area of the 15^{th} Kulite sensor, i.e. at 50.04% of the wing chord.

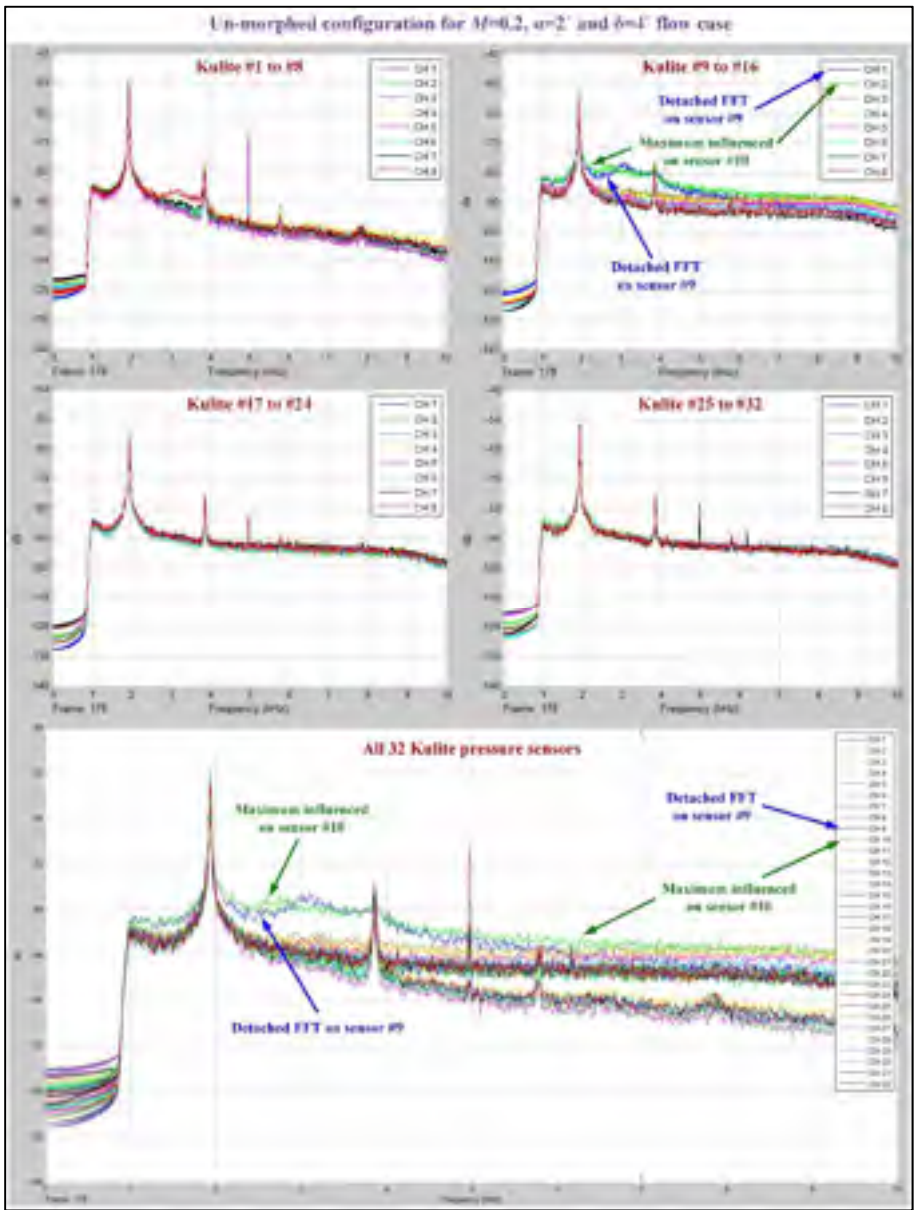

Figure 5.17. FFT results for the wing un-morphed configuration in *M*=0.2, α=2˚, δ=4˚ flow conditions.

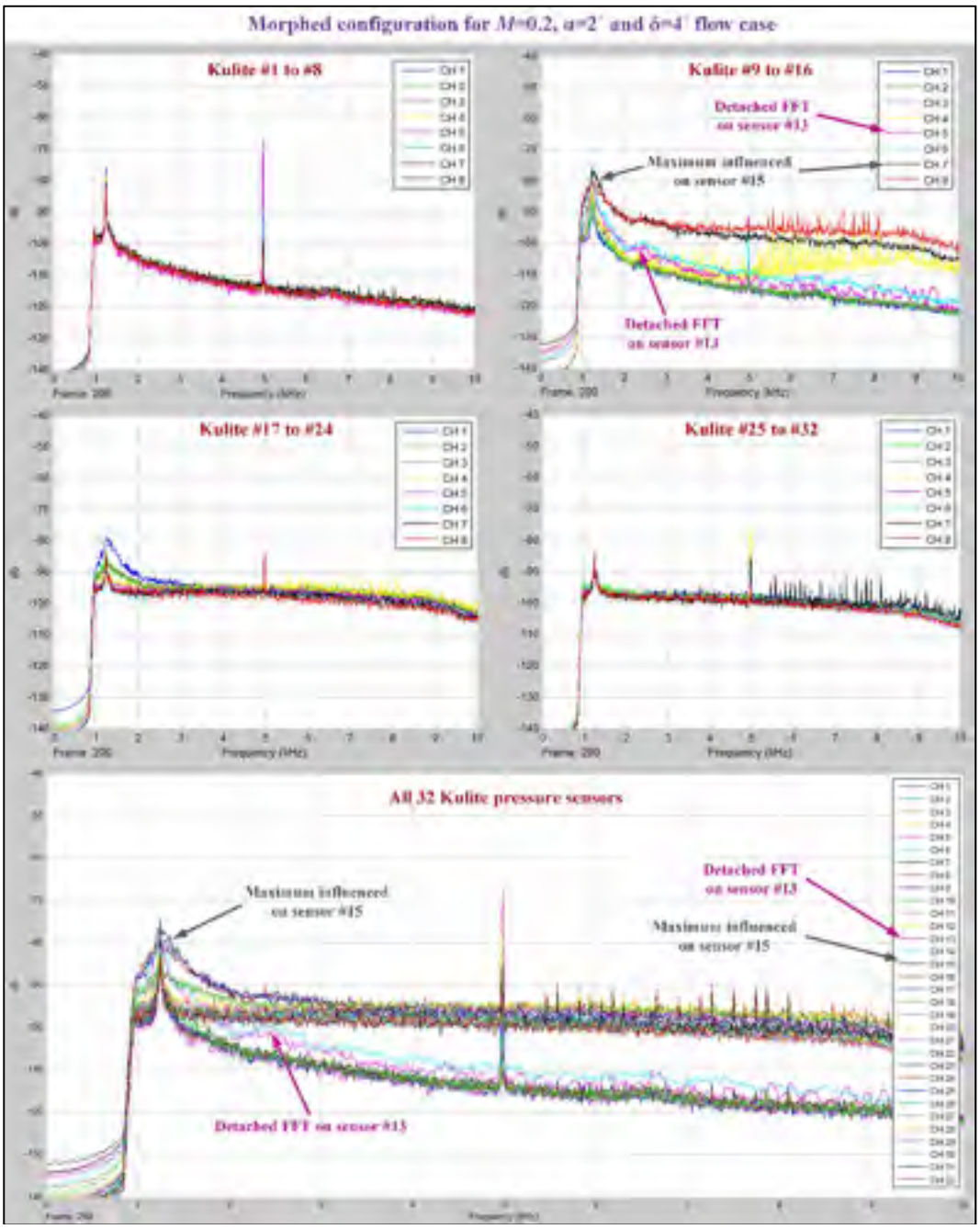

Figure 5.18. FFT results for the wing morphed configuration in M=0.2, α=2˚, δ=4˚ flow conditions.

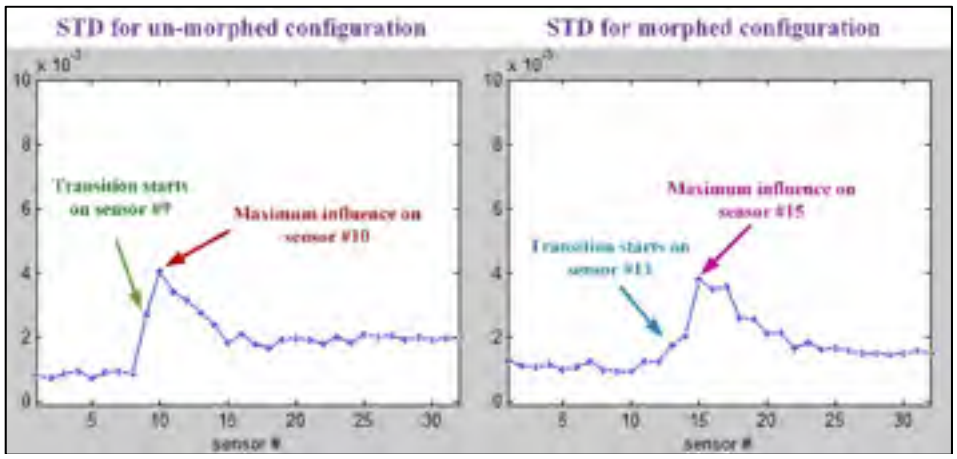

Figure 5.19. STD results for

M=0.2, α=2˚, δ=4˚ flow conditions.

The second method facilitating the estimation of the position for the laminar-to-turbulent airflow transition region, but this time along the whole wing span, was the Infrared (IR) thermography (3D estimation of the transition position). The IR results for M=0.2, α=2˚ and δ=4˚ flow conditions are shown in Figure 5.20 for both un-morphed and morphed configurations of the wing. In the two pictures from Figure 5.20 the doted white lines mark the transition fronts obtained after the next operations were performed with the IR captions: image decimation, detection using gradient image analysis, filtering and thresholding. In the same pictures, the black lines mark the mean transition between the two transition fronts, while the red dot highlights the transition point position for the Kulites section evaluated with IR technique. The IR evaluation for M=0.2, α=2˚ and δ=4˚ flow conditions provided an average value for the laminar to turbulent transition point position along the wing span (the average of all points on the black line) of 43.9767% from the wing chord for un-morphed configuration, and of 47.9681% from the wing chord for morphed configuration. Also, the position of the red dots, i.e. the transition point position for the Kulites station evaluated with IR technique, was found at 42.6925% from the wing chord for un-morphed configuration, and at 49.3381% from the wing chord for morphed configuration, validating in this way the results obtained with the technique based on the FFT and STD evaluation.

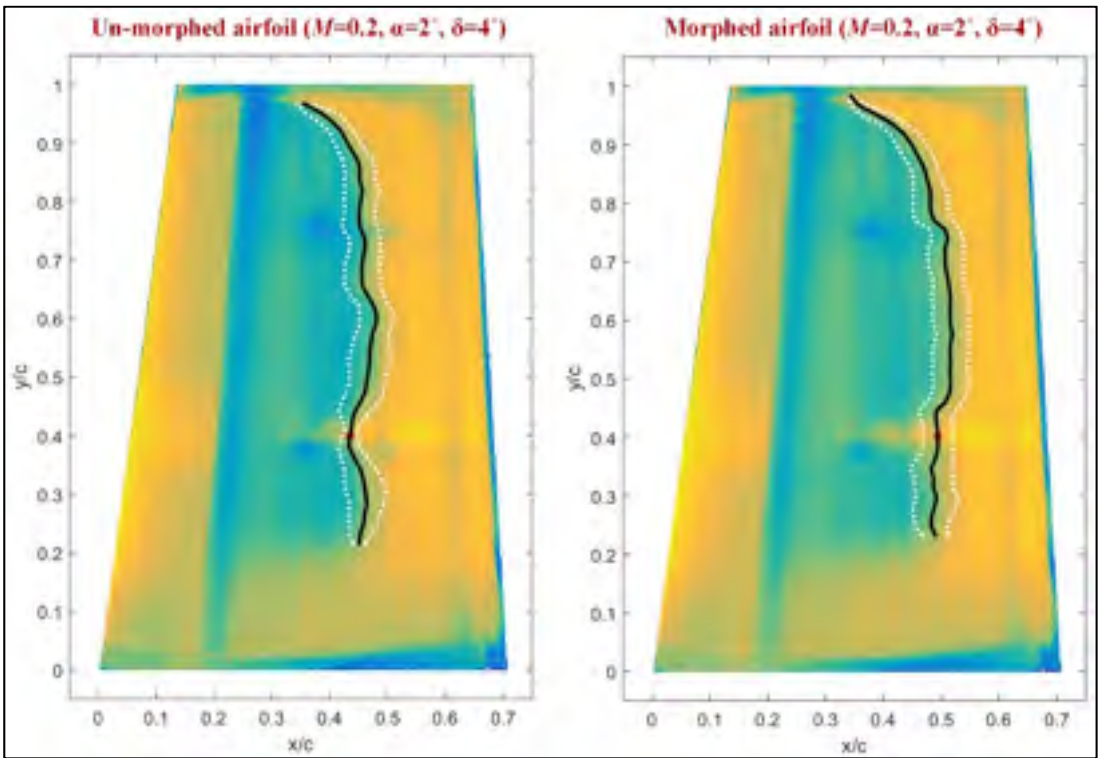

Figure 5.20. The infrared thermography results

for M=0.2, α=2˚ and δ=4˚ flow conditions.

Therefore, the IR technique proved an improvement (the difference between morphed and un-morphed configuration) of the 47.9681% - 43.9767% = 3.9914% from the wing chord, related to the average value for the laminar to turbulent transition point position along the wing span, and of 49.3381% - 42.6925% = 6.6456% from the wing chord, related to the transition point position for the Kulites station. In the same time, the technique based on the FFT and STD evaluation shown an improvement of 50.04%-42.45%=7.59% of the wing chord, related to the transition point position for the Kulites station.

The final analyze of the FFT, SDT and IR results for both un-morphed and morphed airfoils revealed that the morphing technology improved the average position of the laminar to

turbulent flow transition over the whole wing with more than 2.5% of the wing chord for the great majority of the studied flow cases.

5.6 Conclusions

The paper exposed a part of the work done in a major morphing wing international research project developed as a collaboration between Canadian and Italian partners from industry, research and academic fields. The project intended to demonstrate the feasibility of the morphing wing technology for the next generation of aircraft by developing a morphing wing-aileron experimental model, starting from a full scaled portion of a real aircraft wing, and testing it in the wind tunnel.

The work presented here proved the team obtained an experimental wing model able to morph in a controlled manner and to provide in this way an extension of the laminar airflow region over its upper surface, producing a drag reduction with direct impact on the fuel consumption economy. The paper highlighted the results obtained in the design, numerical simulation and wind tunnel experimental testing of a fuzzy logic based control variable for the morphing wing-tip actuation system, but also the aerodynamic gain produced by the morphing technology on our experimental model.

The control system structure for the morphing actuation system included three loops, the designed fuzzy logic based control variant leading to the next configuration: a Proportional-Derivative architecture in the position control loop, a Proportional-Integral-Derivative architecture for the speed control loop, and a Proportional-Integral architecture in the electrical current control loop. All tests demonstrated a very good operation of the control system in all of the three control loops.

From another perspective, the wind tunnel testing of the integrated morphing wing-aileron experimental model shown a promising aerodynamic gain for the morphed configuration in front of the un-morphed one. A set of the 97 flow cases were studied by the research team, both from numerical and experimental points of view, to estimate the added value of the morphing technology. Also, during the wind tunnel testing, the team used two techniques to

monitor the airflow over the upper surface and to evaluate in this way the position of the laminar-to-turbulent airflow transition region: 1) the processing of the pressure data for a section along the wing chord, which were collected by using 32 Kulite pressure sensors (2D estimation of the transition position); 2) the Infrared (IR) thermography (3D estimation of the transition position).

The analyze of the results for the estimation of the transition position, for both un-morphed and morphed airfoils, revealed that the morphing technology improved the average position of the laminar to turbulent flow transition over the whole wing with more than 2.5% of the wing chord for the great majority of the 97 studied flow cases.

Author Contributions: Control design, implementation and testing, software development, control validation, Shehryar Khan, Grigorie Teodor Lucian and Ruxandra Mihaela Botez; system integration and monitoring methodologies, Ruxandra Mihaela Botez and Mahmoud Mamou; concept of pressure data post-processing software for analyze and validation, Grigorie Teodor Lucian; writing—original draft preparation, Shehryar Khan and Grigorie Teodor Lucian; research project concept, aerodynamic optimization, funding acquisition, supervision, project administration, writing—review and editing, Ruxandra Mihaela Botez; wind tunnel testing, infrared thermography analysis, Mahmoud Mamou and Youssef Mébarki.

Funding: This research was funded by the Consortium for Research and Innovation in Aerospace in Quebec (CRIAQ) and the National Sciences and Engineering Research Council of Canada (NSERC), grant CRIAQ MDO 505.

5.6 Acknowledgments: The authors would like to thank the Thales Avionics team (Mr. Philippe Molaret, Mr. Bernard Bloiuin, and Mr. Xavier Louis) and Bombardier Aerospace team (Mr. Patrick Germain and Mr. Fassi Kafyeke) for their help and financial. We would like also to thank the Consortium for Research and Innovation in Aerospace in Quebec (CRIAQ) and the National Sciences and Engineering Research Council (NSERC) for their funding of the CRIAQ MDO 505 project.

5.7 OVER ALL CONCLUSION AND RECOMMENDATION

The research work presented in this thesis is resulting from the major international research collaboration between Canadian and Italian industrial and academic partners. The goal of the research was to develop a new morphing wing mechanism for the new generation of the commercial aircraft wings. This new morphing technology is capable of reducing the drag on the wing of the aircraft and hence to lead to the fuel optimization. The novel wing is composed of a morphing wing with both morphing and non-morphing aileron configurations. Four morphing actuators are placed inside the morphing wing box, two on the each actuation line chord-wise. The new morphing actuator is composed of the BLDC motor, and a screw linked to the motor through a gearbox that would convert the rotary motion of the motor into linear displacement, which is used to morph the wing skin. The combination of the BLDC motor, gear and screw makes it a complex nonlinear system. The work in this thesis focuses on the modelling, simulation, actuation control design, bench testing and wind tunnel testing of this new morphing actuator.

Detailed mathematical modelling of the morphing actuator was presented. The transfer functions were derived from the differential equations representing the dynamics of the BLDC motor. Also, the mathematical modelling of the gear and screw mechanism was presented. The linear actuator model was thus developed based on the transfer function analysis. The simulation revealed that the linear model satisfies the specifications mentioned in the data sheet. However, BLDC motor in real life is composed of three phase windings, permanent magnet rotor, hall sensors and power electronics circuit for the purpose of commutation. The Simulink power system library was used to develop the non-linear model of the actuator which simulates the three phases of winding, power electronics and hall sensors. A classical approach known as Internal Model Control (IMC) was used to design the respective current, speed and position control. The obtained controller gains were successfully able to control the linear and nonlinear models of the actuator with zero steady state error. Finally, the designed controller

was tested in the wind tunnel, and it was able to successfully perform the morphing wing actuation in the presence of aerodynamic loads.

Following which the heuristic approach known particle swarm optimization to the controller design of the new morphing wing mechanism is presented. Since this new morphing actuator is a complex nonlinear system, therefore Particle Swarm Optimization (PSO) was considered as a potential candidate to solve this problem. The PSO belongs to the family of artificial intelligence algorithms, and is famous for solving optimization problems. The controller gains were successfully obtained using the PSO algorithm, and were successfully verified using the simulation results and zero steady state error was obtained. Finally, the designed controller was tested in the wind tunnel, and the infrared and kulite sensors results revealed the improvement of the laminar flows over the morphing wing.

Finally design of a fuzzy controller for the new morphing actuator was presented. The need to design the fuzzy logic controller was considered due to both the nonlinear dynamics of the BLDC motor, the gear box and screw mechanism. Their analysis revealed that fuzzy logic proportional derivative controller could be designed for the position loop, proportional derivative fuzzy plus integral controller for the velocity loop and the proportional integral fuzzy controller for the current loop. Z, S and triangular type membership functions were used for the antecedents and consequents of the fuzzy controller. The universe of discourse for the membership functions was designed based on our experience with the classical actuator controller. Simulation results revealed the successful operation of the designed controller and obtained zero steady state error. Finally, the designed controller was tested in the wind tunnel using the NI PXI and Maxon motor drives. The Infrared and kulite sensor data revealed the improvement in the laminar flows over the morphing wing.

Finally, to conclude, three different controllers were successfully validated in simulations and using the wind tunnel testing based on the National Instruments (NI) PXI technology, however,

more improvement can be achieved in the future in terms of space, weight and cost if the NI actuator control is replaced by the Digital Signal Processor (DSP) technology.

Regarding future work, it is also important to indicate in this thesis that the conditions of the Robust Control design were not taken into considerations. During the real flight the aircraft wing can get exposed to the uncertain aerodynamic loads such as wind gusts as well as other uncertain loads caused by the wing structure itself due to uncertain vibrations caused by the various parts of the wing structure. It is therefore deemed as an important future work, that an H-infinity robust controller shall be designed using the application of Artificial Intelligence (AI) algorithms. One of the journal papers presented the application of PSO algorithm for the design of the PI actuator controller, therefore as a future work the plan is to extend the application of PSO algorithm application should be extended to the design of a robust controller. All the uncertain aerodynamic loads will be modelled within bounded limits and the performance of the robust controller will be tested in the presence of these aerodynamic uncertainties.

Another important future milestone is the upgrade of the performance of the H-infinity Robust Controller to an adaptive Robust Controller for which the controller can tune the parameters of the controller online if the system dynamics alters over the period of time. In contrast to robust control which relies on a priori information about the limits of uncertain disturbances in order to modify the control laws, the adaptive control uses system identification and parameter estimation methods to detect the changes in the plant dynamics and accordingly to modify the control laws.

Appendix A

Specification of the BLDC motor used in the morphing actuator

Nominal voltage	12 volts
No load speed	4610 rpm
No load current	75.7 mA
Nominal speed	2810 rpm
Nominal torque	25.1 mNm
Nominal current	1A
Stall torque	84.1 mNm
Starting current	3.49 A
Terminal resistance	3.43 ohm
Terminal inductance	1.87 mH
Torque constant	24.1 mNm/A
Speed constant	397 rpm/v
Mechanical time constant	20.7 ms

Appendix B

Specification of the equipment used in the bench testing and wind tunnel testing

PXIe-chasis

PXI chasis houses various kinds of PXI modules with varying computational capabilities and it can provide up to 18 slots as shown in Figure B-1.

Figure B-1. PXI chasis

NI PXIe 8135 controller

NIPXIe 8135 controller is used in architectures where high computational power as well as modular instrumentation and high speed data acquasition is required as shown in figure B-2. Following are the salient features of the PXI 8135 controller

i. Intel Core i7 embedded controller for PXI Express systems
ii. Two 10/100/1000BASE-TX (Gigabit) Ethernet ports
iii. Two SuperSpeed USB ports
iv. Four Hi-Speed USB ports
v. Integrated hard drive
vi. Serial port

Figure B-2. NI PXIe
8135 controller

Appendix C

NI SC Express 4330 signal conditioner

The NI SC express is used in signal conditioning applications where high speed data acquisition and signal conditioning is involved. This module provides high speed, accuracy and synchronization capabilities.The module has eight sampled input channels for connection to strain gage bridges and wheat stone bridge based sensors as shown in figure C-1.

Figure C-1. NI SC
Express 4330 signal conditioner

CAN Breakout Box

A CANopen box can be connected to 14 different interfaces.

Figure C-2. CAN Breakout box

Appendix D

XCQ-062 Pressure transceducer

XCQ-062 is ultraminiature pressure transceducer. It is used in both dynamic and static pressure distribution in harsh envirnments. Following are some of its features

I. Applications: Automotive, motorsports, Flight test, General test and measurment
II. Pressure range: High pressure(above 500 psi), Low pressure (0-500psi)
III. Temperature range: -65°F to +275°F (-55°C to 135°C)
IV. Excitation: 10 v
V. Operational mode: Absolute, Differential
VI. Output: Unamplified millivolt Output

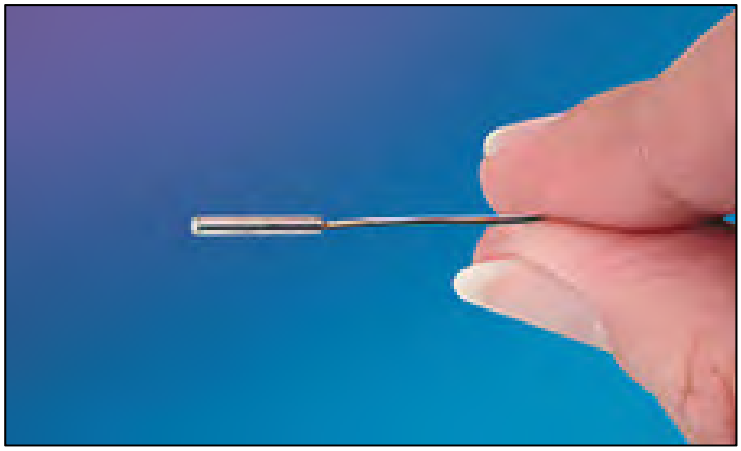

Figure D-1. XCQ-062 Pressure transceducer

Appendix E

LD340 LVDT series

LD340 series is an ideal choice for applications involving linear position measurment as shown in Figure E-1. Following are some of the features of the LD340 LVDT

I. Range : ± 1.5mm to ±12.5 mm
II. Small diameter only 9.52 mm
III. Ideal for use with small actuators
IV. High performance displacment transceducers
V. Sensitivity at 5 kHz ±10% (mV/V/mm)

Figure E-1. LD340
LVDT series

EPOS 2 Positioning controller

EPOS 2 provides various modes for the motor control namely position, speed and current regulation as shown in figure E-2.

Figure E-2. EPOS 2
position controller

Appendix F

NI PXI 8531

It provides a high speed interface for applications with CAN open interface for industrial automation applications. It is mostly used in motor control applications involved in medical equipment, maritime applications and building automation.

Figure F-1. NI PXI 8531
CAN open interface

NI SCXI 1000

SCXI is chasis that powers all SCXI modules and also handles timming, trigger and signal routing issues between SCXI and other PXI modules.

NI SCXI 1315

NI SCXI 1315 is terminal block used for connecting to LVDT ‘s .

Appendix G

Snaps of the bench testing equipment

LIST OF REFERENCES

Barbarino, S., Bilgen, O., R. M. Ajaj., M. I, Friswell., Inman and D. J, Inman. 2011. «Review of Morphing Aircraft ». *journal of intelligent material systems and structures*, vol. 22, pp.823-877.

R. W, Wlezien., G. C, Homer., A. R, McGowan., S. L, Padula., M. A, Scott., R. J, Silcox., and J.O,Simpson. 1998.«https://ntrs.nasa.gov/archive/nasa/casi.ntrs.nasa.gov/19980053567.pdf». *The aircraft morphing program*, NASA Langley Research Center.

Rim, Misun, Kim, Eunho, Kang, Wooram and Lee. 2014. «Development of a shape memory alloy wire actuator to operate a morphing wing». *Journal Of Theoretical And Applied Mechanics*, vol. 52, pp.519-531.

Kang, Wooram, Kim, Eunho and Jeong, Min-Soo and Lee, In and Ahn, Seok-Min. 2012. «Morphing Wing Mechanism Using SMA Wire Actuator». *International journal of Aeronautical and Space sciences*, vol. 18, pp.58-63.

Majji, M., Rediniotis, O., Junkins, J. 2007. «Design of a Morphing Wing: Modeling and Experiments». *AIAA Atmospheric Flight Mechanics Conference*, DOI. 10.2514/6.2007-6310.

XiFengfeng,2009.«https://www.ryerson.ca/content/dam/aerospacemanufacturing/pdfs/research_media.pdf».*Department of Aerospace Engineering Ryerson Institute for Aerospace Design and Innovation*.

Dimino, I., Ciminello, M., Concilio, A., Gratias, A., Schueller, M. 2015. «Control system design for a morphing wing trailing edge». 7th ECCOMAS Thematic Conference on Smart Structures and Materials, vol. 43, pp.175-193.

Popov, A.V., Botez, R.M., Grigorie, T. L., Mamou, M., Mebarki, Y., 2010. «*Modeling and testing of a morphing wing in an open loop architecture*». *AIAA Journal of Aircraft*, vol. 47, pp.917-923.

Botez, R.M., Grigorie, T.L., 2009. «Adaptive neuro-fuzzy controller for an open loop morphing wing». *Journal of Aerospace Engineering*, vol. 223, DOI 10.1243/09544100JAERO487.

Grigorie, T. L., Popov, A.V., Botez, R.M., Mamou, M., Mébarki, Y., 2010. «Design and Experimental Validation of a combined PI and Bi-Positional Laws Controller for Delaying the Transition from Laminar Flow to Turbulent Flow over a Morphing Wing». *International Conference on Informatics in Control and Automation and Robotics,* DOI. 10.1007/978-3-642-19539-6_4.

Popov, A.V., Botez, R.M., Grigorie, T. L., 2010. «Real Time Morphing Wing Optimization Validation Using Wind-Tunnel Tests». *Journal of Aircraft*, vol. 47, pp.1346-1355.

Grigorie, T. L., Popov, A.V., Botez, R.M., Mamou, M., and Mébarki, Y. 2011. «On-off and proportional-integral controller for a morphing wing. Part 1: Actuation mechanism and control design » *Journal of Aerospace*, vol 226 (2), pp.131-145.

Grigorie, T. L., Popov, A.V., Botez, R.M., Mamou, M., and Mébarki, Y., 2011. «On–off and proportional–integral controller for a morphing wing». Part 2: Control validation-numerical simulations and experimental tests, *Journal of Aerospace*, vol 226 (2), pp. 131-145.

Grigorie, T. L., Popov, A.V., Botez, R.M., Mamou, M., and Mébarki, Y., 2011. «An Intelligent Controller based Fuzzy Logic Techniques for a Morphing Wing Actuation System

using Shape Memory Alloy». *AIAA Structures, Structural Dynamics and Materials Conference*, DOI. 10.2514/6.2011-2133.

Grigorie, T. L., Popov, A.V., and R. M. Botez. 2015. «Control Strategies for an Experimental Morphing Wing Model». *AIAA Atmospheric Flight Mechanics Conference*, DOI. 10.2514/6.2014-2187.

Kammegne, M.T., Grigorie, T. L., R. M. Botez., 2015. «Design and validation of a position controller in the Price- païdoussis wind tunnel». *IASTED Conference*, DOI. 10.2316/pp.2014.809-041.

Popov, A.V., Grigorie, T. L., 2010. «Closed Loop Control Validation of a Morphing Wing using Wind Tunnel Tests». *Journal of aircraft*, vol 47, pp.1309-1317.

Kammegne, M.T., Grigorie, T. L., R. M. Botez., 2015. «*Design, Numerical Simulation and Experimental Testing of a Controlled Electrical Actuation System in a Real Aircraft Morphing Wing Model*». *The Aeronautical Journal*, vol 119, pp.1047-1072.

Kammegne, M.J.T., Botez, R. M., Grigorie, L. T., Mamou, M and Mébarki, Y. 2017. «Proportional fuzzy feed-forward architecture control validation by wind tunnel tests of a morphing wing ». *Chinese Journal of Aeronautics*, vol 30, pp.561-576

Nguyen, D.H., Kammegne, M.J.T., Botez, R.M., Grigorie, T.L., 2016. «Open loop morphing wing architecture based ANFIS controller». *AIAA Aviation Technology, Integration, and Operations Conference*, DOI: 10.2514/6.2016-4368.

Kammegne, M.J.T., Botez, R.M., Grigorie, L.T., 2016. «Actuation Mechanism Control in a Morphing Application with a Full-scaled portion of an Aircraft wing». *IASTED* Modelling, Identification and Control *Conference*, DOI: 10.2316/pp.2016.830-031.

Kammegne, M.J.T., Botez, R. M., Grigorie, L. T., Mamou, M., Mébarki, Y. 2016. «Aircraft energy consumption limitation through drag reduction based on morphing wing

technology- A new multi disciplinary experimental model». *National Research Council of Canada Document.*

Botez, R. M., Mamou, M., Mébarki, Y., Guezguez, M.S, 2016. «Morphing Wing-Tip Open Loop Controller and its Validation During Wind Tunnel Tests at the IAR-NRC». *INCAS Bulliten*, vol. 8, pp.41–53.

João Loureiro, Raghuraman Ragarajan, Eduardo Tovar. 2015. « Distributed sensing of fluid dynamic phenomenon with the Xdense sensor grid network». *CPSNA conference*, P 54-59, doi.10.1109/CPSNA.2015.19.

Kammegne, M.J.T., Botez, R.M., Grigorie, L.T., Mamou, M. and Mébarki, Y. 2010. «Morphing wing demonstrator tested in a subsonic wind tunnel in open loop configuration». *Journal of Aerospace Science and Technology*, vol 232 (8), pp. 1479-1494.

Wheeler, P.W., Clare, J.C., Trentin, A., Bozhko, S., 2012. «An overview of the more electric aircraft». *Journal of Aerospace Engineering ImechE*, vol 227(4), pp.578-585.

Jänker, P. et al. 2008. «New Actuators for Aircraft and Space Applications».*11th International Conference on New Actuators*, Bremen, Germany.

Skogestad, S. 2001. «Probably the Best Simple PID Tuning Rules in the World». *Journal of Process Engineering*.

Vos1, R, Barrett, R, Breuker,R and Tiso, P. 2007. «Post-buckled pre-compressed elements: a new class of control actuators for morphing wing UAVs». *Journal of Smart Materials and Structures*, vol.16(3), pp.919-926.

Jodin, G., Scheller, J., Duhayon, E., François, J., Rouchon,D. and Braza, M. 2017. «Implementation of a Electro-Active Actuated Morphing Wing in Wind Tunnel». *Solid State Phenomenon,* vol. 260. pp.85-91.

Bilgen, O., Butt, L.M., Day, S.R., Sossi, C.A., Weaver, JP., Wolek, A., Mason, WH. and Inman, D. J. 2012.«A novel unmanned aircraft with solid-state control surfaces: Analysis and flight demonstration». *Journal of Intelligent Materials*, vol.24, pp.147-167.

Trease, B., Kota, S., 2006. «Design of Adaptive and Controllable Compliant Systems With Embedded Actuators and Sensors». *Journal of Mechanical Design Asme*, vol. 131, DOI. 10.1117/12.715919.

Gagne J, Mendoza A-M, Botez RM, Labour D., 2013. «New method for aircraft fuel saving using Flight Management System and its validation on the L-1011 aircraft». *AIAA Aviation Forum, Aviation Technology, Integration and Operations Conference*, pp. 1-10, DOI.10.2514/6.2013-4290.

Patron R-F., Botez, R.M., Labour, D., 2013. «Low calculation time interpolation method on the altitude optimization algorithm for the FMS CMA-9000 improvement on the A-310 and L-1011 aircraft». *AIAA Aviation Forum, Aviation Technology, Integration, and Operations Conference*, pp.1-8, DOI.10.2514/6.2013-4256.

Patron, R.F., Berrou, Y., Botez, R.M., 2014. «Climb, Cruise and Descent 3d Trajectory Optimization Algorithm for a Flight Management System». *AIAA Aviation Forum,*

Aircraft Noise and Emissions Reduction Symposium, pp.1-12, 10.2514/6.2014-3018.

Dancila, B., Botez, R.M., Labour, D., 2012. «Altitude optimization algorithm for cruise, constant speed and level flight segments». *AIAA Guidance, Navigation, and Control Conference*, pp.1-12, DOI. 10.2514/6.2012-4772.

Patron, R.F, Owono, A., Botez, R.M., Labour, D., 2013. «Speed and Altitude Optimization on the FMS CMA-9000 for the Sukhoi Superjet 100 Using Genetic Algorithms». *AIAA Aviation Forum, Aviation Technology, Integration, and Operations Conference*, pp. 1-10.

Dancila, R., Botez, R.M., Ford, S., 2014. «Fuel burn and emissions evaluation for a missed approach procedure performed by a B737-400». *The Aeronautical Journal*; vol .118**(**1209), pp. 1329-1348.

Mendoza, A.M., Botez, R.M., 2014. «Vertical navigation trajectory optimization algorithm for a commercial aircraft». *AIAA Aviation Forum, Aircraft Noise and Emissions Reduction Symposium*, pp. 1-10. DOI. 10.2514/6.2014-3019.

Dancila, B., Botez, R.M., 2014. «Construction of an aircraft's VNAV flight envelope for in-FMS flight trajectory computation and optimization». AIAA, *Aviation Technology, Integration, and Operations Conference*, pp. 1-7, DOI.10.2514/6.2014-2291.

Patron, R.F., Kessaci, A., Botez, R.M., 2013 «Flight Trajectories Optimization under the Influence of Winds Using Genetic Algorithms». *AIAA Guidance, Navigation, and Control (GNC) Conference*, pp. 1-11. DOI. 10.2514/6.2013-4620.

Mota, S., Botez, R.M., 2009. «New Identification Method Based on Neural Network for Helicopters from Flight Test Data». *AIAA Atmospheric Flight Mechanics Conference*, pp. 1-31, DOI.10.2514/6.2009-5938.

Labib, M., Popov, A., Fays, J., Botez, R.M., 2008. «Transition Point Displacement Control on a Wing Equipped with Actuators». *AIAA Guidance, Navigation and Control Conference and Exhibit*. pp. 1-27, DOI.10.2514/6.2008-6490.

Popov, A.V., Labib, M., Fays, J., Botez, R.M., 2008. «Closed-Loop Control Simulations on a Morphing Wing». *Journal of Aircraft*, vol 45(5), pp. 1794-1803.

Popov, A.V, Grigorie, T.L, Botez, R.M, Mamou, M, Mébarki, Y., 2010. «Real time morphing wing optimization validation using wind-tunnel tests». *Journal of Aircraft* 47(4), pp. 1346-1355.

Grigorie, T.L, Botez, R.M, Popov, A.V., 2012. «Design and experimental validation of a control system for a morphing wing». *AIAA Atmospheric Flight Mechanics Conference*; 2012. pp. 1-12, DOI.10.2514/6.2012-4639.

Grigorie, T.L, Botez, R.M., 2010. «Adaptive Neuro-Fuzzy Inference Controllers for Smart Material Actuators», *51st AIAA/ASME/ASCE/AHS/ASC Structures, Structural Dynamics, and Materials Conference*. pp. 1-12, DOI.10.2514/6.2010-2987.

Grigorie, T.L, Botez, R.M., 2010. «Neuro-Fuzzy Controller for SMAs for a Morphing Wing Application», *51st AIAA/ASME/ASCE/AHS/ASC Structures, Structural Dynamics, and Materials Conference*, 2010, pp. 1-21, DOI./10.2514/6.2010-2745.

Popov, A.V, Grigorie, T.L, Botez, R.M, Mamou, M, Mébarki, Y., 2011. «An Intelligent Controller Based Fuzzy Logic Techniques for a Morphing Wing Actuation System Using Shape Memory Alloy», *52nd AIAA/ASME/ASCE/AHS/ASC Structures, Structural Dynamics and Materials Conference*. pp. 1-12., DOI./10.2514/6.2011-2133.

Popov, A.V., Grigorie, T.L., Botez, R.M., Mamou, M., Mébarki, Y., 2011. «A New Morphing Wing Mechanism Using Smart Actuators Controlled by a Self-Tuning Fuzzy Logic Controller». *11th AIAA Aviation Technology, Integration, and Operations (ATIO) Conference*. 2011, pp. 1-12. doi.org/10.2514/6.2011-7071.

Grigorie, T.L., Popov, A.V., Botez, R.M., 2013. «Control of Actuation System Based Smart Material Actuators in a Morphing Wing Experimental Model». *AIAA Atmospheric Flight Mechanics (AFM) Conference*, pp. 1-10, DOI.10.2514/6.2013-4918.

Popov, A.V., Grigorie, T.L., Botez, R.M., Mamou, M., Mébarki, Y., 2011. «Controller and Aeroelasticity Analysis of a Morphing Wing» *AIAA Atmospheric Flight Mechanics*

Conference, pp. 1-14, DOI/10.2514/6.2011-6460.

Grigorie, T.L, Popov, A.V, Botez, R.M., 2014. «Control Strategies for an Experimental Morphing Wing Model». *AIAA Aviation 2014, AIAA Atmospheric Flight Mechanics (AFM) Conference*, pp. 1-13, doi.org/10.2514/6.2014-2187.

Popov, A.V, Grigorie, T.L, Botez, R.M, Mamou, M., Mébarki, Y., 2010. «Modeling and testing of a morphing wing in open-loop architecture». *Journal of Aircraft*, vol. 47(3), pp. 917-923.

Popov, A.V, Botez, R.M, Mamou, M., Grigorie, T.L., 2009 «Variations in Optical Sensor Pressure Measurements due to Temperature in Wind Tunnel Testing». *Journal of Aircraft*, 46(4), pp. 1314-1318.

Silisteanu, P.D, Botez, R.M., 2010. «Transition-Flow-Occurrence Estimation: A New Method». *Journal of Aircraft,* 47(2), pp. 703-708.

Pern, N.J., Jacob, J.D., 1999. «Aerodynamic Flow Control Using Shape Adaptive Surfaces». *ASME Design Engineering Technical Conferences*; 12-15. pp. 1-8.

Munday, D., Jacob, J., Hauser, T., Huang, G., 2002. «Experimental and Numerical Investigation Of aerodynamic Flow Control Using Oscillating Adaptive Surfaces». *1st AIAA Flow Control Conference*; pp. 1-8, DOI./10.2514/6.2002-2837.

Rivero, A.E, Fournier, S., Weaver, P.M, Cooper, J.E, Woods, BKS. 2018. «Manufacturing and characterisation of a composite FishBAC morphing wind tunnel model». *29th International Conference on Adaptive Structures and Technologies (ICAST2018)*, pp. 1-14.

Yokozeki, T., Sugiura, A., Hirano, Y., 2014. «Development of Variable Camber Morphing Airfoil Using Corrugated Structure». *Journal of Aircraft*, vol. 51(3): pp. 1023-1029.

Vasista, S., Nolte, F., Monner, HP., Horst, P., Burnazzi, M., 2018. «Three-dimensional design of a large-displacement morphing wing droop nose device». *Journal of Intelligent Material Systems and Structures*, vol. 29(16), pp. 3222-3241.

EU Project MOET (More Open Electrical Technologies) - Technical Report. Financed in the EU 6th Framework Research Program FP6-AEROSPACE, Grant agreement ID: 30861, July 2006-December 2009. Coordinated by: Airbus Operations SAS France.https://trimis.ec.europa.eu/sites/default/files/project/documents/20121218_094726_85827_MOET_Public_Technical_report.pdf.

Jänker, P., Claeyssen, F., Grohmann, B., Christmann, M., Lorkowski, T., LeLetty, R., Sosniki, O., *2008.* «New Actuators for Aircraft and Space Applications». *11th International Conference on New Actuators*, pp. 346-354.

Koreanschi, A., Sugar.Gabor, O., Botez, R.M., 2014. «New Numerical Study of Boundary Layer Behavior on a Morphing Wing with-Aileron System». *32nd AIAA Applied Aerodynamics Conference.* pp. 1-18.

Botez R.M, Koreanschi A, Sugar-Gabor O, Mebarki Y, Mamou M, Tondji Y, Guezguez M, Tchatchueng Kammegne J, Grigorie LT, Sandu D, Amoroso F, Pecora R, Lecce L, Amendola G, Dimino I, Concilio A., 2018. «Numerical and Experimental Transition Results Evaluation for a Morphing Wing and Aileron System». *The Aeronautical Journal*, vol. 122(1251), pp. 747-784.

Koreanschi, A., Sugar-Gabor, O., Acotto, J., Brianchon, G., Portier, G., Botez, R.M, Mamou, M., Mebarki, Y., 2017. «Optimization and design of an aircraft's morphing wing-tip demonstrator for drag reduction at low speeds, Part I - Aerodynamic optimization using genetic, bee colony and gradient descent algorithms». *Chinese Journal of Aeronautics*, vol. 30(1): pp. 149-163.

Koreanschi, A., Sugar-Gabor, O., Acotto, J., Brianchon, G., Portier, G., Botez, R.M, Mamou, M., Mebarki, Y. 2017. «Optimization and design of an aircraft's morphing wing-tip demonstrator for drag reduction at low speeds, Part II - Experimental validation using Infra-Red transition measurement from Wind Tunnel tests». *Chinese Journal of Aeronautics*, vol. 30(1): pp. 164-174.

Amendola, G., Dimino, I., Magnifico, M., Pecora, R., 2016. «Distributed actuation concepts

for a morphing aileron device». *Aeronautical Journal*, vol. 120(1231), P 1365-1385.

Arena, M., Amoroso, F., Pecora, R., Amendola, G., Dimino, I., Concilio, A., 2018. « Numerical and experimental validation of a full scale servo-actuated morphing aileron model». *Smart Materials and Structures*, vol. 27(10), pp. 1-21.

Vincent, J-B, Botez, R.M., 2015. «Systemic modeling and design approach for morphing wing aileron controller using Matlab/Simulink». *AIAA Modeling and Simulation Technologies Conference*, pp. 1-10, DOI./10.2514/6.2015-0904.

Tchatchueng-Kammegne, M.J, Khan, S., Grigorie, L.T, Botez, R.M., 2015. «New methodology for the controller of an electrical actuator for morphing a wing». *23rd AIAA/AHS Adaptive Structures Conference*. pp. 1-12.

Tchatchueng Kammegne, M.J, Botez, R.M, Grigorie, L.T, Mamou, M., Mébarki, Y. 2017. «Proportional fuzzy feed-forward architecture control validation by wind tunnel tests of a morphing wing». *Chinese Aeronautical Journal*, vol. 30(2), pp. 561-576.

Tchatchueng Kammegne, M.J, Tondji, Y., Botez, R.M, Grigorie, L.T, Mamou, M., Mébarki, Y., 2017. «New control methodology for a morphing wing demonstrator». *Proceedings of the Institute of Mechanical Engineers Part G: Journal of Aerospace Engineering*, vol. 232(8): pp. 1479-1494.

Chang-Liang Xia., 2012. «*Permanent Magnet Brushless DC Motor Drives and Controls*». John Willey & Sons, ISBN. 978-1-118-18833-0.

Haipeng, R., Ding, L., 2001. «A Novel Digital Position Servo System Using DSP and Fuzzy PID». *Proceedings of the Fifth International Conference Electrical Machines and Systems (ICEMS)*, vol 2, pp. 722-725.

Rubaai, A., 2003. «Implementation of an Intelligent-Position-Controller-Based Matrix Formulation Using Adaptive Self-Tuning Tracking Control». *IEEE Transactions on Industry Applications*, vol 39(3), pp. 627-636.

Tan, Y-K, Panda, S-K., 2004. «Iterative Learning Based Sliding-Mode Position Controller for Linear Permanent Magnet Brushless DC Servo Motors». *30th IECON Annual Conference*, vol. 3, pp. 2864-2869.

Jeong, D-S, Choi, K-J, Kim, J-G, Woo, H-W., 2007. «Controller Design of Missile Actuator Using DSP». *International Conference on Control, Automation and Systems*, pp. 2110-2113.

Ansari, U., Alam, S., Jafri, SMN., 2011. «Modeling and Control of Three Phase BLDC Motor Using PID with Genetic Algorithm». *International Conference on Computer Modelling and Simulation,* pp. 189-194, DOI: 10.1109/UKSIM.2011.

Rivera, D.E, Morari, M., Skogestad, S., 1986. «Internal model control. 4. PID controller

design. *Industrial & Engineering Chemistry Process Design and Development*». vol. 25(1): pp. 252–265.

Skogestad S., 2001. «Probably the Best Simple PID Tuning Rules in the World». *AIChE Annual Meeting* pp. 1-28.

Postlethwaite I, Skogestad S., 2002. «*Multivariable Feedback Contro*». John Willey & Sons;

Ming T Tham., 2005 «*Introduction to Robust Control*. Chemical and Process Engineering», University of Newcastle Document.

Rivera, D.E., 1999. «Internal model control: a comprehensive view» Department of Chemical, Bio and Materials Engineering.

Keeping, S., 2013. «An Introduction to Brushless DC Motor Control. Contributed by electronic Products», http://www.digikey.ca/en/articles/techzone/2013/mar/an-introduction-to-brushless- dc-motor-control.

EPOS2 Positioning Controllers, Maxon Motor Application Notes. Switzerland, https://www.maxonmotor.com/medias/sys_master/root/8823581507614/EPOS2-Application-Notes-Collection-En.pdf.

United States Government Accountability Office., 2014. « Impact of Fuel Price Increases on the Aviation Industry», Report to Congressional Committees GAO-14-331.

Popov, A.V., Grigorie, T.L., Botez, R.M., Mamou, M., and Mébarki, Y., 2010. «Real Time Morphing Wing Optimization Validation Using Wind-Tunnel Tests», *Journal of Aircraft,* vol. 47, pp. 1346-55.

Skillen, M.D., Crossley, W.A., 2007. «Modeling and Optimization for Morphing Wing Concept Generation», NASA/CR-2007-214860, *Langley Research Center*.

Yang, J., Sartor, P., Cooper, J.E., Nangia, R.K., 2015. «Morphing Wing Design for Fixed Wing Aircraft», AIAA Science and Technology Forum (SciTech).

Sleesongsom, S., Bureerat, S., Tai, K., 2013. «Aircraft morphing wing design by using partial topology optimization». *Structural and Multidisciplinary Optimization*, vol. 48, (6), P 1109-1128.

De-Gaspari, A., Ricci, S.A.G, 2015. «Knowledge-Based Shape Optimization of Morphing Wing for More Efficient Aircraft», *International Journal of Aerospace Engineering*,.

Zhoujie-Lyu, Z., Martins, J.R.R.A., 2015. «Aerodynamic Shape Optimization of an Adaptive Morphing Trailing Edge Wing», *Journal of Aircraft*, vol. 52(6), pp. 1951-1970.

Gamboa, P., Vale, J., Lau, F.J.P., Suleman, A., 2009. «Optimization of a Morphing Wing Based on Coupled Aerodynamic and Structural Constraints», *AIAA Journal*, vol. 47(9).

Fincham, J.H.S., Friswell, M.I., 2015. «Aerodynamic optimisation of a camber morphing aerofoil», Aerospace Science and Technology, vol. 43, pp. 245-255.

Molinari, G., Quack, M., Dmitriev. V., Morari, M., Jenny, P., Ermanni, P., 2011. «Aero-Structural Optimization of Morphing Airfoils for Adaptive Wings». *Journal of Intelligent Material Systems and Structures*, vol. 22, pp. 1075-1089.

Namgoong, H., Crossley, W.A., Lyrintzis, A.S., 2007. «Aerodynamic Optimization of a Morphing Airfoil Using Energy as an Objective», *AIAA Journal*, vol. 45(9), pp. 2113-2124.

Woods, B.K.S., Friswell, M.I., 2015. «The Adaptive Aspect Ratio morphing wing: Design concept and low fidelity skin optimization». *Aerospace Science and Technology*, vol. 42, pp. 209-217.

Usher, T.D., Ulibarri Jr., K.R., Camargo, G.S., 2013. «Piezoelectric Microfiber Composite Actuators for Morphing Wings», *ISRN Materials Science*, vol. 2013, pp. 1-8.

Bilgen, O., Friswell, M.I., 2014. «Piezoceramic composite actuators for a solid-state variable-camber wing». *Journal of Intelligent Material Systems and Structures*, vol. 25(7), pp. 806–817,.

Ohanian III, O.J., Karni, E.D., Olien, C.C., Gustafson, E.A., Kochersberger, K.B., Gelhausen, P.A., Brown B.L., 2011. «Piezoelectric composite morphing control surfaces for unmanned aerial vehicles». *Sensors and Smart Structures Technologies for Civil, Mechanical, and Aerospace Systems*, vol. 7981. DOI. 10.1117/12.881770.

Debiasi, M., Bouremel, Y., Khoo, H. H., Luo, S. C., Tan, E. Z., 2011. «Shape Change of the Upper Surface of an Airfoil by Macro Fiber Composite Actuators», AIAA 29th *AIAA Applied Aerodynamics Conference*, DOI./10.2514/6.2011-3809.

Vos, R., Barrett, R., de Breuker, R., Tiso, P., 2007. «Post-buckled precompressed elements: a new class of control actuators for morphing wing UAVs», *Smart Materials and Structures*, vol. 16, pp. 919-926.

Bil, C., Massey, K., Abdullah, E.J., 2013. «Wing morphing control with shape memory alloy actuators», *Journal of Intelligent Material Systems and Structures*, vol. 24(7) ,pp 879–898.

Kang, W.R., Kim, E.H., Jeong, M.S., Lee, I., 2012. «Morphing Wing Mechanism Using an SMA Wire Actuator», *International Journal of Aeronautical & Space Sciences*, vol. 13, pp. 58-63.

Karagiannis, D., Stamatelos, D., Spathopoulos, T., Solomou, A., Machairas, T., Chrysohoidis, N., Saravanos, D., Kappatos, V., 2014. «Airfoil morphing based on SMA actuation technology", Aircraft Engineering and Aerospace Technology». *An International Journal*, vol. 86, pp. 295-306.

Barbarino, S., Pecora, R., Lecce, L., Concilio, A., Ameduri, S., De Rosa, L. 2011. «Airfoil Structural Morphing Based on S.M.A. Actuator Series: Numerical and Experimental Studies» *Journal of Intelligent Material Systems and Structures*. vol. 22(10), pp. 987-1004.

Botez, R. M., Molaret, P., Laurendeau, E., 2007. «Laminar Flow Control on a Research Wing Project Presentation Covering a Three Year Period». CASI Aircraft Design and Development Symposium. *Canadian Aeronautics and Space Institute Journal*.

Grigorie, T.L., Popov, A.V., Botez, R.M., Mamou, M., Mébarki, Y. 2012. «On–off and proportional-integral controller for a morphing wing. Part 1: Actuation mechanism and control design», Proceedings of the Institution of Mechanical Engineers, Part G: *Journal of Aerospace Engineering,* vol. 226 (2), pp. 131-145.

Grigorie, T.L., Popov, A.V., Botez, R.M., Mamou, M., Mébarki, Y. 2012 «On–off and proportional-integral controller for a morphing wing. Part 2: Control validation–numerical simulations and experimental tests», *Proceedings of the Institution of Mechanical Engineers, Part G: Journal of Aerospace Engineering,* vol. 226 (2): pp. 146-162.

Grigorie, T.L., Popov, A.V., Botez, R.M., Mamou, M and Mébarki, Y., 2012. «A hybrid fuzzy logic proportional-integral-derivative and conventional on-off controller for morphing wing actuation using shape memory alloy. Part 1: Morphing system mechanisms and controller architecture design», *The Aeronautical Journal*, vol. 116(1179), pp. 433-450.

Grigorie, T.L., Popov, A.V., Botez, R.M., Mamou, M and Mébarki, Y., 2012 «A hybrid fuzzy logic proportional-integral-derivative and conventional on-off controller for morphing wing actuation using shape memory alloy. Part 2: Controller implementation and validation», *The Aeronautical Journal*, vol. 116(1179), pp. 451-465.

Grigorie, T.L., Popov, A.V., Botez, R.M., 2014 «Control Strategies for an Experimental Morphing Wing Model», AIAA Aviation 2014, *AIAA Atmospheric Flight Mechanics (AFM) Conference*, doi.org/10.2514/6.2014-2187.

Popov, A.V., Grigorie, T.L., Botez, R.M., Mamou, M and Mébarki, Y., 2010. «Closed-loop control validation of a morphing wing using wind tunnel tests», *Journal of Aircraft*, vol. 47(4), pp. 1309-1317.

Popov, A.V., Grigorie, T.L., Botez, R.M., Mamou, M., Mébarki, Y. 2010«Modeling and testing of a morphing wing in open-loop architecture», *Journal of Aircraft*, 47 (3) pp. 917-923.

Koreanschi, A., Sugar-Gabor, O., Botez, R.M., 2016. «Numerical and Experimental Validation of a Morphed Wing Geometry Using Price-Païdoussis Wind Tunnel Testing», *The Aeronautical Journal*, vol. 120 (1227), pp 757- 795.

Sugar-Gabor, O., Simon, A., Koreanschi, A., Botez, R. M., 2016 «Aerodynamic Performance Improvement of the UAS-S4 Éhecatl Morphing Airfoil using Novel Optimization Techniques» Proceedings of the Institution of Mechanical Engineers, Part G: *Journal of Aerospace Engineering*, vol. 230(7), pp 1164-1180.

Kammegne Tchatchueng, M.J., Grigorie, T.L., Botez, R.M., Koreanschi, A., 2014 «Design and validation of a position controller in the Price-Païdoussis wind tunnel», *IASTED Modeling, Simulation and Control conference*.

Tchatchueng Kammegne, M.J., Grigorie, T.L., Botez, R.M., Koreanschi, A., 2016 «Design and wind tunnel experimental validation of a controlled new rotary actuation system for a morphing wing application», Proceedings of the Institution of Mechanical Engineers, Part G: *Journal of Aerospace Engineering*, vol. 230, pp 132-145.

Koreanschi, A., Sugar-Gabor, O., Botez, R.M., 2016. «Drag Optimization of a Wing Equipped with a Morphing Upper Surface», *The Aeronautical Journal*, vol. 120(1225), pp. 473-493.

Khan, S., Botez, R. M., Grigorie, T.L., 2015. «A New Method for Tuning PI Gains for Position Control of BLDC Motor Based Wing Morphing Actuators», *AIAA Modeling and Simulation Technologies Conference*, https://doi.org/10.2514/6.2015-2497

Kennedy, J., Eberhart, R., 1995. «Particle Swarm Optimization», *in Proceedings of IEEE International Conference on Neural Networks (ICNN)*, pp 1942-1948.

Venter, G., Sobieszczanski-Sobieski, J., 2002. «Multidisciplinary optimization a transport aircraft wing using particle swarm optimization», *9th AIAA/ISSMO Symposium on Multidisciplinary Analysis and Optimization,* Atlanta, Georgia, 4-6 September,.

Venter, G., Sobieszczanski-Sobieski, J., 2004. «Multidisciplinary optimization of a transport aircraft wing using particle swarm optimization», *Structural and Multidisciplinary Optimization*, vol. 26, Issue 1-2, pp. 121-131.

Blasi, L., Del Core, G., 2007. «Particle Swarm Approach in Finding Optimum Aircraft Configuration», *Journal of Aircraft*, vol. 44(2).

Pontani, M., Conway, B.A., 2010. «Particle Swarm Optimization Applied to Space Trajectories», Journal of Guidance, *Control, and Dynamics*, vol. 33(5).

Grant, M.J., Mendeck, G.F., 2007. «Mars Science Laboratory Entry Optimization Using Particle Swarm Methodology», *AIAA Atmospheric Flight Mechanics Conference*, doi.org/10.2514/6.2007-6393.

Hassan, R., Cohanim, B., de Weck, O., 2005. «A comparison of particle swarm optimization and the genetic algorithm». 46th AIAA/ASME/ASCE/AHS/ASC Structures, *Structural Dynamics and Materials Conference, Structures, Structural Dynamics, and Materials and Co-located Conferences*. https://doi.org/10.2514/6.2005-1897

Van den Bergh, F., 2002. «An Analysis of Particle Swarm Optimizers», PhD thesis, Department of Computer Science, University of Pretoria, Pretoria, South Africa,.

Poli, R., Kennedy, J., Blackwell, T., 2007. «Particle swarm optimization. An overview». Swarm Intelligence, vol 1(1), pp 33-57.

NOvel Air Vehicle Configurations: «From Fluttering Wings to Morphing Flight» (NOVEMOR), Grant Agreement ID: 285395, Programme FP7-TRANSPORT - Specific Programme "Cooperation": Transport (including Aeronautics). Available *online: https://cordis.europa.eu/project/rcn/99991/factsheet/*en.

Smart Intelligent Aircraft Structures (SARISTU), Grant Agreement ID: 284562, Programme FP7-TRANSPORT - Specific Programme "Cooperation": Transport (including Aeronautics). Available online: https://cordis.europa.eu/project/rcn/100047/factsheet/en.

Wings of the future (FUTUREWINGS), Grant Agreement ID: 335042, Programme FP7-TRANSPORT - Specific Programme "Cooperation": Transport (including Aeronautics). Available online: https://cordis.europa.eu/project/rcn/109751/factsheet/en.

Leading Edge Actuation Topology Design and Demonstration (LeaTop), Grant agreement ID: 271861, Programme FP7-JTI - Specific Programme "Cooperation": Joint Technology Initiatives. Available online: https://cordis.europa.eu/project/rcn/102033/factsheet/en.

Kota, S., Osborn, R., Ervin, G., Maric, D., Flick, P., Paul, D., 2009. «Mission Adaptive Compliant Wing - Design, Fabrication and Flight Test» In RTO-MP-AVT-168, NATO AVT-168 Morphing Vehicles Symposium, pp 1-19.

Ameduri, S.; Brindisi, A.; Tiseo, B.; Concilio, A.; Pecora, R., 2012. «Optimization and integration of shape memory alloy (SMA)-based elastic actuators within a morphing flap architecture». *International Journal of Materials Systems and Structures*, vol 23(4), pp 381-396.

Barbarino, S.; Pecora, R.; Lecce, L.; Concilio, A.; Ameduri, S.; De Rosa, L., 2011 «Airfoil Structural Morphing Based on S.M.A. Actuator Series: Numerical and Experimental Studies». *International Journal of Materials Systems and Structures***,** vol 22, *Issue 10*, pp 987-1004.

Peel, L.D.; Mejia, J.; Narvaez, B.; Thomson, K.; Lingala, M. 2008. «Development of a simple morphing wing using elastomeric composites as skins and actuators». In ASME *Conference on Smart Materials, Adaptive Structures and Intelligent Systems*. pp 839-847, DOI.10.1115/SMASIS2008-544.

Larco, C., Constatin, L., Demșa, M., Mustata, S., 2018. «Wing lift-drag ratio optimization». In The 20th Edition of the *International Conference Scientific Research and Education in the Air Force* (AFASES 2018), pp 191-196.

Pahonie, R.C., Larco, C., Mihaila Andres, M., Nastasescu, V.; Barbu, C., Costuleanu, C.L, 2017. «Experimental characterisation of hyperelastic materials for use in a passive-adaptive membrane on MAVs wing». volume 54(4), pp 768-772.

Pahonie, R.C., Mihai, R.V., Larco, C. 2014. «Towards Flexible-Winged Unmanned Aircraft Systems». In *International Conference of Aerospace Sciences* "AEROSPATIAL 2014", Bucharest, Romania, September 18-19.

Larco, C., 2008. «Analyse des instabilités dans l'écoulement transsonique». In Proceedings of the International Symposium Research and Education in an Innovation Era - Engineering Sciences. Universitatea, Aurel Vlaicu, Arad.

Wereley, N.M., Kothera, C., Bubert, E., Woods, B., Gentry, M., Vocke, R., 2009.«Pneumatic Artificial Muscles for Aerospace Applications». In 50th AIAA/ASME/ASCE/AHS/ASC Structures, *Structural Dynamics, and Materials Conference*.

Kudva, J.N. 2004. «Overview of the DARPA Smart Wing Project». Journal of Intelligent Material Systems and Structures, vol. 15, pp. 261-267

Martinez, J.M., Scopelliti, D., Bil, C., Carrese, R., Marzocca, P., Cestino, E. and Frulla, G., 2017. «Analysis and Experimental Testing of a Morphing Wing». *In 25th AIAA/AHS Adaptive Structures Conference, Grapevine*, vol 15(4), pp. 261-267.

Kumar, D., Faruque, Ali., Arockiarajan, A., 2018. «Structural and Aerodynamics Studies on Various Wing Configurations for Morphing». In 5th IFAC Conference on Advances in Control and Optimization of Dynamical Systems ACODS, vol. 51(1), pp. 498-503.

Yokozeki, T., Sugiura, A., Hirano, Y., 2014. «Development of variable camber morphing airfoil using corrugated structure». *Journal of Aircraft*, vol.51(3), pp. 1023-1029.

Liauzun, C., Le, Bihan., D, David, J-M., Joly, D., and Paluch, B., 2018. «Study of Morphing Winglet Concepts Aimed at Improving Load Control and the Aeroelastic Behavior of Civil Transport Aircraft». *AerospaceLab Journal* No 14, DOI, 10.12762/2018.AL14-10, *AerospaceLab*, Issue 14, pp. 1-16.

Popov, A.V., Grigorie, T.L., Botez, R.M., Mamou, M. and Mebarki, Y., 2010. «Real Time Morphing Wing Optimization Validation Using Wind-Tunnel Tests». *Journal of Aircraft*, vol(47), Issue 4, pp. 1346-1355.

Popov, A.V., Grigorie, T.L., Botez, R.M., Mébarki, Y. and Mamou, M. 2010. «Modeling and testing of a morphing wing in open-loop architecture». *Journal of Aircraft*, vol (47)3, pp. 917-923.

Grigorie, T.L., Botez, R.M., Popov, A.V., 2015. «How the Airfoil Shape of a Morphing Wing is Actuated and Controlled in a Smart Way». *Journal of Aerospace Engineering*, vol.28(1).

Grigorie, T.L., Popov, A.V., Botez, R.M., Mamou, M., Mebarki, Y., 2011. «A New Morphing Wing Mechanism Using Smart Actuators Controlled by a Self-Tuning Fuzzy Logic Controller». In *11th AIAA Aviation Technology, Integration, and Operations (ATIO) Conference*, pp. 1-12, doi.org/10.2514/6.2011-7071.

Grigorie, T.L., Popov, A.V., Botez, R.M., 2014. «Control strategies for an experimental morphing wing model». *In AIAA Atmospheric Flight Mechanics Conference*, pp. 1-12, https://DOI./10.2514/6.2014-2187.

Popov, A.V., Grigorie, T.L., Botez, R.M., Mamou, M., Mebarki, Y. «Closed-Loop Control Validation of a Morphing Wing Using Wind Tunnel Tests». *Journal of Aircraft* 2010, vol. 47(4), pp. 1309-1317.

Wheeler, P.W., Clare, J.C., Trentin, A., Bozhko, S., 2013. «An overview of the more electrical aircraft». *Journal Of Aerospace Engineering*, vol.227(4), pp. 578-585.

Madonna, V., Giangrande, P., Galea, M., 2018. «Electrical Power Generation in Aircraft: Review, Challenges, and Opportunities». *IEEE Transactions on Aerospace and Electronic Systems*, vol. 4(3), pp. 646-659.

Sun, J., Guan, Q., Yanju, L., Leng, J., 2016. «Morphing aircraft based on smart materials and structures». *Journal of Intelligent Materials Systems and Structures,* vol. 27(17), pp. 2289-2312.

Koreanschi, A., Sugar-Gabor, O., Botez, R.M., 2016. «Drag Optimization of a Wing Equipped with a Morphing Upper Surface». *Aeronautical Journal*, vol.120(1225), pp. 473-493.

Amendola, G., Dimino, I., Magnifico, M., Pecora, R., 2016. «Distributed actuation concepts for a morphing aileron device». *Aeronautical Journal*, vol. *120*(*1231*) pp. 1365-1385.

Arena, M., Amoroso, F., Pecora, R., Amendola, G., Dimino, I., Concilio, A., 2018. «Numerical and experimental validation of a full scale servo-actuated morphing aileron model». *Journal of Smart Materials and Structures*, vol. 27(10), pp. 1-21.

Choosing between Brush and Brushless DC Motors - Allied Motion Technologies Inc., Available online: https://www.alliedmotion.com/wp-content/uploads/whitepapers/Choosing-Between-Brush-Brushless-Motors-201801.

Maxon Motor Inc. Available online: http://www.maxonmotor.com/maxon/view/content/index.

Grigorie, T.L., Popov, A.V., Botez, R.M., Mamou, M., Mebarki, Y., 2011. «An Intelligent Controller based Fuzzy Logic Techniques for a Morphing Wing Actuation System using Shape Memory Alloy». *In 52nd AIAA/ASME/ASCE/AHS/ASC Structures, Structural Dynamics and Materials Conference*. DOI./10.2514/6.2011-2133.

Mahfouf, M., Linkens, D.A., Kandiah, S. and Kang, T-S., 1999 «Model predictive control for process engineering». In IEEE Workshop on Model Predictive Control: Techniques and Applications.

Mohamed Sadok Guezguez, 2016. «Morphing wing system integration with wind tunnel testing», Master's Thesis in Aerospace Engineering, 2016.

Gianluca, Amendola., 2016. «Full Scale Servo-Actuated Morphing Aileron for Wind Tunnel Tests», PhD thesis in Aerospace Engineering.

Kelvin, P., Atta, O., 2014, "Morphing Wings Using Macro Fiber Composites", Embry Riddle Aeronautical University, McNair Scholars Research Journal.

Bilgen, O., Kevin B., and Daniel J. Inman, 2010, "Novel, Bi-Directional**,** Variable Camber Airfoil via Macro-Fiber Composite Actuators", Journal of aircraft, Vol. 47(1):pp-303-314.

Bilgen, O., Alper Erturk, Daniel J. Inman, 2010 “Analytical and Experimental Characterization of Macro-Fiber Composite Actuated Thin Clamped-Free Unimorph Benders”, Journal of Vibration and Acoustics, Vol. 132 - 051005-1.

Daniel, J., lnman, Harley, H., Cudney, 1998, “Center for Intelligent Materials Systems and Structures Virginia Polytechnic Institute and State University”, Final Report to NASA Langley Research Center.